Model Predictive Control for Dissolved Oxygen and Temperature to Study Adeno-Associated Virus (AAV) Production in Bioreactor

by

Farzaneh Bannazadeh

Thesis submitted to the University of Ottawa
in partial Fulfillment of the requirements for the
Master of Applied Science in
Biomedical Engineering

Ottawa-Carleton Institute for Biomedical Engineering
School of Electrical Engineering and Computer Science
Faculty of Engineering
University of Ottawa

Abstract

Gene therapy is advancing rapidly, with Recombinant Adeno-associated virus (rAAV) being investigated for potential use in treating cancer and neurological disorders. Plasmid DNA transfection and viral infection are standard methods for producing large-scale rAAV vectors. However, improving yield production requires careful monitoring and control of process state variables, which can be expensive and time-consuming. This thesis proposes a model predictive control (MPC) model that can efficiently monitor, predict, and optimize the final product by controlling state variables like DOT and temperature. The model relies on an unstructured mechanistic kinetic model designed explicitly based on rAAV upstream production. Monitoring viral vector production based on substrate or biomass concentration enhances bioprocess production efficiency. However, other state variables like dissolved oxygen (DO), pH, and temperature should also be considered.

The objective of this thesis is to enhance cell growth in bioreactors by regulating dissolved oxygen and temperature levels using a Model Predictive Control (MPC) system. This model can be employed in different processes to enhance cell growth and examine the impact of control measures. The goal is to achieve a high cell density, increase productivity, and lower costs in a shorter duration. Simulink, a software tool developed by MATLAB, seamlessly integrates Ordinary Differential Equations (ODEs) to optimize bioprocesses in bioreactors. The Model Predictive Control (MPC) controller expertly regulates Dissolved Oxygen Tension (DOT) and temperature, thereby increasing cell growth concentrations. This sophisticated controller efficiently manages multiple variables simultaneously and exceeds the Proportional Integral Derivative (PID) controller. The model is straightforward to comprehend and promptly responds to anomaly data.

To evaluate the suggested resolution, we conducted tests on both PID and MPC controllers by introducing measurement noise to the DOT. Our analysis indicated that MPC demonstrated superior performance based on the ISE (Integral of Squared Error), IAE (Integral of Absolute Error), and ITAE (Integral of Time-

weighted Absolute Error), all of which were substantially higher for the PID controller. Regardless of changing conditions, MPC adeptly tracks the setpoint and optimizes the variable to enhance production efficiency.

Co-Authorship

I hereby verify that this thesis is entirely my own work unless otherwise indicated. I am aware of the University of Ottawa regulations concerning plagiarism, which carry possible disciplinary repercussions. If I have incorporated another author's work, I have given appropriate credit and recognition to their contribution.

Acknowledgements

I would like to thank the National Research Council Canada (NRC) for funding the project. I would like to express my deep gratitude to Dr. Amine and his team at McGill for generously sharing their data and for the valuable discussions and guidance they provided.

I am incredibly grateful for the support and assistance those around me gave me while creating my thesis. Without their kindness, I could not have completed this document. My supervisor, Dr. Miodrag Bolic, gave invaluable guidance and advice, and I genuinely appreciate his insightful comments and suggestions. My loved ones, including my parents, siblings, and significant others, have always provided emotional support, even from afar, as I pursued my aspirations. I owe them my deepest gratitude.

Table of Contents

List of Figures

List of Tables

List of Abbreviations

AAV	*Adeno-associated virus*
rAAV	*Recombinant adeno-associated virus*
Ad	*Adenovirus*
MPC	*Model predictive control*
PID	*Proportional-Integral-Derivative*
ODE	*Ordinary Differential Equation*
ITR	*Inverted terminal repeats*
HEK293	*Human Embryonic Kidney 293*
HSV	*Herpes simplex virus*
BEVS	*Baculovirus expression vector system*
PEI	*Polyethyleneimine*
ISE	*Integral Square Error*
IAE	*Integral Absolute Error*
ITAE	*Integral Time Squared Error*
SISO	*Single-input single-output*
MIMO	*Multi-input multi-output*
N_P	*Prediction horizon*
N_C	*Control horizon*
y(t)	*Output variables at instant t*
u(t)	*Input variables at instant t*
$\Delta u(t + m)$	*Future incremental control at sample m*
ΔU	*Parameter vector for the control sequence*

$w(t)$	*Reference trajectory*
$x(t)$	*State variables at instant t*
$r(t)$	*Set-point signal*
A	*State matrix of the state-space model*
B	*Input-to-state matrix of the state-space model*
C	*State-to-output matrix of the state-space model*
F, Φ	*Pair of matrices used in the prediction equation* $Y = Fx(ki) + \Phi\Delta U$
Y	*Predicted output data vector*
J	*The performance index for optimization*
I^*	*Optimal control*
φ	*Performance criterion*
R_s	*Pair of weight matrices in the cost function of predictive control*
X	*Biomass concentration*
X_0	*Initial biomass concentration*
X_P	*Product concentration*
μ	*Specific growth rate*
K_s	*Saturation constant*
$Y_{x/O}$	*Yield from oxygen to biomass*
P_{O2}	*Partial pressure of* O_2
p	*State Parameter (Italic)*
E	*Internal energy of the system*
V	*Volume*
S	*Substrate concentration*
$F(t)$	*Flow rate*

q_g	*Rate of fresh cell biomass production*
q_p	*Rate of production*
X	*State variable vector*
t_f	*Final culture time*

Chapter 1

Introduction and Motivation

1.1 Introduction

The field of gene therapy is rapidly advancing and presents many exciting opportunities in the treatment of genetic disorders, infectious diseases, and cancer. This innovative approach uses nucleic acids to target specific cells through gene expression and RNA interference. Given the inherent instability of RNA and DNA within biological systems, viral vectors - notably recombinant Adeno-associated virus (rAAV) - offer a highly effective means of delivering genes to their intended targets. rAAV is non-pathogenic, exhibits low immunogenicity, and enables long-term gene expression. The FDA has approved rAAV-based therapies for rare monogenic diseases like spinal muscular atrophy and Leber congenital amaurosis. With over 200 clinical trials, rAAV-based gene therapies are under investigation for various conditions, including cancer and neurological disorders [1–5]. The AAV is a non-enveloped virus and has a single-stranded DNA genome. For infections to occur, helper viruses are required. Researchers have developed recombinant AAV (rAAV) vectors since 1984, allowing the expression of foreign genes in mammalian cells. Multiple AAV serotypes and variants have been identified, facilitating the creation of diverse "pseudotyped" vectors. Several methods, including plasmid DNA transfection and viral infections, are established for large-scale rAAV vector production [1, 6, 7].

Bioreactors are used to grow genetically modified microorganisms and mammalian cells for producing recombinant therapeutic proteins. However, controlling these processes to their maximum yield is difficult due to their nonlinear and non-stationary nature. Automatic control systems need improvement to meet safety standards and operational restrictions. Bioreactors currently have simple, conventional automatic control systems [8–11]. Current bioreactor

monitoring and control studies employ PID, Artificial Neural Networks (ANNs), or model predictive control (MPC) controllers to optimize crucial factors like the specific growth rate, substrate concentrations (e.g., glucose, glutamine), and biomass levels in microbial and recombinant protein production. These controllers are instrumental in overseeing diverse bioreactor operations, encompassing fed-batch and batch-to-batch processes. Nonetheless, bioprocesses are inherently intricate, and various environmental variables, such as pH, temperature, dissolved oxygen (DO), CO_2 uptake, and agitation, can profoundly influence growth rates. Unfortunately, the cost associated with upgrading sensors or hardware for bioreactors often necessitates the utilization of embedded feedback controllers to regulate these parameters [8–16].

In this thesis, we developed a model predictive controller (MPC) tailored for precisely regulating dissolved oxygen and temperature, two pivotal factors influencing cell growth within a laboratory-scale bioreactor dedicated to producing Adeno-associated virus. We achieved this by simulating the bioreactor model using ordinary differential equations (ODEs) that capture the dynamic behaviour of the bioprocess. In order to optimize cellular growth and maintain control over critical parameters, we employed Model Predictive Control (MPC). To evaluate its effectiveness, we conducted a comparative analysis against a conventional PID controller in the presence of noisy data. This research advances our understanding of MPC's applicability in bioprocess control and optimization of AAV.

1.2 Motivation and Problem Statement

The recent approval of two adeno-associated virus (AAV) drugs by the U.S. Food and Drug Administration (FDA) indicates AAV-based gene therapy's maturity [6, 17]. This development highlights the growing significance of AAV-based gene therapy in medicine. Pre-clinical and clinical investigations have consistently shown that AAV is effective, regardless of the manufacturing method used [6]. Manufacturing Adeno-associated virus (AAV) viral vectors is a

complex procedure requiring inventive strategies to address safety, effectiveness, clinical and market requirements, and cost objectives. Maintaining the stability of viral vectors is a crucial challenge AAV manufacturers face during the process. This includes preventing degradation during various stages such as manufacturing, handling, and storage and ensuring long-term stability which is related to the production situation. Developing scalable and robust manufacturing processes for gene therapy products necessitates integrating both traditional approaches and novel technologies to monitor the system. The workflow includes unit operations: upstream, downstream, formulation, and fill/finish processing [18]. The upstream process involves several key steps, including plasmid development and production, cell expansion, plasmid transfection, and viral vector production. Nevertheless, the upstream process, which includes triple transfection, leads to low titers (low final product) and significant variability in product quality. This restricts the ability to scale up the process, making it unsuitable for long-term solutions [4, 18].

Ensuring adequate oxygen supply and proper heat removal are critical design considerations for large fermenters used in industrial settings [19]. The oxygen demand is essential for the proper upstream processes, as low amounts may prevent cell growth, while excessive levels can lead to oxidative damage. The regulation of oxygen levels is crucial to achieve maximum product output. The oxygen demands vary across different processes, particularly in scale-up production. Ensuring equilibrium between the culture's oxygen intake rate and the bioreactor system's oxygen transfer rate is highly significant. Increased cell concentrations have the potential to result in a lack of oxygen, whereas the specific growth rate shows variability in response to changes in dissolved oxygen. An explicit knowledge of oxygen requirements is crucial for effective manufacturing endeavours [20, 21]. Maintaining optimal temperature is vital for achieving high cell concentration. While temperature can accelerate the growth rate, exceeding the ideal range can lead to a decline in growth and even result in thermal death. Temperature also significantly impacts product formation and yield factor and can even affect the rate-limiting step in bioprocess [20].

Due to the importance of controlling dissolved oxygen (DO) and temperature for optimal cell growth, the control concept may become important in scale-up upstream processes. Cutting-edge gene therapy techniques are currently working to streamline production and reduce expenses through data-driven and mechanistic methodologies. Nonetheless, the intricacy of bioprocesses and the inquiry of assumptions can present obstacles to practical application. Therefore, combining mechanistic and data-driven models to create a hybrid model shows promise in better describing and optimizing the rAAV production process. Mechanistic models define reactions in cell metabolism and rAAV production, while data-driven models connect process parameters and define and estimate unknown system parameters [17]. Table 1.1 provides a compilation of existing solutions for controlling and monitoring various upstream processes in bioreactors.

This thesis is motivated by a notable gap in the current state of research on regulating dissolved oxygen and temperature using mechanistic kinetic models in AAV production by triple plasmid transfection of HEK293SF-3F6 cells. While significant progress has been made in bioprocess control, much-existing literature and studies focus on processes not involving mammalian cell cultures. The specific complications and requirements of AAV, CHO, or MAb production within mammalian cell cultures have received different attention and investigation. Existing research has primarily centred on controlling biomass or substrate concentration to enhance production yield, often overlooking the critical aspects of dissolved oxygen and temperature regulation.

Table 2-1 Existing solutions for bioprocess control

Model Characteristics	***Control Parameters***	***Goal of study***	***Ref.***
Adaptive nonlinear controller with parameter estimator for HEK-293 cell	*Maintaining a low-glucose concentration*	*Decreasing the rate of glycolysis and lactate accumulation.*	*Siegwart et al. 1999*[22]
Artificial neural network (ANN)+ MPC	*Temperature*	*Dynamic modelling of yeast fermentation (complex model)*	*Nagy 2006* [15]
Simulation of biochemical process model	*Flow rate*	*Simulation of the effect of pH, DO, and temperature with considering ionic strength*	*Assadzadeh et al. 2010*[23]
Nonlinear model predictive controller (NMPC) in CHO mammalian cell fed-batch process	*Glucose concentration fixed setpoint*	*Improving product quality, batch-batch reproductivity, and cost reduction*	*Craven et al. 2014* [24]
Nonlinear model predictive controller (NMPC)	*Glucose and glutamine concentration*	*Optimal culture condition in the production of Mab. Estimation of glucose and glutamine concentration*	*Dewasme et al. 2015* [14]
Model reference adaptive control (MRAC)	*Dissolved oxygen (DO) for bacteria and yeast culture*	*Control of DO as a secondary state variable*	*Chitra et al. 2018* [25]
MPC based on adapted metabolic-genetic model in batch growth of E. coli	*Oxygen uptake rate (OUR)*	*Optimization of ethanol productivity*	*Jabarivelisdeh et al. 2020*[26]
Sliding mode nonlinear control (SMNC)	*Biomass and volume*	*Maintaining maximum biomass dynamics, avoiding overflow metabolism*	*Lopez-Perez et al. 2022*[27]
Digital-twin framework for intelligent biomanufacturing (BioDT)	----	*Prediction of glucose consumption and lactic acid production, cell growth rate, oxygen transfer*	*Zhao et al. 2023* [28]

1.3 Objective and Contribution

This thesis is dedicated to achieving several primary objectives. The primary objectives of this thesis are:

- Develop comprehensive mechanistic kinetic models encompassing the bioreactor and bioprocess behaviour, focusing on several important parameters like dissolved oxygen (DO), temperature, cell growth, glucose and glutamine consumption, and lactic acid production. The developed models optimize cell growth concentration precisely within the bioreactor. This model will offer outstanding insights into the complexities of the upstream.
- Develop the model predictive control (MPC) system specifically customized for regulating DO and temperature in AAV's upstream process. The model conducted a comparative analysis and evaluation of the MPC controller's performance in the presence of measurement noise alongside the conventional PID controller.
- The MPC controller's practical utility extends to predicting and applying control actions for DO and temperature in batch or fed-batch processes, thereby enhancing cell growth compared to AAV processes lacking advanced control mechanisms.
- Develop the Proportional-Integral-Derivative (PID) control model for the bioreactor with similar characteristics to the actual bioreactor in the production of AAV. This model is utilized for comparison of the MPC controller's performance.

Through these multifaceted objectives, this thesis strives to significantly advance our understanding of rAAV production within bioreactors, offering mechanistic insights and practical control solutions.

The initial data were utilized in the formulation of the proposed ordinary differential equations (ODEs), and Model predictive control (MPC) data was gathered from the production of adeno-associated virus (AAV) through triple plasmid transfection of HEK293SF-3F6 cells in a 3 L bioreactor. The necessary specific growth rate values were obtained by estimating parameters using Neural Ordinary Differential Equations. These limitations arise due to the lack of knowledge of the required parameters for our bioprocess. [4]. Additional constants and unknown values were obtained from relevant literature sources and related biological processes.

1.3.1 Boundaries

This thesis consists of several boundaries that are going to be listed here. The ODE model and the MPC controller are only developed but not verified with real data. The MPC controller modelled DOT, and temperature and pH values were considered constant. The initial values for various parameters were collected from similar studies due to the lack of information about the rAAV production experiment. This thesis does not cover all the materials presented in the actual bioreactor as they focus on cell growth rate and main dependents.

The contributions of this study lie in its effort to advance the development of a high cell density and high yield strategy for the scale-up production of recombinant Adeno-associated virus (rAAV) as a viral vector for gene therapy with implementing an MPC controller. This thesis represents an important step in an ongoing attempt to achieve this objective. As aforementioned, existing control models introducing a different point of view in controlling AAV production can lead these monitoring concepts to the environmental parameters that directly affect the final results. The

proposed model can be developed in the real environment and verified its performance efficiency in experiments.

1.4 Thesis Outline

This thesis is divided into five chapters, each exploring different aspects of the thesis. Chapter 1 introduces the objectives and motivation behind this research. Chapter 2 provides a background and literature review of prior work related to the production of AAV in bioreactors and the control strategies of bioprocesses. This chapter delves into the biology of AAV and its production methods, as well as the optimization of these methods. The use of bioreactors in bioprocesses is discussed, and PID and MPC control strategies are examined. Chapter 3 outlines the steps for implementing bioprocess models. It includes sections on mathematical modelling, environmental factors such as DO and temperature, the bioreactor's mechanistic model, and the implementation of PID and MPC controller models. Chapter 4 presents simulation results and discussions, accompanied by multiple graphs illustrating the novelty of the work. Chapter 4 presents simulation results and discussions, along with the performance of the proposed model. The model is evaluated using various performance curves and plots, including simulated data good and anomaly ones for the MPC controller. Chapter 5 presents our conclusion, a summary of contributions to this thesis and possible future work.

Chapter 2

Background and Literature Review

This chapter presents an overview of the context and previous studies on producing and monitoring adeno-associated virus (AAV) and related bioprocesses. The text discussed the general aspects of adeno-associated virus (AAV) and its biological characteristics, along with the utilization of bioreactors in bioprocesses. Additionally, an overview of proportional-integral-derivative (PID) and model predictive control (MPC) control mechanisms was mentioned to comprehend control strategies in various processes.

2.1 Introduction to Adeno-associated virus (AAV)

Viruses are responsible for numerous diseases, and developing antiviral agents is crucial in drug discovery. However, viruses also play a significant role in bioprocessing technology. For example, the attack of phages on an E. coli fermentation that produces a recombinant protein product can result in severe destruction, leading to the loss of an entire culture in vessels containing multiple litres. Nevertheless, phages can also serve as agents for transporting desired genetic material into E. coli. Modified animal viruses can function as vectors for genetically engineering animal cells to generate proteins through recombinant DNA technology [20]. In the middle of the 1960s, laboratory adenovirus (AdV) preparations developed the first evidence of adeno-associated virus (AAV), which was later discovered in human tissues [29–32]. Researchers attempted to explore the biological characteristics of AAV based on their interest in science regardless of its enormous potential as a human gene therapy technology [32, 33].

Over the first 15-20 years, the main aspects of AAV were defined, including AAV's genome configuration and composition [32, 34, 35], DNA replication and transcription [32, 36, 37],

infectious latency [32, 38–40] and virion assembly [32, 41]. These achievements have helped the successful cloning of the wild-type AAV2 sequence into plasmids, making it possible for genetic research and study of the AAV2 genome. These initial studies gave researchers an essential understanding of AAV's gene delivery ability [32]. Adeno-associated virus (AAV) vectors are the leading gene delivery platform for treating various human diseases. AAV has shown promising results in preclinical and clinical trials for gene replacement, silencing, and editing, leading to regulatory approvals for two AAV-based therapies. Ongoing research in AAV biology and therapeutic challenges will open the way for future clinical advancements [32]. Recombinant adeno-associated viral (rAAV) vectors have gained widespread attention and have been extensively used in numerous clinical trials. These vectors have demonstrated impressive safety records and notable effectiveness in treating genetic disorders. Additionally, rAAVs are being increasingly utilized as a valuable tool in gene-editing methodologies due to their unique ability to infect both dividing and non-dividing cells and act as efficient substrates for homologous recombination [6].

In clinical-stage experimental medicine, researchers are focused on non-encapsulated adeno-associated virus (AAV). Specifically, this virus can be modified to transport DNA into specific cells, offering promising applications in various therapeutic strategies. Developing recombinant AAV particles without viral genes, carrying desired DNA sequences, has shown potential in therapeutics [42].

2.1.1 AAV Biology and Replication

Adeno-associated viruses (AAVs) are a particular category of viruses that require the assistance of other viruses, like adenovirus and herpes simplex virus, or substances that damage DNA to replicate successfully within host cells. AAVs must create a symbiotic relationship with helper viruses or factors to complete their reproduction cycle. The helper modifies the cellular environment on each occasion, which may enhance AAV expression and replication. At every lifecycle stage,

molecular interactions between the virus and its host cell control AAV's infection outcome [43]. AAV2 is the most studied serotype of AAV and is used as a prototype for the family of AAVs. General features of AAVs are described using information obtained from AAV2. The genome of AAV is a 4.7 kb single-stranded DNA molecule with inverted terminal repeats (ITRs) that contain the cis-elements required for packaging and replication. The rep and cap genes encode four non-structural proteins and three structural proteins that contain the capsid. The virus can be introduced by using the Ad helper function through transfection, and then AAV vectors can be produced by removing rep and cap genes and replacing them with a transgene.

It has been observed that Adeno-Associated Virus (AAV) may have developed an optimal association with its human host [44]. It is important to note that without the presence of helper and normal healthy cells, AAV is replication-defective [44, 45]. However, under certain conditions that can be characterized as unfavourable to the host, such as co-infection or superinfection with a helper virus, AAV can replicate to a significant extent, ranging from 100,000 to 1,000,000 copies per cell [44].

AAV Production Methods

Adeno-associated virus (AAV) has become a progressively favoured instrument in the scientific laboratory, expediting its clinical utilization. Although AAV is widely used in scientific laboratories and clinical settings, its production can be complex and time-consuming. Nonetheless, considerable endeavours have been committed to refining, enhancing, and streamlining the methods employed to generate premium AAV with amplified production outputs [3]. The classical method for producing AAV vectors involves tri-transfection of the adherent human embryonic kidney 293 (HEK293) cell line, which requires transfection of three distinct plasmid constructs. The first plasmid contains the transgene of interest, viral inverted terminal repeat (ITR) sequences, serotype-dependent rep and cap gene sequences, and adenoviral helper genes. This system

effectively produces functional AAV vectors, but its adhesive nature makes it challenging to increase industrial-scale production. Alternative production methods include tri-transfection of HEK293 cells grown in suspension, production through stable cell lines, or using the Herpes simplex virus (HSV) as a vector for AAV production by mammalian cells [3].

The AAV production protocol outlined in [3] begins with preparing bacterial cell cultures for genome and helper plasmids. For maintaining bacterial health proper incubation and subsequent DNA purification methods were used. CsCl density centrifugation is highlighted as a method for obtaining high-quality supercoiled DNA. The implementation of gel electrophoresis for DNA quality control is emphasized to guarantee the integrity and purity of the samples. The maintenance of Human Embryonic Kidney (HEK293) cells depends on adhering to specific culture conditions and appropriate cell passage strategies. The importance of achieving cell confluency for effective transfection is highlighted with using Polyethyleneimine (PEI) as a transfection agent. The next step involves using tangential flow filtration (TFF) for the purpose of purifying AAV from substantial waste. For achieving high-quality outcomes in molecular biology applications, it is important to follow all the steps accurately.

In 2002, a baculovirus expression vector system (BEVS) was introduced to circumvent technological lockdowns and expand AAV production in insect cells. This method provides enough AAV vectors for preclinical projects in large animal models or research projects focusing on repeatability and reproducibility in vitro and in vivo experimental approaches [3].

2.1.2 Bioprocess Optimization

The metabolism of HEK-293 cells at low glucose concentrations was investigated by implementing fed-batch cultures. Siegwart [46] assessed glucose concentration at regular intervals of 30 minutes and effectively regulated at a level of 1 mM with the implementation of an adaptive nonlinear controller. The controller exhibited effective performance across various cell concentrations,

covering low and high values, without requiring recalibration during transitions between different culture phases. The estimation of a single parameter was conducted in order to diagnose the physiological condition of the culture. The concentration profiles obtained from both culture modalities have been divided into three stages for analysis and interpretation. The initial stage exhibited notable increases in the specific growth rate, glucose consumption, and lactate generation. In the subsequent phase, there was a decline in glucose intake, lactate generation, and glutamine uptake. The last stage showed a deceleration in cellular proliferation and minimal glutamine utilization. The respiration rate remained constant during the initial two phases. The lactate generation and glycolysis rate reduction were achieved by maintaining a low glucose concentration. The energy generated through glycolysis was shown to be non-essential for cellular growth.

In the pursuit of developing a controller that can maintain the glucose concentration at 1mM in HEK-293 mammalian cells in serum-free cultivation, optimal control was considered unreliable due to its susceptibility to model inaccuracies and the intricacy of the setup. The metabolism of mammalian cells is complex, time-varying, and nonlinear, with the dynamics determined by cell concentration. The obstacle of replicability persists from batch to batch, and the behaviour is subject to the cell's history. Due to the complexity and non-linearity of mammalian cell metabolism, optimal control for maintaining glucose concentration is unsound, and standard proportional integral derivative (PID) controls are considered ineffective. The effectiveness of an adaptive proportional integral derivative (PID) controller with time-evolving parameters has been seen. However, tuning parameters for ordinary PID controllers becomes increasingly challenging when including the suitable parameter evolution method [46].

Nguyen et al. [47] have developed a mathematical model for synthesizing rAAV viral vectors through triple plasmid transfection based on biological processes from wild-type AAV. The model covers significant steps from exogenous DNA delivery to the reaction cascade that forms viral proteins and DNA, resulting in filled capsids. The Rep protein plays a crucial role as a regulator of

packaging plasmid gene expression and a catalyst for viral DNA packaging. Their model predicts productivity changes due to varied input plasmid ratios. It suggests that a poorly coordinated timeline of capsid synthesis and viral DNA replication results in a low ratio of complete virions in harvest. The model provides testable hypotheses for evaluation and identifies potential process bottlenecks for investigation.

2.2 Bioreactor

A bioreactor is a vessel or machine supporting one or more biological processes that transform an initial substance, raw material, or substrate into a final product. For this bioprocess, a biocatalyst is used, which may include enzymes, bacteria, animal or plant cells, as well as subcellular components like chloroplasts and mitochondria. The starting material or substrate that can be transformed into a product within a bioreactor may include organic chemicals like sugar or penicillin, inorganic chemicals like carbon dioxide, or complex materials like meat and animal manure that lack definition. This conversion process could result in cells or biomass, viruses, or various chemicals, depending on the specific process occurring within the bioreactor [48].

These reactors are typically cylindrical and range in size from a few cubic metres to a few litres, depending on the industrial bioprocesses' design and mode of operation [49]. The production of food products like soy sauce, the treatment of home and industrial wastewater, the production of vaccines, antibiotics, and a variety of other essential compounds all include the usage of bioreactors. Fermenters are the name given to bioreactors that produce both animal and plant and microbial cells. In addition to producing cells, a fermenter can produce additional compounds or change a chemical added to a different molecule. A fermenter may contain either one type of cell (known as a monoseptic operation) or a mixed population of many cell types. For monoseptic operation, sealed units with barriers that prevent environmental microorganisms from compromising the process are utilized. Only nonviable things, such as cells, isolated enzymes, and cellular organelles, may be

present in other bioreactors [48]. Compared to cells and organelles, enzymes are soluble in liquid media. To achieve reusability, a soluble enzyme can be retained within the bioreactor by employing ultrafiltration membranes or can be immobilized within an insoluble matrix [48].

There are three types of bioreactor operation modes: batch processes, fed-batch processes, and continuous processes. These operation modes are typically applied to submerged or liquid fermentations in addition to cell culture processes such as tissue or algal growth [49].

Batch processes are widely used to produce specialty biomolecules for various industries, including chemical, biotechnological, and pharmaceutical. These bioproducts generate a substantial and growing portion of revenue and earnings for bioprocess industries [49]. Batch processes can be classified as a partially enclosed system where most of the necessary materials are loaded onto the bioreactor in an aseptic manner and removed at the operation's end. The only materials added or removed during the operation are air/gas exchange, antifoam, and pH-controlling agents. In contemporary bioprocesses, modifications to the medium are typically made to regulate conditions and provide nutrients and compounds that encourage the biosynthesis of the desired product [49].

A substantial category of bioprocesses uses bioreactors for fed-batch processes, primarily in the food and pharmaceutical industries but also, for instance, in biopolymer applications. Optimizing the production of a synthesis product, such as enzymes, penicillin, or even biomass, is one of the main obstacles in operating fed-batch reactors [49]. In a fed-batch, a semi-continuous bioreactor, the sterile substrate is provided while outflow from the fermenter is absent. The bioreactor experiences an increase in volume, resulting in the accumulation of total mass. This type of bioreactor can effectively showcase critical characteristics such as quasi-ready state, linear growth, and the utilization of alternative feed strategies [49, 50]. In addition to substrate, necessary nutrients are continuously or occasionally added to the initial medium when cultivation begins or halfway through the batch process. Fed-batch processes have been used to avoid substrates that, in high concentrations, could reduce growth rate, to get around catabolic repression, to require less initial

biomass, to get around contamination issues, and to avoid change and plasmid instability that is present in continuous culture [49, 51].

In continuous culture, a new medium is added to the batch system when the microbial growth is exponential, and the product-containing media is withdrawn. Continuous cultivation leads to balanced growth with minimal variations in nutrients, metabolites, cell counts, and biomass. Any bioreactor can use batch operating methods. However, fed-batch and continuous operation systems need to be examined by the various bioreactor types and the procedure itself. Although they require significant funds, stringent instrumentation, and control, these activities have several advantages over batch systems [49].

2.2.1 Upstream Process in Bioreactor

Bioprocesses have been employed to generate food products that meet specific quality standards for a long time. Antoni van Leeuwenhoek (1632–1723) made significant improvements to bioprocesses by introducing microbes into the manufacturing of beer and ethanol, enhancing understanding in this area [10]. The 20th century saw substantial improvements in process development, including a fed-batch process for baker yeast production and the patent for acetone and butanol production [10]. The model proposed by Monod in 1949 discusses the growth rate of microorganisms. Process measurement systems, such as spectroscopy, evolved, and industrial penicillin and glutamic acid production began in 1957. Rudolf E. Kalman's Kalman filter introduced a new approach to linear filtering and prediction problems in 1960 [10]. A successful outcome combines robust technology, outstanding initial materials, and creative process design. Developing a reliable, high-yielding upstream process is a challenging task. A complete understanding of the fundamental process principles and the underlying biological phenomena is necessary to succeed in the upstream production stage and the entire bioprocess. Upstream processing has improved significantly during the past few decades, and modern fed-batch systems can provide 10 g/L or more

of monoclonal antibodies. An improved understanding of cell cultures, which has produced better cell culture media, more sophisticated feeding techniques, stronger cell lines, and bioreactor control customized for specific processes, can explain this progress [21].

2.2.2 General features in bioreactors

- **Mixing and Shear Effects:** In bioreactors, it is essential to maintain a small amount of mixing to suspend biocatalyst and substrate particles effectively, minimize the occurrence of pH and temperature gradients, and enhance the efficiency of heat and mass transfer processes. Mixing improves nutrient and substrate transfer, eliminates inhibitory metabolites, and disrupts biofilms. Mixing can be achieved through mechanical agitation or compressed gas bubbles. High agitation has the potential to cause harm to cells, leading to their destruction, as well as the decomposition of immobilized biocatalyst pellets and the dislodgement of biofilms. Microorganisms in a state of free suspension exhibit a certain degree of tolerance towards hydrodynamic pressures. However, it is essential to note that animal cells, plant cells, microalgae, and protozoa are more vulnerable to the negative impacts of shear damage. Minimizing damage can be achieved by utilizing lower aeration velocities, larger bubble sizes, and adding protective additives [52].
- **Dissolved Oxygen:** Oxygen is crucial for the survival of animal and plant cells and many microorganisms, although some organisms are susceptible to its toxicity. The amount of oxygen required during fermentation depends

on various factors, such as the microorganism, degree of substrate oxidation, and rate of oxidation. Oxygen is generally supplied to the culture by sparging air into the broth, but this process can be challenging in highly viscous broths. Once the dissolved oxygen concentration drops below a critical level, microbial growth becomes limited, and this value differs for various microorganisms. The concentration of dissolved carbon dioxide also impacts microbial and cell growth, and too much can harm most aerobic fermentations. Carbon dioxide is added to sparging gas in animal cell cultures using a carbonate-bicarbonate system to buffer the broth. While normal mammalian cells require carbon dioxide as a substrate for the carboxylation of pyruvate to oxaloacetic acid, established cell lines may not need it [48].

The dissolved oxygen level is crucial for cellular respiration and is achieved through complete aeration in biotechnological applications. The equilibrium state with air is called 100% Dissolved Oxygen Tension (DOT), the standard unit for measuring dissolved oxygen in industrial settings. To measure dissolved oxygen tension (DOT), the electrodes must be calibrated to 100% of the air by measuring the partial pressure of oxygen in the exit air. The reading of DOT from the electrode during the process will depend on the partial pressure of oxygen inside the bioreactor [53].

- **Heat Removal and Temperature Control:** All fermentations generate heat, with up to 15 $kW \cdot m^{-3}$of the heat output from microbial activity and mechanical agitation. Temperature must be controlled to prevent damage to

the culture, typically by circulating cooling water in a jacket that surrounds the bioreactor vessel. In large-scale bioreactors, internal cooling coils are needed to regulate temperature. Another method for cooling the broth is recirculating it through an external ringlet coil. However, removing heat is challenging since the temperature of the cooling water is slightly lower than that of the broth. Depending on variables, including the surface area available for exchanging heat, the temperature differential between the broth and coolant, and the design of the bioreactor design, heat capacity may be a constraint for industrial fermentations. Maintaining a temperature of 37 ˚C during animal cell culture may need significant heat [48].

2.2.3 Batch Growth Patterns

Cell growth refers to increased cell volume and surface area resulting from chemical, biological, and physical mechanisms [54, 55]. The growth kinetics phenomenon can be described as a cell growth process dependent on cells' concentration [55, 56]. Upon injection of a liquid nutrient media with seed culture, known as inoculums, the microorganisms selectively absorb nutrients that are dissolved from the medium and transform them into biomass [20].

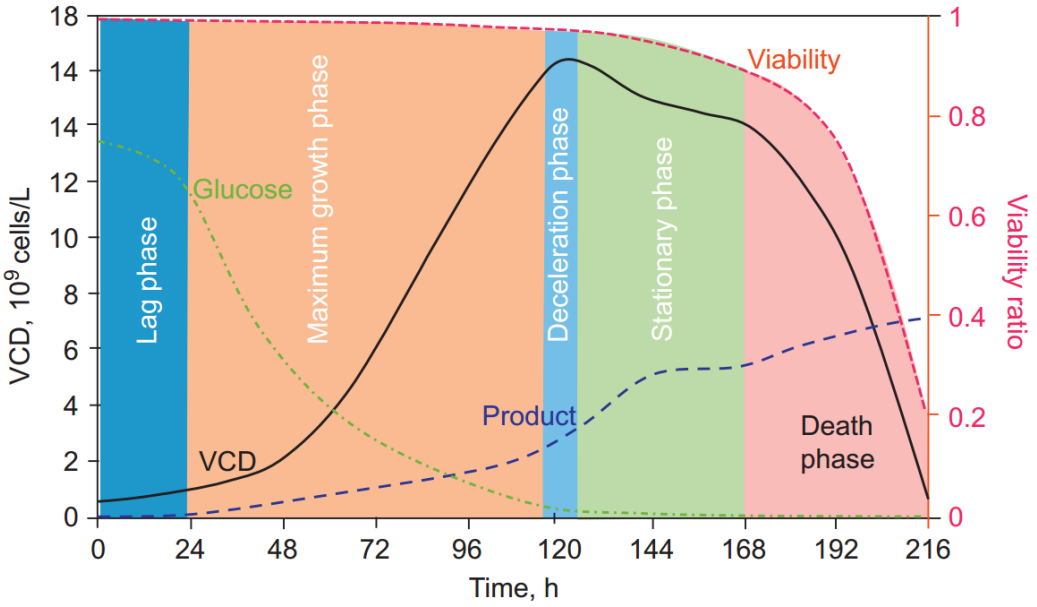

Figure 2-1. A batch growth pattern [20]**.**

A growth curve can describe the kinetics of batch growth; the standard batch growth curve comprises several phases: lag phase, logarithmic or exponential growth phase, deceleration phase, stationary phase, and death phase. The curve illustrates the growth cycle of mammalian cells in batch culture in Fig. 2.1, which is also representative of microbial cells. The primary classification of the growth phase is the cell count viable cell density (VCD) or cell biomass. However, various other metrics are also considered in the curve [20]. The lag phase is observed right after the inoculation process and represents the period in which cells adapt to a novel environment [20, 55]. Microorganisms undergo molecular reorganization upon their transfer to a different media. The synthesis of enzymes is influenced by the nutrient content, leading to the production of new enzymes and inhibition of specific existing enzymes. The internal cellular machinery also experiences adaptations in response to the changing environmental conditions. Numerous lag periods occur when the media is given many sugars; this development is known as diauxic growth [20, 55].

The Log phase characterized by the maximum growth rate is also called the exponential growth phase. During this stage, the cells become adapted to their new conditions. Following the Lag phase,

cell expansion reaches its maximum rate; consequently, cells' mass and density experience exponential growth. The Log phase is characterized by a condition of equilibrium growth, where every component of a cell encounters uniform and simultaneous growth (referred to as pseudo steady state). During this period of growth, it can be observed that the average composition of a single cell remains relatively stable. In the context of balanced growth, the net-specific growth rate remains consistent regardless of whether it is measured based on cell number or mass [20]. The exponential growth phase typically ends when a vital nutrient is depleted or metabolic by-products accumulate to a growth-inhibiting concentration. This is followed by a stationary phase, where there is no net growth, and a death phase, in which biomass is lost. The biomass growth rate in a bioreactor depends on the viable concentration of biomass at any given time and is self-catalyzing [48, 53]. Determining specific rates, such as glucose, glutamine, and amino acids, as well as metabolite synthesis rates, including ammonia, lactate, and monoclonal antibodies, are essential in evaluating and controlling the performance and management of cell culture systems. During exponential growth, the growth rate is expressed mathematically as [55]:

$$\frac{dX}{dt} = \mu X \tag{2-1}$$

X is the biomass concentration, and μ is a constant known as the *specific growth rate*. The biomass growth rate in a bioreactor relies on the level of viable biomass concentration at all times. More specifically, it depends on the rate of change in biomass concentration over time (dX/dt). It can be said that growth demonstrates a self-catalyzing or autocatalytic nature. The Equation (2-1) can be written below to show the exponential behaviour of biomass growth:

$$ln\frac{X}{X_0} = \mu t \tag{2-2}$$

X and X_0 are cell concentrations at time t and initial time t = 0, respectively.

A deceleration phase is observed as harmful components accumulate, followed by the stationary phase, which has a mortality rate equivalent to the rate of rise [55]. In the stationary phase, the net growth rate decreases to zero (indicating an absence of cell division), or the growth rate becomes equivalent to the mortality rate. Cellular metabolic activity persists in producing secondary metabolites, even when the net growth rate decreases during the stationary phase [20].

The death phase commences at the endpoint of the stationary phase due to the lack of nutrients or the buildup of toxic substances. However, it is crucial to acknowledge that certain occurrences of cellular mortality may occur either during or before the phase of stationarity, thereby posing challenges in establishing a well-defined boundary between the two stages. In certain situations, dead cells may undergo lysis, which releases internal nutrients into the surrounding environment. Living organisms can then utilize these nutrients during the stationary phase. The death phase occurs at the end of the stationary phase when nutrients are depleted, or toxic substances accumulate [20].

2.2.4 Kinetic Models

Process characterization and modelling are critical for establishing control and automation methods and improving and documenting processes. A vital component of the "quality by design" (QbD) architecture is models. The availability of more powerful computers and recent developments in understanding metabolic processes have led to the creation of highly complex upstream models for animal cells. Although the modelling of bioprocesses is still in its early stages compared to many other industries, the complexity of the process increases as the modelling becomes more challenging. One fundamental reason is that, despite continuous improvements, there still needs to be more knowledge about the complexity of living cells [21].

The following principles offer a foundational comprehension of modelling in upstream bioprocessing: non-segregated and unstructured models. Non-segregated models assume that all cells exhibit identical behaviour, thus simplifying the computational process. Unstructured models

characterize reaction rates by considering input and output variables, wherein cells are regarded as black boxes devoid of any consideration for interdependencies [21]. Mathematical models become more complex when considering environmental conditions like multi-substrate consumption, pH, temperature, rheological changes, multi-phasic variability, and nonideality of mixing and stirring [57]. The kinetic model has seen advancement from basic exponential growth to intricate mathematical formulations, allowing the prediction of cellular heterogeneity, numerous reactions, internal regulatory mechanisms, and genetic variability in bacteria [57]. A key aspect of modelling involves the consideration of either homogeneous or heterogeneous situations. A homogeneous system is associated with a singular and continuous phase in this context. Bioreactors are commonly characterized as single-liquid phases in the majority of applications.

Nevertheless, if the investigation includes the biofilm, it becomes necessary to account for a solid or semi-solid phase inside the model. In contrast, heterogeneous systems pertain to characterizing multiple continuous steps and the interplay among them. Complex heterogeneous systems can be explained by many phases: liquid, solid, semi-solid, and gaseous. An example of such a system is solid-state fermentation. By this classification, the parameters of a model can be categorized as either distributed or nondistributed (sometimes referred to as lumped). Distributed parameter models are predicated on the assumption that operational parameters exhibit spatial variation. Explaining key variables as a parameter distribution function typically involves considering one, two, or three dimensions. Consequently, the system can be characterized by a collection of partial differential equations (PDEs).

In contrast, using a lumped model becomes essential in this context, as it allows for describing the system using a collection of ordinary differential equations (ODEs). This approach is suitable due to the constancy of the parameters involved, which lack variations in space [57]. The application of ordinary differential equations (ODEs) is a popular method in computational systems biology to conduct simulations [58].

2.2.5 Unstructured Mechanistic Kinetic Growth Model

Applying a kinetic model is crucial in understanding the complex relationship between cell growth, substrate consumption, inhibitory effects, and the dynamic changes in substrate concentrations during extracellular protein synthesis. The model's representations are explained by mathematical equations within a logical framework, offering an extensive overview of the fermentation process for the given species under ideal circumstances. Furthermore, it provides an apparent separation of the cellular structure and the individual components present in a given solvent. Unstructured mechanistic kinetic growth models (UMKMs) are formulated based on conservation equations, which consider many elements such as cell mass, nutrients, metabolites, and species production and consumption rates. Most UMKMs can be classified into three categories: rate expressions for cell growth, nutrient consumption, and metabolite production [57].

The ordinary differential equation (ODE) framework represents the concentration of various organisms such as RNAs, proteins, and other species. These concentrations are described using time-dependent variables controlled by a rate equation system. This modelling approach applies to well-mixed systems that exhibit continuous kinetics, wherein the reaction rates are proportional to molecule concentration. The concept is rooted in the belief that concentrations fluctuate in a predictable and uninterrupted manner. ODE models often ignore spatial heterogeneity and stochasticity in the occurrence of biological events in contrast to stochastic approaches, which take into account individual molecules and their interactions [59]. A cellular system comprises a complex network of interconnected biochemical reactions, including various processes such as transcription, translation, dimerization, protein or mRNA degradation, enzyme-catalyzed reactions, transport, diffusion, binding or unbinding, DNA or histone methylation, histone acetylation, and phosphorylation [59].

When developing a kinetic model, several steps should be taken. Cell growth and death rates, nutrient uptake, metabolite production, and protein secretion are typically measured in mammalian

cell cultures. These rates are analyzed to determine the rate-limiting steps and to formulate hypotheses. The general equations that correctly model batch or continuous cultures of multiple mammalian cell lines have been discovered through experimental data [60].

$$\mu = \frac{dX_t}{X_v dt} \tag{2-3}$$

The main specific growth rate equation for mammalian cell cultures is Equation (2-3), used in kinetic analysis. X_t is total cell production; X_v is viable cell concentration.

Michaelis-Menten [20] kinetics models or their variations explain enzymatic reactions. The kinetic equation observed in DNA and RNA replication and manipulation is similar to the one mentioned before. However, calculating cell growth while considering all the genetic steps, metabolic pathways, and governing parameters can be daunting. Simplifying the kinetics becomes important to quantify cell growth and bioreactions. The Michaelis-Menten equation or the Monod equation can be used to express the growth and product formation rate equations for a system limited by a single substrate:

$$\mu = \frac{r_X}{X} = \frac{\mu_{max} S}{K_s + S} \tag{2-4}$$

where r_x is the generation rate, K_s is the saturation constant for the substrate, and S is the substrate concentration. Equation (2-4) shows that when the concentration of the limiting substrate is significantly higher than the substrate saturation constant ($S \gg K_S$), the specific growth rate (μ) remains constant and is equal to the maximum growth rate (μ_{max}) and cell growth is occurring at its highest rate. The change in the growth rate can be caused by variations in substrate concentration [20].

2.3 Control Strategies for Bioreactors

The synthesis of products in biotechnological manufacturing processes depends on cells, as shown in Figure 2.2 [61]. Bioreactors act as the primary unit operating in several industries, including biopharmaceuticals. The performance of each bioreactor is dependent on the functioning of billions of individual cellular reactors. Process control aims to ensure uniform manufacturing of the desired product at the designated level of quality [60]. Process dynamics influence the choice of control strategy. Process dynamics are affected by inherent process lag and variations in bioreactor volumes, which influence control strategy selection. Microbial growth produces metabolites that affect biomass, pH, and temperature. Advanced controllers based on mathematical modelling are designed to meet process targets due to nonlinear characteristics in measured variables. Supervisory systems adjust control loop tuning parameters using controller-controlled variables and available information. The successful design and implementation of control strategies necessitate utilizing a multidisciplinary approach to tackle various requirements effectively, ultimately delivering viable solutions [60].

The importance of monitoring and control systems for bioprocess optimization and malfunction detection is increasing due to industry changes. However, only some installations have implemented such procedures. The complexity of biological processes involving living organisms and nonlinear solid interactions makes off-the-shelf controllers inadequate. Variations in state variables and interactions must be considered in controller design due to microorganisms' tendency to switch metabolic pathways based on operating conditions [60]. For instance, ethanol fermentation and E. coli cultivation depend on glucose and oxygen levels. Accumulation of acetate reduces protein production. A feeding strategy can constrain microorganisms for higher protein production in these cases. Despite bioprocesses' inherent variability and unpredictability, it is possible to effectively lead

the process toward the intended trajectory and control it inside the design area by applying accurate control mechanisms [60].

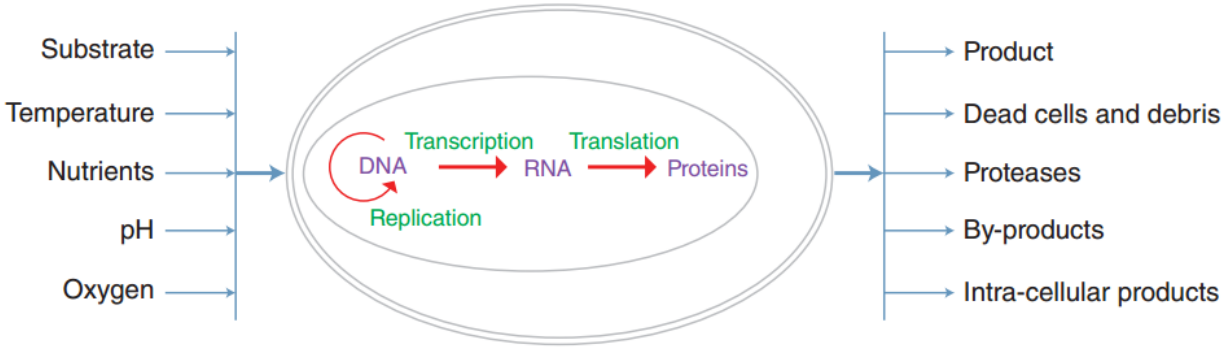

Figure 2-2. Illustration of the intricate nature of biomanufacturing (From [60]**)**

The variability in behaviour exhibited by industrial cultures of microbial and animal cells cannot be characterized as random. As previously mentioned by Sonnleitner and Fiechter (1992), discrepancies in experimental findings can mainly be attributed to improperly regulated process operations. To minimize variability, it is imperative to maintain strict control over temperature, pH, and oxygen levels [60].

A bioreactor has a complicated network of pipes, fittings, cables, and sensors and is subject to operational issues. Online monitoring and diagnosis tools now make it feasible to identify a wide range of potential process problems [49]. Monitoring key variables and parameters in bioprocesses is vital for analyzing and controlling these processes, particularly in industrial settings where measurements are restricted in availability [62].

The traditional control techniques are primarily utilized in industrial bioreactor control systems, with the control system being adapted to the specific facility [63]. The evaluation of bioreactor performance covers both productivity and product quality, which can be impacted by variations in

process variables and raw components [63]. To compute PID controller settings, the process dynamics are utilized. These dynamics can also predict the trajectory of process outputs from past inputs for future model predictive control (MPC) applications in bioreactors. While MPC technology has been primarily used in continuous processes, promising batch applications have emerged, and bioreactor applications are expected to be possible [61].

2.3.1 Proportional Integral Derivative (PID) Control

The Proportional-Integral-Derivative (PID) controller is a widely used three-term controller in the field of automatic control, with a history going back to the early 20th century [64]. The PID controller is commonly used in industries to regulate various processes effectively. Digital technology is now widely utilized, leading to a shift from traditional components in many applications. This component is present in many types of control equipment, acting either as an independent controller or as a functional unit within Programmable Logic Controllers (PLCs) and Distributed Control Systems (DCSs) [64].

The primary objective of a control system is to achieve the desired output for a specified method. The task can be completed using an open-loop control system, in which the controller establishes the input signal to the process solely based on the reference signal. On the other hand, a closed-loop control system can be employed when the controller sets the input signal to the process by calculating the output measurement [64]. Feedback control is crucial to maintain process variables despite disturbances and variations. Feedback control methodologies have had a significant impact on the field of engineering. The control system's performance can be optimized by selecting the appropriate components. The dynamics of actuators and sensors are frequently disregarded during controller design. The block diagram shown in Figure 2.3 depicts the use of various components like *P* as a process, *C* as a controller, F as a feedforward filter, r as the reference signal, e as a

control error, *u* as a manipulated variable, y as a process variable, d as load disturbance signal, and *n* as measurement noise signal as a part of a feedback control system [64].

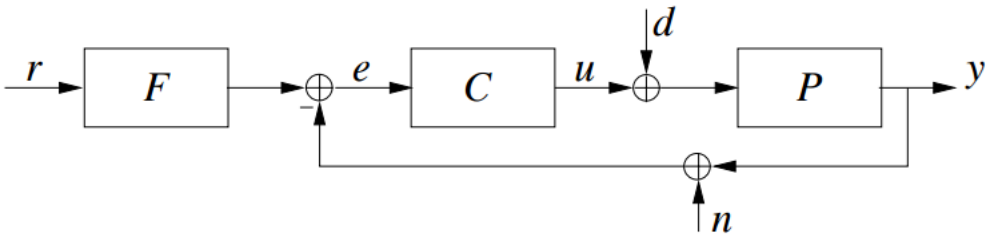

Figure 2-3. Schematic block diagram of a feedback control loop (from [64]**)**

2.4 The Three Actions of PID Control

Application of a PID control law requires the appropriate implementation of three distinct control actions, including proportional, integral, and derivative. The subsequent activities are individually described in the following parts.

Proportional Action: The proportional control action is directly proportional to the present control error, as indicated by the given statement [64]:

$$u(t) = K_p e(t) = K_p(r(t) - y(t)) \tag{2-5}$$

where K_p is the proportional gain, the typical method of increasing the control variable occurs when the control error is significant, with the appropriate sign. The transfer function of a proportional controller can be determined easily when the control error is substantial with the proper character [64]. The transfer function of a proportional controller can be derived easily as:

$$U(s) = K_p \cdot E(s) \tag{2-6}$$

Integral Action: The integral action is directly proportional to the integral of the control error:

$$u(t) = K_i \int_0^t e(\tau) d\tau \tag{2-7}$$

The variable K_i represents the integral gain. The integral action is believed to be linked to the previous values of the control error. The transfer function that corresponds to the given system is:

$$U(s) = \frac{K_i}{s} \cdot E(s) \tag{2-8}$$

Integral control, represented by the I-term in the PID controller, is employed when the controller must make up for a uniform deviation from a fixed reference signal value. Integral control is a method that addresses the limitations of proportional control by effectively reducing offset without the need for highly high controller gain [64, 65].

Derivative Action: The proportional action in control systems is determined by the present control error value, while the integral step includes the historical importance of the control error. On the other hand, the derivative action is influenced by the probable future values of the control error by considering the rate of change of the error signal, enabling the controller to anticipate and respond to upcoming changes in the system. The expression of an optimal derivative control law can be expressed as [64, 65]:

$$u(t) = K_d \frac{de(t)}{dt} \tag{2-9}$$

as K_d is the derivative gain, the corresponding controller transfer function is:

$$U(s) = K_d \cdot E(s) \tag{2-10}$$

2.4.1 Parallel PID Controllers

Integrating the proportional, integral, and derivative actions can be implemented using multiple techniques. The PID controller in its ideal or non-interacting form can be mathematically represented by the following transfer function [64, 65]:

$$U_c(s) = \left[K_p + K_i \frac{1}{s} + K_d s\right] E(s) \tag{2-11}$$

where $U_c(s)$ is controller output, and $E(s)$ is controller input error. The previously mentioned parallel or textbook formula is commonly called the decoupled PID form. The PID controller consists of three parallel channels, as illustrated in Figure 2.4. The graphic illustrates that modifying any specific coefficient, namely K_p, K_i, or K_d, alone affects the contribution size inside the corresponding term. For instance, only the magnitude of the derivative action changes if the value of K_d is altered, and this change is independent of the sizes of the proportional and integral terms. The separation of the three terms results from the parallel structure employed in the PID controller [64, 65].

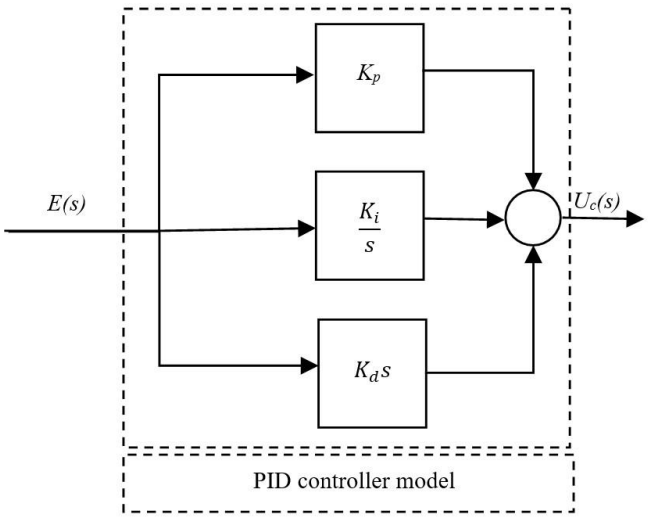

Figure 2-4. Parallel architecture for PID controller (illustrated from [65]**)**

2.5 Model Predictive Control (MPC)

The optimum control theory is the hypothetical foundation for model predictive control (MPC). To obtain the optimal control decision at any given time, MPC predicts the behaviour of the system by using dynamic models. Therefore, models are an essential part of all MPC methods. In addition to relying on a dynamic model to predict system behaviour, model predictive control (MPC) considers the system's initial state as a critical factor in determining the optimal control decision. However, accurately choosing the initial state of a dynamic system can be challenging. To address this challenge, MPC employs a second elemental concept, using past data to estimate the most probable initial state of the system. In other words, the MPC technique leverages previous measurements and the dynamic model to establish the present state value. Both regulation and estimation quandaries hinge on dynamic models and optimization, with the former generating the most efficient control action through a model-based prediction and the latter providing optimal state estimates based on previous measurements. By incorporating these approaches, MPC offers a powerful tool for optimizing control decisions in various applications [66].

In the last 20 years, industry and academia have shown great interest in advancing process control. In the 1960s, advanced control referred to any algorithm different from the traditional three-term Proportional-Integral-Derivative (PID) controller. However, in industries, 80% of feedback control devices are automated with PID. They are essential for ensuring quality products, safe processes, and economic efficiency [67]. Other self-tuning controllers, such as Minimum Variance, generalized Minimum Variance, Pole Placement, and Model Predictive Control, have been developed to handle dead time and non-minimum phase systems. Model Predictive Control is widely accepted in the industry and modifies generalized Minimum Variance [67].

The following studies on MPC presented at the Chemical Process Control (CPC) conference (1996) are an excellent starting point for MPC technology. Qin and Badgwell compare algorithms of

industrial MPC, which is useful for practitioners [68]. MPC was introduced as a field of control by Chen and Allgower [69, 70] with a particular focus on nonlinear control. They also discussed estimation of moving horizon, which is the dual of MPC. Morari and Lec [70] provided a detailed analysis of MPC's theoretical basis and practical applications, including progress and remaining challenges for nonlinear systems. These resources can be valuable for researchers and practitioners seeking a deeper understanding of MPC and its applications [71].

2.5.1 Definition and Strategy of Model Predictive

Model predictive control (MPC), or receding or moving horizon control, is a regulation method that the model predicts the future impact of manipulated variables on output. To obtain a control signal, it minimizes a cost function that reflects the desired control objectives while adhering to system constraints. The effectiveness of the controller depends on the accuracy of the input-output model used to design it, which must precisely capture the system's dynamics. Therefore, MPC involves an iterative model refinement process, control design, and performance evaluation to ensure optimal control under varying operating conditions [67].

Model Predictive Control, or MPC, typically encompasses the following three concepts:

1) Employing a model to forecast the process output in the future,
2) computing a control sequence to optimize a performance index,
3) utilizing a receding horizon strategy, the horizon is continuously shifted towards the future, and the first control signal of the calculated sequence is executed at each step.

The approach of the MPC methodology is identified by the plan illustrated in Figure 2.5 [72]:

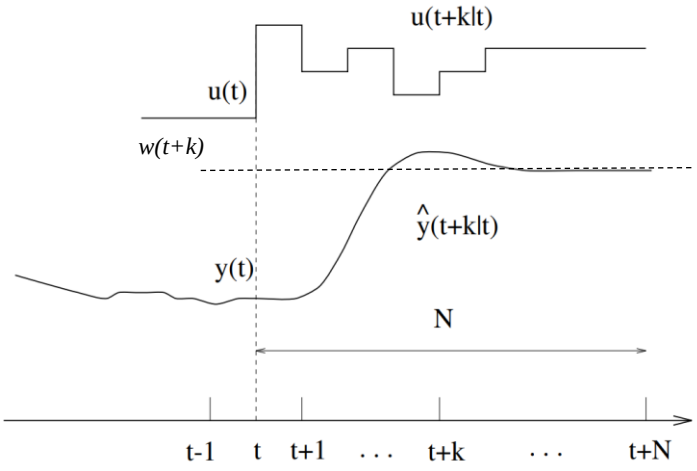

Figure 2-5. MPC strategy (Copied from Camacho and Bordons, 1999 [72]**)**

1) To predict future outputs for a given period, called the prediction horizon *N*, a process model is used at each instant *t*. *u(t)* is the input variable at instant *t*; it denotes the measure the controller takes at instant t to lead the system toward a desired state or setpoint. *y(t)* refers to output variables at instant *t*, and it stands for the quantifiable reaction of the system to the control input u(t) at instant t. These predictions for outputs $y(t+k|t)$[1] for each value of $k = 1 \ldots N$ depends on both past inputs and outputs up to *t*, as well as future control signals (as the input for t+k) $u(t+k|t)$, $k = 1 \ldots N-1$, which will be calculated and applied to the system [70, 72].
2) Determining the future control signals involves optimizing a specific criterion to maintain the process near the reference trajectory. The reference trajectory, *w(t+k)*, can be the setpoint or a close approximation of it. Typically, the

[1] This notation denotes the variable's value at time $t + k$, computed at time t.

criterion is a quadratic function considering the predicted output signal and reference trajectory errors. Additionally, the control effort is usually included in the objective function. An explicit solution can be found in the linear model; the criterion is quadratic, and there are no constraints. However, an iterative optimization method must be used if there are constraints, or the model is nonlinear. Sometimes, assumptions are made about the future control law's structure, such as constant from a particular time.

3) The process receives the control signal, $u\ (t|t)$, while the subsequently calculated control signals are discarded. This is because $y\ (t+1)$ is already known at the next sampling moment, and the first step is repeated with this new information, updating all the sequences. This approach, known as the receding horizon concept, allows the calculation of $u\ (t+1|t+1)$, which may differ from $u\ (t+1|t)$ due to the new information available [70, 72].

The fundamental framework presented in Figure 2.6 is utilized to implement this strategy. The plant uses a model that forecasts future production outcomes based on prior and current values alongside the recommended optimal future control actions. The optimizer calculates these actions while considering the cost function, which considers future tracking errors and constraints. As a result, in the controller, the process model plays a critical role. The model chosen should be able to understand the process dynamics accurately to predict the future outputs precisely, and it should be simple to execute and comprehend. Since MPC is not a singular technique but a range of different methodologies, several models are employed in various formulations [72].

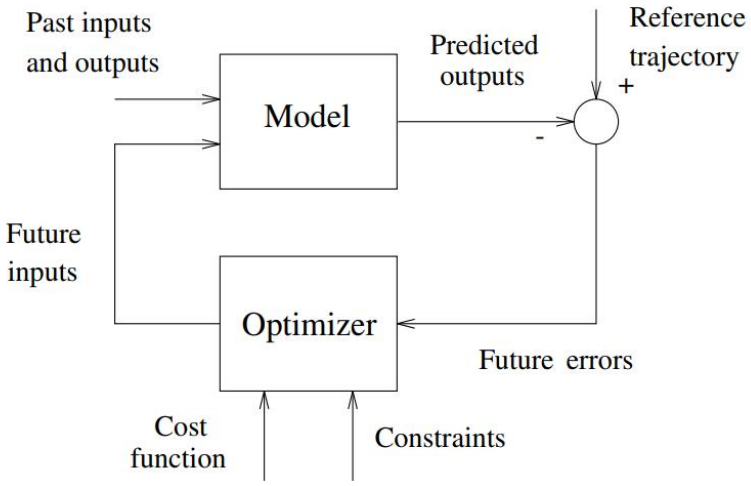

Figure 2-6. The basic structure of MPC (Copied from Camacho and Bordons, 1999 [72]**)**

The strategy relies on the optimizer to provide control actions. When the cost function takes on a quadratic form, the minimum can be calculated using a linear function considering prior inputs and outputs in addition to the future reference trajectory. However, if inequality constraints are present, numerical algorithms are required to find the solution, which can be computationally taxing. The complexity of the optimization problem is determined by quantity of variables and prediction horizons involved, and it is typically a relatively straightforward matter that does not necessitate advanced computer coding. However, in constrained and robust scenarios, the computational time required can substantially exceed that of unconstrained cases, and the applicability of constrained MPC to various processes is notably constrained [70, 72].

2.5.2 MPC Design and Implementation

Model predictive control systems rely on the plant's mathematical model for their design. The chosen model for the control system is typically a state-space model. This model type represents the information necessary for predicting future outcomes by using the state variable at the present

moment [73]. With relative ease, the model predictive control (MPC) methodology can be initially developed for single-input and single-output (SISO) systems in discrete time conditions. This methodology can also be extended to multi-input and multi-output (MIMO) systems.

2.5.2.1 General Formulation of the Model

It is assumed that independent control of each measured output with zero steady-state errors cannot be achieved if the number of outputs exceeds the number of inputs (i.e., q > m) in a plant with n_1 states, m inputs, and q outputs, where number of outputs are not greater than number of inputs. The general predictive control problem formulation also accounts for plant noise and disturbance [72, 74].

$$x_m(t+1) = A_m x_m(t) + B_m u(t) + B_d \omega(t) \quad (2\text{-}13)$$

$$y(t) = C_m x_m(t) \quad (2\text{-}14)$$

where u is the manipulated input variable, y is the output of the process; and the vector x_m is the state variable, and it is assumed to have a dimension of n_1. It should be noted that the input for this plant model is u(t). $\mathbf{A_m}$ describes how the state of the system evolves over time in the absence of inputs or disturbances, and $\mathbf{B_m}$ describes how the system inputs affect the state of the system, $\mathbf{C_m}$ describes how the state of the system is related to the outputs of the system are the system matrices, $\mathbf{B_d}$ describes how the system disturbances affect the state of the system. $\mathbf{A_m}$, $\mathbf{B_m}$, $\mathbf{C_m}$ are system matrices that are arranged in the state-space equation. As a result, the model must be modified to fit the design objectives, which involve incorporating an integrator. The input disturbance at time t, denoted as ω(t), represents the integration of white noise. This means that it is connected to a white noise sequence, denoted as $\epsilon(t)$, with zero mean, through the difference equation [72, 74]:

$$\omega(t) - \omega(t-1) = \epsilon(t) \quad (2\text{-}15)$$

It is important to note that equation (2-13) also implies equation (2-16):

$$x_m(t) = A_m x_m(t-1) + B_m u(t-1) + B_d \omega(t-1) \tag{2-16}$$

To relate the state variable $\Delta x_m(t)$ to the output y(k), the difference equation

$$\Delta y(t+1) = C_m \Delta x_m(t+1) = C_m A_m \Delta x_m(t) + C_m B_m \Delta u(t) + C_m B_d \epsilon(t) \tag{2-17}$$

can be deduced by subtracting equation from (2-13), where:

$$\Delta x_m(t) = x_m(t) - x_m(t-1) \tag{2-18}$$

$$\Delta u(t) = u(t) - u(t-1) \tag{2-19}$$

$$\Delta y(t+1) = y(t+1) - y(t) \tag{2-20}$$

$\Delta u(t)$ likely refers to a change in the input at time t, relative to some reference value. The process of connecting $\Delta x_m(t)$ to the output y(t) involves defining a new set of state variables that capture the connection between the input and output. This is typically done by defining a new state variable vector that includes the original state variables as well as additional variables that describe the input-output relationship.

$$x(t) = [\Delta x_m(t)^T \; y(t)]^T \tag{2-21}$$

The superscript $^{\mathbf{T}}$ is matrix transpose. By considering:

$$\begin{aligned} \Delta y(t+1) &= C_m(\Delta x_m(t+1) - \Delta x_m(t)) = C_m \Delta x_m(t+1) \\ &= C_m A_m \Delta x(t) + C_m B_m \Delta u(t) \end{aligned} \tag{2-22}$$

Combining equations (2-21) and (2-22) results in the subsequent state-space representation:

$$\underbrace{\begin{bmatrix}\Delta x_m(t+1)\\ y(t+1)\end{bmatrix}}_{x(t+1)} = \underbrace{\begin{bmatrix}A_m & O_m^T\\ C_m A_m & 1\end{bmatrix}}_{\mathrm{A}} \underbrace{\begin{bmatrix}\Delta x_m(t)\\ y(t)\end{bmatrix}}_{x(t)} + \underbrace{\begin{bmatrix}B_m\\ C_m B_m\end{bmatrix}}_{\mathrm{B}} \Delta u(t) \tag{2-23}$$

$$y(t) = \overbrace{[0_m \quad 1]}^{\mathrm{C}} \begin{bmatrix}\Delta x_m(t)\\ y(t)\end{bmatrix}$$

Where 0_m is zero matrices and (**A**, **B**, **C**) is called the augmented model that is used to design predictive control.

2.5.3 Prediction of State and Output Variables in MPC

The subsequent stage in development of predictive control comes after the formulation of mathematical model is predicting output of plant from consideration of the future control signal as a variable that is adjustable within a specific optimization window. This window is examined in detail, assuming the present time is t and the optimization window is N_p samples. Initially, single-input and single-output (SISO) systems are considered before extending to multi-input and multi-output (MIMO) systems [72, 74].

Availability of state variable vector x(t) by measurement, it offers up-to-date information about the present state of the plant. The trajectory of future control is indicated by:

$$\Delta u(t), \Delta u(t+1), \ldots, \Delta u(t+N_C+1),$$

where N_c is the control horizon determines the quantity of parameters employed to represent the future control path, and predictions are made for the future state variable accordingly, where N_p is the prediction horizon and the optimization window's length. The forecasted output variables are

expressed using the available current state variable information x(t) in conjunction with the future control action Δu(t +j), where j = 0, 1, . . . N_c−1 [72, 74].

Define vectors:

$$Y = \left[y(t+1|t), y(t+2|t), y(t+3|t), \ldots y\left(t+N_p\middle|t\right)\right]^T \quad (2\text{-}24)$$

$$\Delta U = [\Delta u(t), \Delta u(t+1), \Delta u(t+2), \ldots \Delta u(t+N_c-1)\ ]^T \quad (2\text{-}25)$$

Utilizing the state-space model (A, B, C) as a basis, the future state variables are computed step using the step by step employing the set of upcoming parameters and from the predicted variables, the predicted output variables are y. The compact form of predicted output variables with accordance of equations (2-21) and (2-24), and (2-25) will be:

$$Y = Fx(t) + \Phi\Delta U \quad (2\text{-}26)$$

Where F is the state prediction matrix and Φ is the input prediction matrix, the vector can be shown below:

$$F = \begin{bmatrix} CA \\ CA^2 \\ CA^3 \\ \vdots \\ CA^{N_p} \end{bmatrix}; \Phi = \begin{bmatrix} CB & 0 & 0 & \ldots & 0 \\ CAB & CB & 0 & \ldots & 0 \\ CA^2B & CAB & CB & \ldots & 0 \\ \vdots & & & & \\ CA^{N_p-1}B & CA^{N_p-2}B & CA^{N_p-3}B & \ldots & CA^{N_p-N_c}B \end{bmatrix}$$

The goal of a control prediction is to minimize the error between the setpoint signal r(t) at time t and the predicted output in the prediction horizon, assuming the set-point signal remains constant. This is achieved by finding the optimal control parameter vector, ΔU, through an error minimization design. The setpoint information is assumed to be included in a data vector [75]. R_S^T the transpose of the matrix that is a data vector which contains the set-point information, with a matrix size of N_p×1. Each element of the matrix $\mathbf{R}_s$ equals the set-point signal r(t) at the corresponding sample time t within the prediction horizon of length N_p. The matrix $\mathbf{R}_s$ is constructed by stacking N_p copies of the set-point signal r(t) on top of each other.

$$R_S^T = [1\ 1 \ldots 1]r(t),$$

Representation of the control objective is the cost function J, is defined as follows [75]:

$$J = (R_s - Y)^T (R_s - Y) + \Delta U^T \bar{R} \Delta U \quad (2\text{-}27)$$

The first term in the equation (2-27) is focused on reducing the errors between the predicted output Y and the set-point signal $\mathbf{R}_S$, while the second term takes into account the magnitude of ΔU in order to minimize the objective function J. $\bar{R} = r_w I_{Nc \times Nc}$ (where $r_w \geq 0$), which acts as a tuning parameter for the desired performance of the closed-loop. When $r_w = 0$, the cost function (2-27) prioritizes minimizing the error $(R_s - Y)^T(R_s - Y)$ without considering the magnitude of ΔU. Conversely, a large r_w value means that the cost function will prioritize reducing the error $(R_s - Y)^T(R_s - Y)$ while carefully considering the magnitude of ΔU. The optimal ΔU for minimizing J can be found using this equation that is obtained from equation (2-26). This allows us to determine the control signal's ideal solution as:

$$\Delta U = (\Phi^T \Phi + \bar{R})^{-1} \Phi^T (R_s - Fx(t)) \quad (2\text{-}28)$$

Φ is the input prediction matrix, and $(\Phi^T \Phi + \bar{R})^{-1}$ is the Hessian matrix in the optimization literature because it is crucial in determining the optimal values of the regression coefficients in ridge regression. the Hessian matrix is a matrix of second partial derivatives of a function, and it can be used to determine whether a critical point of the function is a maximum, or minimum [76]. With the aim of optimizing a given set-point signal r(t) within a prediction horizon. The objective is to bring the predicted output as close as possible to the set-point signal by finding the 'best' control parameter vector ΔU. The set-point signal r(t) and the state variable x(t) are connected to the control signal's optimal solution by the following equation [75]:

$$\Delta U = (\Phi^T \Phi + \bar{R})^{-1} \Phi^T (R_s r(t) - Fx(t)) \quad (2\text{-}29)$$

2.5.4 State estimation:

In MPC, the system frequently receives a reference trajectory, and the controller uses this trajectory to provide control inputs that move the system in the direction of the desired state. State estimation

is crucial to MPC because it gives the controller the up-to-date state data required to match the reference trajectory precisely. Particle filters, Extended Kalman filters, and Kalman filters are a few of the methods used in MPC for state estimation. These techniques calculate the system's current state using measurements of its inputs and outputs as well as a mathematical model of the system. The effectiveness of MPC depends on how accurate state estimation is. The controller may not produce control inputs that result in the expected system behavior if the state estimation is off. In order to build the MPC controller to be robust to estimate mistakes, it is crucial to choose the proper state estimation approach carefully.

The state estimation problem involves estimating hidden variables using a noisy set of observations in an optimal way. This can be seen as a probabilistic inference problem, which is solved using the recursive Bayesian estimation algorithm. For linear Gaussian systems, the optimal solution is the Kalman Filter. For non-linear and non-Gaussian systems, sub-optimal approximated solutions must be used, such as the EKF algorithm or the more recent UKF. The UKF uses the Unscented Transformation and sigma points to approximate probability distributions without the need for Jacobians. The UKF has a similar structure to the EKF but is more suitable for strong nonlinearities. This work focuses on the UKF formulation with an assumption of additive noise with zero mean [77].

2.5.5 Literature Review of Control Strategies

Jabarivelisdeh et al. [26] introduced an adaptive control approach for bioprocesses, concentrating on dynamic flux balance models in their study. It employs a model predictive control (MPC) framework and a real-time moving horizon estimation algorithm to mitigate model uncertainties. The approach maximizes the productivity of a target metabolite under microaerobic conditions by dynamically adjusting oxygen-limitation online. The research emphasizes the efficacy of constraint-based approaches in bioprocess optimization but acknowledges model uncertainties and

biological variability. The adaptive MPC effectively manages various biological states and uncertainties during the bioprocess. The study suggests the adaptability of the deFBA-based control scheme for diverse bioprocesses with dynamic system behavior. The approach is flexible in accomplishing engineering objectives through temporal manipulations of metabolism while managing process uncertainties.

Siegwart et al. [22] employed investigation on fed-batch cultures to examine the metabolism of HEK-293 cells. An adaptive nonlinear controller was employed to regulate the glucose concentration at a level of 1 mM. The concentration was measured every 30 minutes using an FIA biosensor system. The controller demonstrated outstanding performance over a wide range of cell concentrations without requiring adjustment. By keeping glucose concentration at a low level, the production of lactate and the rates of glycolysis were lowered. The study delineated many metabolic phases, encompassing glucose uptake, lactate production, and rates of growth. The program exhibited excellent control performance across all cellular states, effectively adjusting to various cell line cultures and demonstrating strong scalability. The study further discovered a self-regulatory mechanism that leads to a reduction in glycolysis when cell densities surpass 1×10^6 cells/mL.

Pachauri et al. [78] prioritized attaining accurate temperature regulation and the necessary level of product excellence in a given procedure. The authors suggest a new control technique that integrates fractional mathematics with IMC-PID, leading to the development of a fractional-order IMC-PID controller. The controller is enhanced (MFOIMC-PID) by integrating an extra control loop to minimize offset error. The controller's design parameters are optimized by utilizing a water cycle algorithm, resulting in the creation of a WMFOIMC-PID controller. The paper incorporates a comparative analysis including fractional order PID (FOPID) and regular PID controllers. The simulation results indicate that the WMFOIMC-PID controller outperforms the other controllers in terms of performance. It achieves a reduction in Integral Absolute Error (IAE)

of 57% and 72% compared to the FOPID and PID controllers, respectively, for set-point tracking, disturbance rejection, and noise reduction. The results indicate that the WMFOIMC-PID controller has superior resilience and effectiveness in achieving accurate temperature regulation in the examined procedure.

Craven et al. [24] investigate the utilization of a non-linear model predictive controller (NMPC) to improve product quality, maintain consistent results between batches, and produce substantial cost savings in a Chinese hamster ovary (CHO) mammalian cell fed-batch process. A nonlinear model was created to simulate the CHO mammalian cell fed-batch bioprocess. This model helps in configuring and adjusting the NMPC through offline simulation. Afterwards, the optimized Nonlinear Model Predictive Control (NMPC) algorithm was used on a 15 L pilot-plant bioreactor to regulate the glucose concentration at a predetermined target value. Conventional bioprocesses have significant gaps between measuring key process parameters (CPP), but advancements in Process Analytical Technology (PAT) have enabled more frequent assessment of CPP. This work utilized in situ Kaiser RXN2 Raman spectroscopy to continuously monitor glucose levels at frequent intervals of 6 minutes. Although faced with difficulties such as significant process variability, measurement noise, and lengthy measurement intervals, the NMPC successfully achieved closed-loop fixed set-point control in the examined bioprocess.

The employed control strategies entail in previous investigations are a combination of one or two distinct control methods, thereby introducing heightened intricacy to the bioprocess control system. This complexity is particularly relevant in the context of developing an Adeno-Associated Virus (AAV) production system, which currently utilizes a conventional Proportional-Integral-Derivative (PID) controller. The forthcoming chapter will delve into a detailed discussion of the methodology employed in this study.

Chapter 3

Methodology and Model Framework

This chapter presents a mathematical model describing the bioprocess occurring in a bioreactor that produces Recombinant Adeno-Associated Virus rAAV. To ensure optimal growth rates, the dissolved oxygen (DO) and temperature in the bioreactor are controlled using an oxygen sparger and heating jacket. By handling these environmental conditions, the low rAAV production rate and growth rate can be eliminated. The ordinary differential equations (ODEs) describing the bioreactor dynamics, DO, and temperature have been developed into a controller design. The control objectives and intricacies of the controller design are explained in detail in the following terms.

3.1 Mathematical Modelling

As mentioned in section 2.2, there are three different modes for bioreactor operation [49]:

- *Batch*, which is no additional feeding implemented during all process stages.
- *Fed-batch*, the utilization of substrate and supplements in the process of feeding, has the potential to extend the culture duration, leading to increased cell densities or a shift in metabolic activity towards the production of a specific protein, such as a recombinant protein.
- In microbiology, it is possible to maintain a consistent state in microbial cultures through *continuous culture* methods such as a chemostat or turbidostat. A chemostat regulates cell density by controlling the feed rate of a growth-limiting substance, while a turbidostat uses cell density to determine the feed rate of the substrate. Another option is cell retention,

which can be highly productive through perfusion. A balanced feeding system can be achieved by matching the incoming feed rate with the rate of removal of harvest. This allows for a stable state lasting for days to months, making it an ideal environment for studying microbial metabolism and long-term production.

This thesis aims to model the batch bioreactor on a laboratory scale. Therefore, the discussions in the continuation of the work have mainly focused on batch systems. However, to ensure that the overall scope of the work is maintained, we have made an effort to generalize the model presented for batch systems so that it can also accurately describe fed-batch methods.

Initially, the growth stages are reviewed in cellular and bacterial cultures. Afterwards, the mathematical representation of the system is described. Figure 3.1 illustrates the typical growth curve observed in a batch culture. This system exhibits multiple growth stages, which can be listed as follows: 1) lag phase, 2) logarithmic or exponential growth phase, 3) stationary phase, and 4) death phase.

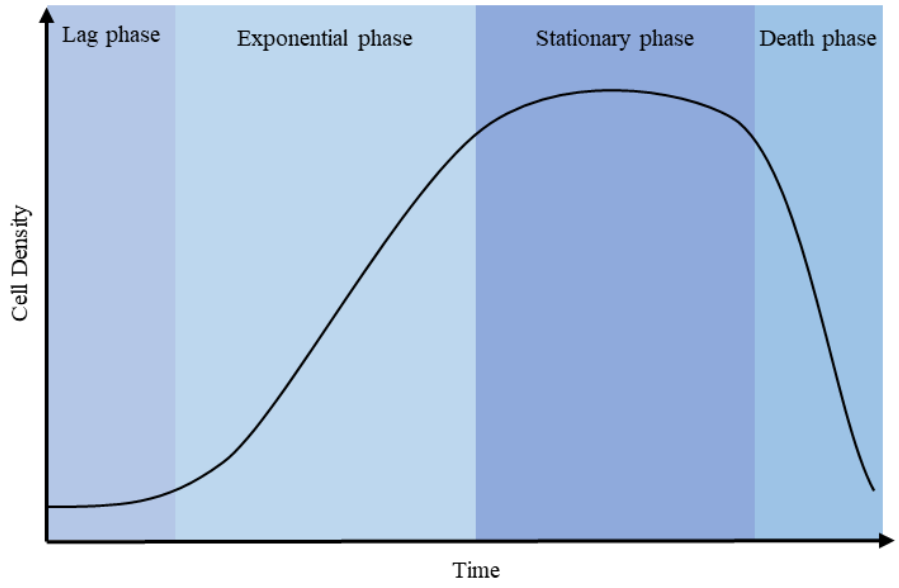

Figure 3-1. Cell growth pattern

This figure shows the different stages of cellular growth and their basic characteristics. However, it is essential to remember that this is a simplified representation, and the actual processes may differ.

The growth of a culture begins with a lag phase followed by an exponential growth phase marked by a rapid increase in biomass concentration. The process will continue until all nutrients have been eaten and the growth enters the stationary phase. In batch execution, an initial addition of essential nutrients is made at elevated concentrations to ensure that the growth rate remains unaffected by substrate availability. The biomass concentration exhibits an early period of inactivity, followed by an exponential expansion until the growth rate is diminished due to low substrate concentrations. As mentioned earlier, the phenomenon will decelerate the rate of biomass concentration growth until it reaches a state of equilibrium. Without supplementary nutrients, the culture will undergo a death phase, resulting in a decline in viable cell concentration and ultimately leading to biomass reduction. In batch culture, only specific compounds are introduced to regulate pH, dissolved oxygen, and foaming.

3.1.1 Bioreactor Modelling

To accurately represent species concentration, particularly in cell growth, employing a framework involving nonlinear ordinary differential equations (ODEs) is necessary. Although the general form of these ODEs is similar in different biological processes, modifying the models is crucial to achieve the desired output. Critical environmental factors such as pH, temperature, and dissolved oxygen (DO) must be controlled to achieve a high cell concentration. When it comes to modelling cell growth and microbial fermentation, there is a significant difference in the complexity of the cell media. The substance that limits microbial growth is often a carbon source, such as sugar. However, the medium can contain diverse components consumed to produce a specific cell type in cell culture. As a result, it is challenging to identify a single limiting substance and create a mathematical representation.

The maximum growth phase, also known as the exponential or logarithmic growth phase, is a period of balanced growth where all cell components grow at the same rate, ensuring a constant average composition of a single cell. In balanced growth, cells' net specific growth rate remains constant, whether measured by number or mass. This consistent rate allows for developing a phenomenological model that explains the exponential growth phase [79]:

$$\frac{dX}{dt} = \mu X \tag{3-1}$$

Based on Equation (3-1), the Malthus growth model states that biomass concentration changes with biomass generation, and the mass balance equation can be integrated to determine biomass generation rates with an exponential expression (3-2b):

$$ln\frac{X}{X_0} = \mu t \tag{3-2a}$$

$$X = X_0 e^{\mu t} \tag{3-2b}$$

where X_0 is the initial biomass concentration or cell at time $t = t_0 = 0$, as shown in Figure 3.1, exponential growth represents the number of cells doubled during each fixed time interval using the definition of derivative for Equation (3-2a):

$$t_d = \frac{ln\,2}{\mu} \tag{3-3a}$$

or

$$\mu = \frac{ln\,2}{t_d} \tag{3-3b}$$

The doubling time t_d refers to the time it takes for a new cell generation to emerge during an exponential growth period [79].

It is important to note that the bioreactor has additional components that impact the specific growth rate μ. The main nutrients, namely glucose (Glc), glutamine (Gln), lactate (Lac), ammonium (Amm), and recombinant adeno-associated virus (rAAV), influence the specific growth rates. The increase in cell concentration is proportional to the consumption or production of these components. Therefore, the following relationship can be employed to determine the substrate concentration in batch systems:

$$\frac{dS}{dt} = -\frac{\mu}{Y_{S/X}}X \tag{3-4}$$

S is the substrate concentration, and $Y_{S/X}$ .The yield coefficient means the ratio of the mass of cells formed to the mass of substrate consumed. In order to formulate an ordinary differential equation for each substrate, appropriate Ys/x values are determined and incorporated into the current set of differential equations. If studying a fed-batch setup in which substrate is continuously introduced into the reactor, the correlation mentioned above is rephrased as follows:

$$\frac{dS}{dt} = \frac{F}{V}(S_i - S) - \frac{\mu}{Y_{S/X}}X \tag{3-5}$$

S_i[2] is the inlet flow of substrate concentration, F is the inlet flow, and V is the current volume. In a fed-batch system, the rate of cell concentration can be shown by this Equation (3-5):

$$\frac{dX}{dt} = \left(\mu - \frac{F}{V}\right) X \tag{3-6}$$

In order to assess the influence of environmental conditions on cell concentration in a bioreactor, it is imperative to acknowledge that each of these characteristics impacts the specific growth rate:

$$\mu(S, pH, T, DOT) = \mu_{max}.f(S).f(pH).f(T).f(DOT) \tag{3-7}$$

The function f(x) is defined in the range of values between zero and one and characterizes the impact of the variable x on the growth rate. The Monod Equation as mentioned in Chapter 2 is frequently employed in modelling such systems, focusing exclusively on the correlation between growth rate and substrate concentration. The discussed Equation is as follows:

$$\mu(S) = \mu_{max}.f(S) = \mu_{max}\frac{S}{S + K_S} \tag{3-8}$$

[2]Andis i represents the word inlet for S_i

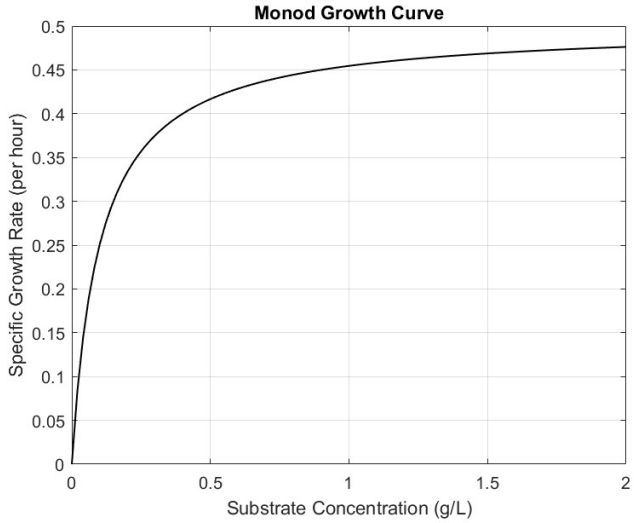

Figure 3-2. Illustration of the Monod function. The following parameters are used K_S =0.5 and μ_{max} = 1. Note that S = K_S gives μ= 0.5 μ_{max}

In the Monod Equation μ_{max} is the maximum growth rate, *S* is the substrate concentration, and K_S is half saturation constant, which is the substrate concentration at $\mu = \frac{1}{2}\mu_{max}$. By modification of the Monod Equation, the new relation can be written [80]:

$$\mu(S, pH, T, DOT) = \mu_{max} \frac{S}{S + K_S} . f(pH) . f(T) . f(DOT) \quad (3\text{-}9)$$

The above functions are linked to the specific growth rate that will be further expanded. The present study investigated the impact of Dissolved Oxygen Tension (DOT) and temperature on AAV production, as these factors have been identified as potential inhibitors. In order to simplify the model, the pH level in the bioreactor was maintained at a constant level.

- pH

  It has been observed that mammalian cell lines tend to flourish when grown at a pH of 7.4, regardless of the strain. Nevertheless, certain modified cell lines exhibit better growth in slightly acidic conditions, ranging from pH

7.0 to 7.4. In contrast, native fibroblast cell lines prefer slightly alkaline environments, with a pH between 7.4 and 7.7 [55]. The pH of this thesis was regulated at a value of 7.2 with the implementation of a control loop that involved CO_2 overlay and the injection of sodium bicarbonate [4].

$$f(pH) = \begin{cases} -(pH_{max} - pH)(pH_{min} - pH) \; if \;\; pH_{min} \leq pH \leq pH_{max} \\ 0 \; else \end{cases} \quad (3\text{-}10)$$

- Temperature

  The temperature range is more difficult to determine because the cells are more tolerant of low temperatures. Different bioprocesses can be classified by the thermal behaviour, psychophiles (T_{opt} < 20˚C), mesophiles (T_{opt} = from 20˚C to 50˚C), and thermophiles (T_{opt} > 50˚C). When the temperature drops to 30°C or lower, growth stops because 37°C is the ideal temperature for growth in this system. The upper limit is set at maximum to achieve a symmetrical second-order polynomial. The constant 1/49 is utilized to scale the maximum function value to 1. The operation temperature of the bioreactor was set at 37°C [53, 80].

$$f(T) = \begin{cases} -\frac{1}{49}(T_{max} - T)(T_{min} - T) \; if \;\; T_{min} \leq T \leq T_{max} \\ 0 \; else \end{cases} \quad (3\text{-}11)$$

  For describing the effects of suboptimal temperatures or pH in microorganisms Ratkowsky et al. (1982) proposed a simple empirical model for specific growth rate. After fitting the model with the experimental data, data were transformed using the square root to stabilize their variability. This model and all its other modifications account for the most

significant group of secondary models in the field of microbiology prediction [80, 81].

- DOT

  The dissolved oxygen tension (DOT) function can be expressed using a Monod function, similar to the substrate function. This is because the level of DOT does not restrict cell growth until it reaches below the critical concentration level of DOT [20]. Beyond this concentration, no significant inhibitory effects are noticeable. Thus, the DOT function Moreover, it should be noted that there are no observable inhibitory effects beyond this particular concentration. Therefore, the definition of the DOT function is as follows:

$$f(DOT) = \frac{DOT}{DOT + K_{DOT}} \tag{3-12}$$

where K_{DOT} is approximately 6, which is the DOT concentration at which the specific growth rate is half of μ_{max} when all other environmental parameters are equal to 1.

3.1.2 Temperature Modelling

Controlling the bioreactor's temperature can lead to an increase in the growth rate. Figure 3.3 illustrates how temperature affects the growth rate according to Equation (3-11). The growth rate decreases as the bioreactor's temperature deviates from its optimal value. Typically, to control the temperature in bioreactors, they are equipped with a cooling jacket. Modifying the bioreactor with a cooling jacket allows for maintaining its temperature near its desired range by adjusting the cooling fluid flow rate within the jacket when the bioreactor's temperature increases.

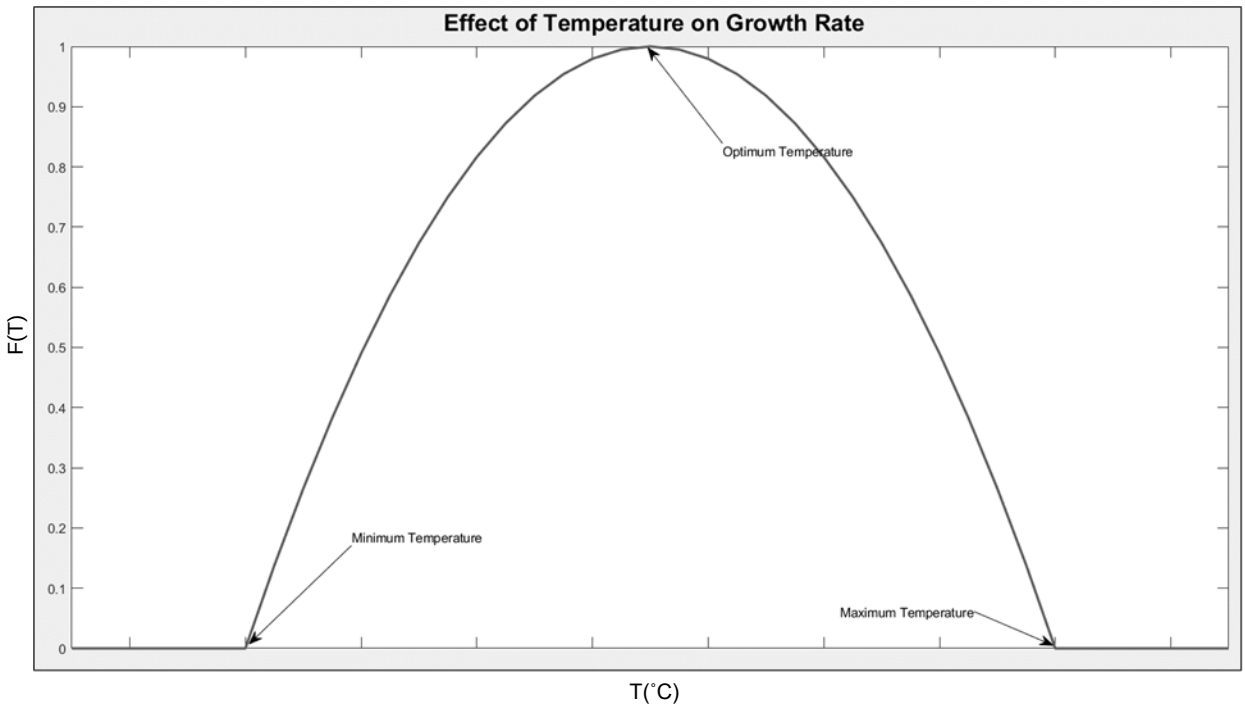

Figure 3-3 Effect of temperature on growth rate

In order to properly analyze the bioreactor and cooling jacket, it is crucial to consider their dynamics and describe the system using a series of differential equations. The ODE can be achieved by applying an energy balance to the bioreactor and the jacket, yielding the following relationships [23]:

$$\begin{bmatrix} heat \\ in \end{bmatrix} \begin{bmatrix} accumulated \\ reactor \end{bmatrix} = \begin{bmatrix} heat \\ inlet \end{bmatrix} \begin{bmatrix} of \\ flow \end{bmatrix} - \begin{bmatrix} heat \\ outlet \end{bmatrix} \begin{bmatrix} of \\ flow \end{bmatrix} + \begin{bmatrix} heat \\ from \end{bmatrix} \begin{bmatrix} generated \\ reaction \end{bmatrix} + \begin{bmatrix} heat \\ to\ the \end{bmatrix} \begin{bmatrix} transferred \\ jacket \end{bmatrix} \quad (3\text{-}13)$$

Each of the mentioned terms in the recent Equation (3-13) is calculated as follows, and all parameters that are going to be mentioned in Equations from (3-14) to (3-19) are listed below [23]:

T_{in} = temperature of the substrate entering reactor
$F_i = flow\ of\ the\ substrate\ entering\ reactor$
$F_e = outlet\ flow\ from\ reactor$

$r_{O2} = rate\ of\ oxygen\ consumption$
$\Delta H_r = heat\ of\ reaction\ in\ fermentation\ (\Delta H_r)$
$\rho_r = density\ of\ the\ mass\ of\ reaction$
$C_{heat,r} = heat\ capacity\ of\ the\ mass\ of\ reaction$
$K_T = heat\ transfer\ coefficient$
$A_T = heat\ transfer\ area$
$T_{ag} = temperature\ of\ cooling\ agent\ in\ the\ jacket$
$V = volume\ of\ mass\ of\ reaction$
$F_{ag} = flow\ of\ cooling\ agent$
$V_j = volume\ of\ the\ jacket$
$T_{in,ag} = temperature\ of\ the\ cooling\ agent\ entering\ the\ jacket$
$\rho_{ag} = density\ of\ the\ cooling\ agent$
$C_{heat,ag} = heat\ capacity\ of\ cooling\ agent$
$T_r = temperature\ in\ the\ reactor$

$$\begin{bmatrix} heat & of \\ inlet & flow \end{bmatrix} = \frac{F_i}{V}(T_{in} + 273) \tag{3-14}$$

$$\begin{bmatrix} heat & of \\ outlet & flow \end{bmatrix} = \frac{F_e}{V}(T_r + 273) \tag{3-15}$$

$$\begin{bmatrix} heat & generated \\ from & reaction \end{bmatrix} = \frac{r_{O_2}\Delta H_r}{32\rho_r C_{heat,r}} \tag{3-16}$$

$$\begin{bmatrix} heat & transferred \\ to\ the & jacket \end{bmatrix} = \frac{K_T A_T (T_r - T_{ag})}{V\rho_r C_{heat,r}} \tag{3-17}$$

By substituting the above terms into the initial Equation (3-13), the following differential Equation is eventually obtained [23]:

$$\frac{dT_r}{dt} = \frac{F_i}{V}(T_{in} + 273) - \frac{F_e}{V}(T_r + 273) + \frac{r_{O_2}\Delta H_r}{32\rho_r C_{heat,r}} + \frac{K_T A_T (T_r - T_{ag})}{V\rho_r C_{heat,r}} \tag{3-18}$$

As mentioned earlier, the bioreactor under investigation in the current project is in batch mode. According to the provided definition for these bioreactors, components have no continuous inlet

and outlet flow. Consequently, heat transfer resulting from it does not occur in recent research. Therefore, the Equation is rewritten as follows [23]:

$$\frac{dT_r}{dt} = \frac{r_{O_2}\Delta H_r}{32\rho_r C_{heat,r}} + \frac{K_T A_T\left(T_r - T_{ag}\right)}{V\rho_r C_{heat,r}} \tag{3-19}$$

The heat transfer for the cooling agent T_{ag} can be modelled similarly to the bioreactor, and the energy balance is written as follows [23]:

$$\begin{bmatrix} heat & accumulated \\ in & jacket \end{bmatrix} = \begin{bmatrix} heat & of \\ inlet & coolant \end{bmatrix} + \begin{bmatrix} heat & of \\ outlet & coolant \end{bmatrix} \tag{3-20}$$

each of the above terms is written as:

$$\begin{bmatrix} heat & of \\ inlet & coolant \end{bmatrix} = \frac{F_{ag}}{V_j}\left(T_{in,ag} - T_{ag}\right) \tag{3-21}$$

$$\begin{bmatrix} heat & of \\ outlet & coolant \end{bmatrix} = \frac{K_T A_T\left(T_r - T_{ag}\right)}{V_j\rho_{ag}C_{heat,ag}} \tag{3-22}$$

the differential Equation will be as follows [23]:

$$\frac{dT_{ag}}{dt} = \frac{F_{ag}}{V_j}\left(T_{in,ag} - T_{in,ag}\right) + \frac{K_T A_T\left(T_r - T_{ag}\right)}{V_j\rho_{ag}C_{heat,ag}} \tag{3-19}$$

3.1.3 Dissolved Oxygen Model

When constructing and operating an aerated bioreactor, it is crucial to ensure that the cells receive enough oxygen transferred from the gas to the liquid phase. However, as oxygen has low solubility in water, with a saturation level of solely 1.26 mmole/L at 25°C, for meeting the requirements of a regular aerated bioreactor 750 times the saturation volume must be consumed per hour. The transfer of oxygen from the sparged gas to the culture media is a critical parameter of bioreactor design and operation [61]. As cell concentrations reach high levels, the pace at which oxygen is consumed may surpass the rate at which oxygen is supplied, resulting in restrictions in oxygen availability. The dissolved oxygen concentration influences the specific growth rate when it becomes the limiting

factor. This relationship follows saturation kinetics, where the growth rate fluctuates with the dissolved oxygen concentration. When the concentration falls below a critical threshold, the growth or respiration rate becomes dependent on the dissolved oxygen concentration in a first-order manner [82].

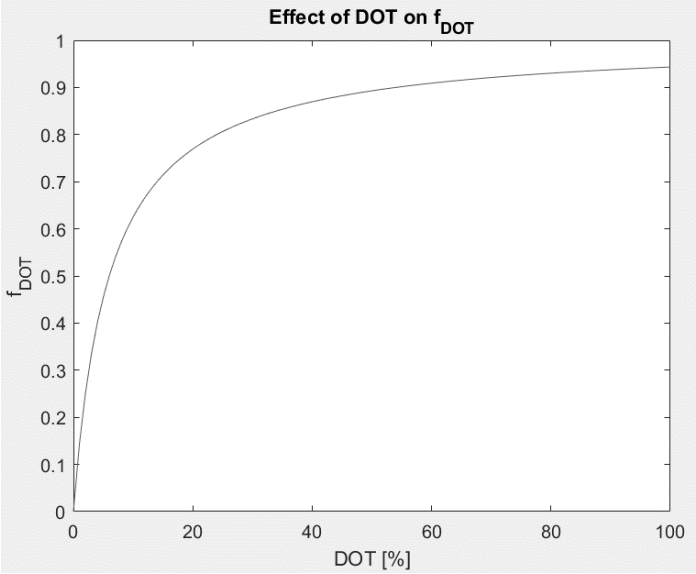

Figure 3-4. Growth rate dependence on DOT

Controlling the oxygen level in the bioreactor can lead to an increase in the growth rate. Figure 3.4 illustrates how Equation (3-12) affects the growth rate. As the level of oxygen in the environment increases, the growth rate will follow. When DO concentration reaches its critical amount, the growth rate becomes independent.

Although measuring oxygen concentration at the gas-liquid interface is impractical, the gas phase's concentration can be directly measured. While dissolved oxygen probes in the bulk liquid may present specific difficulties, a measurement can still be obtained. As specified by Henry's law, the driving force behind oxygen transfer is the difference between the bulk liquid-phase oxygen concentration in equilibrium and the bulk gas-phase oxygen concentration [61, 82].

$$C_G = HC_L^* \tag{3-20a}$$

C_G represents the concentration of oxygen in gas out, C_L^* is the oxygen concentration in equilibrium with the gas out, and H is Henry's law constant [61, 82]. As mentioned, oxygen is usually inserted into the bioreactor by sparging air through the culture. At the steady state condition, the flux of oxygen to the liquid phase is described with:

$$OTR = K_L a\ (DOT^* - DOT) \tag{3-20b}$$

where DOT* is the same as C_L^* and it is a saturated DO concentration of (mg/l). DOT is the actual DO concentration in the system, and OTR is the oxygen transfer rate. The oxygen transfer coefficient, K_L, measures how efficiently oxygen is transferred between gas and liquid in a bioreactor. The oxygen absorption rate is influenced by the surface area of the gas-liquid interface per unit volume of liquid, represented by the parameter a. When combined with K_L, a becomes $K_L a$, the volumetric oxygen transfer coefficient. It is worth noting that this relationship means that the rate of oxygen transfer is equal to the rate at which microbes consume oxygen [61]. Van't Riet (1979) has shown the validity of using power input and gas superficial velocity to estimate oxygen transfer capacity for local mass transfer [82, 83]:

$$K_L a = k\left(\frac{P_g}{V_R}\right)^{0.4} v_s^{0.5} N^{0.5} \tag{3-20c}$$

k is the empirical constant for the characteristic of the bioreactor geometry, P_g is the gassed power input by the impeller (N m s^{-1}), V_R is the bioreactor's volume (m^3), and v_s is the superficial gas velocity (m s^{-1}). N is the rotational speed of the agitator, which is 100 rpm.

The oxygen consumption rate (OCR) is donated as:

$$OCR = q_{O_2} X \tag{3-20d}$$

in this relation q_{O_2} is the specific oxygen uptake. Regarding practical use, sensors usually measure the dissolved oxygen tension (DOT) instead of the oxygen concentration. This measurement is a

direct reflection of the oxygen partial pressure. A dissolved oxygen tension level of 100% suggests that the partial oxygen pressure in the solution is balanced with the surrounding air, creating a fully saturated solution with oxygen. The connection between the dissolved oxygen tension (DOT) and the dissolved oxygen concentration can be explained through Henry's law Equation (3-20a). The constant *H* depends on oxygen solubility [84, 85]. For this discussion, we will use the commonly accepted literature [53] value for water, $H = 1.4 \times 10^3 L \cdot atm/g$, corresponding to oxygen solubility in a growth medium of 7.14 mg/l in equilibrium with air. It is reasonable to assume that DOT*[3] is at or near 100% when working in a laboratory setting. Based on this information, the OCR can be described as follows:

$$OCR = q_{O_2} XH \tag{3-20e}$$

We can demonstrate the mass balance of oxygen concentration through the following Equation [82]:

$$\frac{dDOT}{dt} = K_L a\ (DOT^* - DOT) - q_{O_2} XH \tag{3-21}$$

3.2 Bioreactor Model

3.2.1 Bioprocess Operation

The data used for the present study was obtained by the synthesis of recombinant adeno-associated virus (rAAV) through the triple plasmid transfection technique in HEK293SF-3F6 cells, performed at the National Research Council Canada in Montreal, QC, Canada. The processes were completed in two bioreactors and three shake-flasks, resulting in the manufacture of rAAV9

[3] If the gas is complemented with additional supply of pure oxygen this value will be higher and if complemented vid N2 the value will be lower.

and rAAV6 [86]. The volume of the bioreactor was 3 L, with a performance volume of 2.7 L, which was regulated by the my-Control controller (Applikon Biotechnology, Delft, the Netherlands). The physical characteristics in the bioprocess included dissolved oxygen (DO), pH, and temperature, which were controlled by a control loop employing Proportional-Integral-Derivative (PID) control. Dissolved oxygen concentration was established at 40% air saturation. The culture was agitated at a rotational velocity of 100 rpm. The pH was upheld at 7.2 by adding carbon dioxide (CO_2) overlay and sodium bicarbonate. The temperature of the system was kept up at 37˚C by heating jacket. The initial viable cell density (X_v) used for inoculation into the bioreactor was 0.31×10^6 cells/ml [4]. The model parameters were determined through experimentation, or the estimation techniques reported by [4] using the Extended Kalman Filter to estimate the parameters from online viable cell density. Constraints were set based on the system, and Table 3.1 shows the specific parameter values for this system. This nonlinear model accurately represents the growth and metabolism of the HEK293SF-3F6 mammalian cell batch bioprocess.

Table 3-1 Model Parameters[4] [4, 15]

Parameters	*Unit*	*Value*
μ_{Xv}	$(h^{-1}10^6$ *cells/mL)*	*0.02*
$Y_{Glc/Xv}$	$(\mu mol/10^6$ *cells)*	*2.0*
$Y_{Gln/Xv}$	$(\mu mol/10^6$ *cells)*	*0.56*
$Y_{Lac/Glc}$	$(\mu mol/10^6$ *cells)*	*2.0*
$Y_{O2/Xv}$	$(\mu mol/10^6$ *cells)*	*8.8*
$\boldsymbol{X_{V_0}}$	10^6 *cells/mL*	*0.31*
Glc_0	*mM*	*6.45*

[4] Some of the unknown parameters are used from the literature that are referenced.

Gln_0	*mM*	*3.32*
Lac_0	*mM*	*0.07*
MW_{O2}	*gr/mol*	*32*
$C_{heat,ag}$	*J/gK*	*4.41*
$C_{heat,r}$	*J/gK*	*4.18*
$\Delta \boldsymbol{H_r}$	*kJ/mol* O_2	*518*
DOT_0	*mg/l*	*39.70*
DOT^*	*mg/l*	*100*
K_T	J/hm^2K	3.6×10^5
K_S	*g/l*	*1*
K	*g/l*	*5*
A_T	m^2	*1*
ρ_{ag}	*g/l*	*1080*
ρ_r	*g/l*	*1000*
V	*l*	*1000*
V_j	*l*	*50*

3.2.2 Bioprocess Model

The bioprocess model is a mathematical model that explains cell growth and metabolism. It is a nonlinear and first principle mechanistic model. This approach is based on foundational assumptions, such as having a well-mixed bioreactor and controlling the culture pH. The model consists of eight first-order ordinary differential equations, as Equations 1-8 in Table (3-2), presented in Table 3.2. These equations describe the rate of change of the state variables within the

process. The state variables include the viable cell density (X_V), glucose concentration (Glc), glutamine concentration (Gln), lactate concentration (Lac), dissolved oxygen tension (DOT), and temperature. The growth of the bioprocess mammalian cell line is responsible for influencing the eight state variables. The first Equation describes this.

Table 3-2 ODEs expressions in MATLAB

1.	$\boldsymbol{\mu_{X_v} = \mu_{max}\left[\frac{Glc}{Glc+K_S}\right][f(pH)][f(T)][f(DOT)]}$
2.	$\boldsymbol{\frac{dX_v}{dt} = \mu_{X_v} X_v}$
3.	$\boldsymbol{\frac{dGlc}{dt} = -\mu_{X_v} Y_{Glc/X_v} X_v}$
4.	$\boldsymbol{\frac{dGln}{dt} = -\mu_{X_v} Y_{Gln/X_v} X_v}$
5.	$\boldsymbol{\frac{dLac}{dt} = \mu_{X_v}(Y_{Lac/Glc})(Y_{Glc/X_v})(10^6) X_v}$
6.	$\boldsymbol{r_{O_2} = \mu_{X_v} Y_{O_2/X_v} X_v MW_{O_2}}$
7.	$\boldsymbol{\frac{dT_r}{dt} = \frac{r_{O_2}\Delta H_r}{32\rho_r C_{heat,r}} + \frac{K_T A_T (T_r - T_{ag})}{V\rho_r C_{heat,r}}}$
8.	$\boldsymbol{\frac{dT_{ag}}{dt} = \frac{F_{ag}}{V_j}\left(T_{in,ag} - T_{in,ag}\right) + \frac{K_T A_T (T_r - T_{ag})}{V_j \rho_{ag} C_{heat,ag}}}$
9.	$\boldsymbol{\frac{dDOT}{dt} = K_L a\,(DOT^* - DOT) - q_{O_2} XH}$

3.3 Controller Implementation

Multiple parameters must be controlled and measured for optimal product formation within a bioreactor's intricate environment. Standardly, pH, temperature, and dissolved oxygen levels are regulated by adjusting the rotational speed of the agitator in fermenters. While specific probes and

techniques have been developed to measure ions, substrates, and products, current bioreactor process-control strategies are less sophisticated than those employed in the petrochemical industry. This is due to a need for more reliable sensors for online measurements and precise dynamic models [82].

The current focus is on developing a controller that can manage the environmental parameters of the bioreactor system. To accomplish this, it has been established two control loops. The first control system adjusts the airflow rate to manage the Dissolved Oxygen Tension (DOT). In contrast, the second control system regulates the cooling fluid flow rate to maintain the reactor temperature. PID (Proportional-Integral-Derivative) and MPC (Model Predictive Control) controllers are developed using the ODE models we explored in section 3.1 to design these control loops. The control performance of both controller types is analyzed and aimed to enhance the overall performance by substituting the PID controller with MPC.

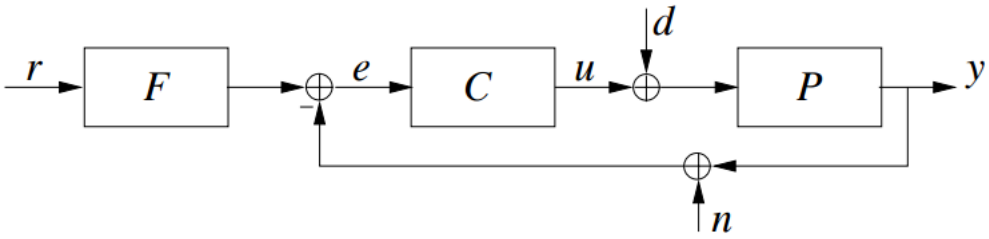

Figure 3-5 General schematic of the control system (copied from [64]**)**

Implementing a control system (Figure 3.5) effectively regulates the system input, u, to ensure that the system output, y, remains near the desired setpoint, r. The controller variable pertains to the system input, whereas the controlled variable relates to the system output. Additionally, the disparity between the output and the setpoint is known as the control error, and the principal aim of devising a controller is to minimize this error.

Figure 3.6 is the block diagram of the bioreactor process. It depicts an open-loop system with airflow and cooling fluid flow rates as input variables and temperature and DOT (Dissolved Oxygen Tension) as output variables.

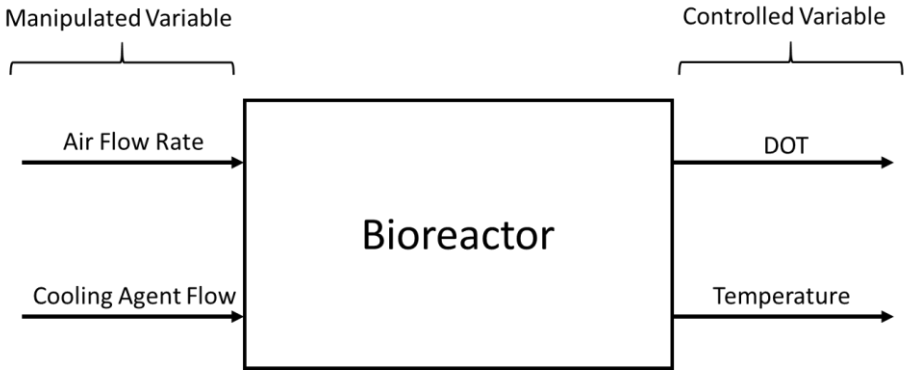

Figure 3-6 Block diagram of bioreactor process

Maintaining the temperature and DOT at their designated setpoints can result in more viable cells. To achieve this, the bioreactor's temperature can be controlled by changing the flow rate of the cooling fluid to the desired level. Similarly, the airflow rate into the bioreactor can be adjusted to control the DOT. A block diagram of the closed-loop system is displayed in the following Figure 3.7.

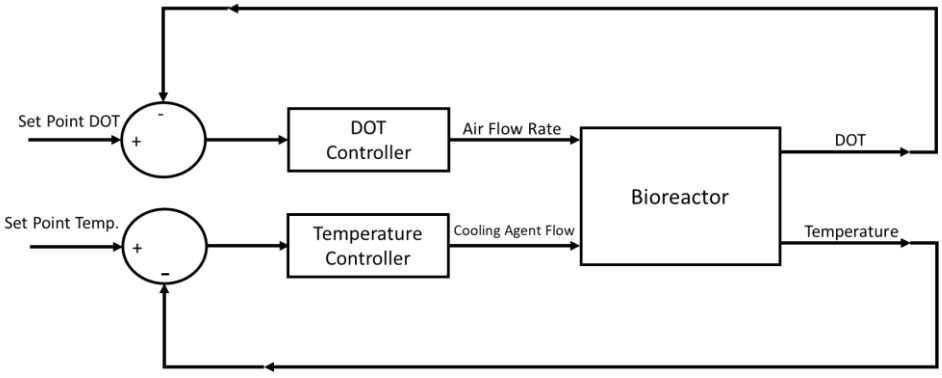

Figure 3-7 Closed-loop block diagram

3.3.1 Design of PID Controller for Bioreactor

The PID controller has gained significant attention in industrial unit control due to its satisfactory performance and simple structure. It consists of three terms: Proportional, Integral, and Derivative, each with advantages and disadvantages. By tuning the coefficients associated with each term, desirable control performance can be achieved. The general concept of PID is investigated in Chapter 2.

3.3.2 Design of MPC Controller for Bioreactor

In order to gain a comprehensive understanding of Model Predictive Control (MPC), it is essential to examine its benefits compared to other control methodologies, such as PID controllers. Numerous advantages of MPC have been identified in works of literature, including [70, 72]:

- This controller boasts an entirely intuitive design, ensuring ease of understanding.
- Tuning the controller is a straightforward process.
- Its effectiveness is demonstrated in controlling a range of systems, from those with basic dynamics to those with more complex dynamics, such as non-minimum phase systems or systems with significant delay times.
- Moreover, it excels in controlling systems with measurable disturbances. The control law obtained is easily implementable, and this control method allows for effortless application of constraints, including output constraints that will be elaborated further.

The advantages mentioned above, along with other benefits beyond the scope of this research to discuss in detail, have led to increased attention and utilization of these controllers. Controllers that utilize MPC rely on a system model to achieve optimal performance. The accuracy of the model

directly correlates with the effectiveness of the controller. By estimating the system's output for a specified number of future time steps, the controller aims to adjust the input to align with the desired setpoint.

To attain the control objective, addressing the implementation of the MPC controller structure is imperative by referring to Figure 3.8. By utilizing the inputs and outputs available along with the system model, we can compute the anticipated output for the subsequent N-time steps. The disparity between this value and the setpoint is the system error for the upcoming N time steps. This error is utilized as the optimizer's input. If constraints need to be included in the MPC controller's design, they are integrated at this stage in the optimization problem. Irrespective of the optimization problem-solving method, it is crucial to accurately specify the cost function and constraints, which we will discuss in detail below. Through solving the optimization problem, we can determine the inputs to the system for the upcoming N time steps. In the design of an MPC controller, the term "Prediction Horizon" refers to the next N time steps. The control horizon is a finite time period during which control inputs are optimized to minimize a cost function and satisfy system constraints. To achieve the best results, the optimizer needs to make N_u (control horizon) calculations.

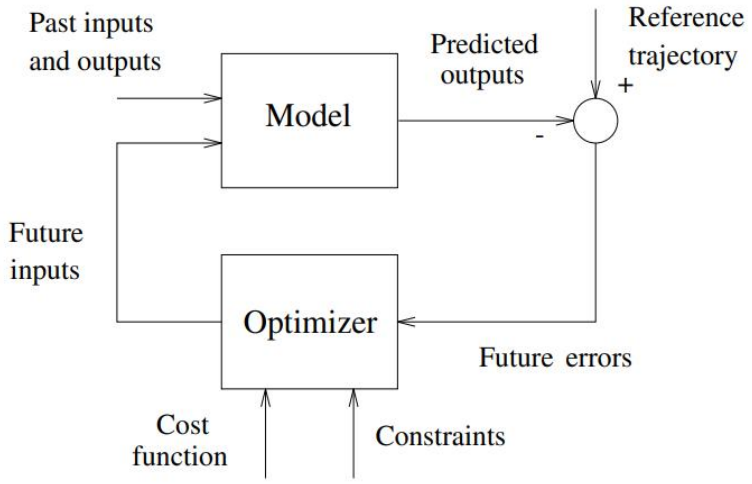

Figure 3-8 Structure of MPC controller (Copied from[72]**)**

The general form of the cost function or objective function in MPC controller design is as follows [70, 72]:

$$J(N_1, N_2, N_u) = \sum_{j=N_1}^{N_2} \delta(j)[\hat{y}(t+j|t) - w(t+j)]^2 + \sum_{j=N_1}^{N_2} \lambda(j)[\Delta u(t+j-1)]^2 \qquad (3\text{-}22)$$

Parameters in the Equation (3-22) are:

$N_1 = minimum\ prediction\ horizon$
$N_2 = \ maximum\ prediction\ horizon$
$N_u = control\ horizon$
$\delta(j) and\ \lambda(j) = \ weighting\ sequences$
$w(t\ +\ j) = future\ reference\ trajectory$
$\hat{y}(t+j\mid t) = \ prediction\ of\ the\ system\ output$

In the cost function, there are two components. The first involves squaring the trajectory error, while the second involves squaring the changes in controller action. The rationale behind incorporating these two elements is easily comprehensible. The first component works towards minimizing the trajectory error, the primary goal of creating the control system. The second component guarantees that the controller executes the appropriate control actions as it is known as

control effort which can prevent the controller from driving the system to its physical limits by penalizing large control inputs. This is crucial in systems with constraints.

3.3.3 Constraint Handling in MPC

Compared to PID controllers, MPC controllers possess a notable advantage as they are adept at accommodating constraints common in physical system modelling. These constraints are an inescapable aspect of many systems, whereby a variable cannot increase or decrease without limit and can be mathematically expressed as inequalities. According to the definition, these constraints can apply to the inputs, outputs, or all system states.

In practical scenarios, all procedures are subjected to certain limitations. Actuators have a limited range of motion and a restricted slew rate, as seen in control valves, which have a fully closed and fully open position and a maximum slew rate. Bounds in process variables are caused by constructive or safety reasons, as well as sensor range, such as tank levels, pipe flows, and deposit pressures. The control system usually operates near the boundaries, which increases the chances of constraint violations. In order to achieve long-term predictive control, the control system must be able to anticipate constraint violations and address them accordingly. Output constraints are mainly implemented for safety reasons and must be controlled beforehand since process dynamics affect output variables. The controller can maintain input (or manipulated) variables within bounds by capping the control action to a value that satisfies amplitude and slew rate constraints [72]. When constraints are only handled by clipping manipulated variables, any violations on output variables are not considered. This approach needs to fully utilize the predictive capabilities of Model Predictive Control (MPC). Control systems, particularly those that involve long-range predictive control, should anticipate constraint violations and address them appropriately. Constraints on a process can stem from various sources, such as amplitude limits in the control signal, actuator slew rate limits, and output signal limits. These are described as follows [72]:

$$u_{min} \leq u(t) \leq u_{max}, \quad \forall t$$
$$du_{min} \leq u(t) - u(t-1) \leq du_{max}, \quad \forall t$$
$$y_{min} \leq y(t) \leq y_{max}, \quad \forall t$$

3.3.4 Measurement of Controlled System Performance

In order to evaluate the performance of the implemented controller, the subsequent criteria may be employed:

Integral Square Error $$ISE = \int ERROR(t)^2 dt \quad (3\text{-}23)$$

Integral Absolute Error $$IAE = \int |ERROR(t)| dt \quad (3\text{-}24)$$

Integral Time Squared Error $$ITAE = \int t|ERROR(t)|^2 dt \quad (3\text{-}25)$$

where *ERROR(t)* is the error between the controlled variable and the defined setpoint.

Three different control measures are used to evaluate controller performance. These measures are known as the ISE, IAE, and ITAE indices. The ISE index considers the squared error over time and is sensitive to significant deviations from the set point. The IAE index, on the other hand, looks at the absolute error over time and does not give any extra weight to errors in system response. Finally, the ITAE index considers the absolute error multiplied by time over time and penalizes errors that persist for an extended period of time. All three indices are precise and commonly used to compare control schemes [24].

Designing a controller with lower ISE, IAE, and ITAE values indicates superior performance, making these indices valuable in controller tuning. This thesis utilized these criteria to compare the performance of PID and MPC controllers in the bioreactor.

3.4 Model Implementation in MATLAB

The Simulink environment within MATLAB has been leveraged in the R2022a version in implementing the bioreactor control system. Moreover, a comprehensive explanation was developed, discussing using specific Simulink blocks to model individual components within the closed-loop system effectively.

3.4.1 Bioreactor S-Function

We have implemented the bioreactor system by employing the S-function block within the Simulink environment. The required parameters for this block are as follows:

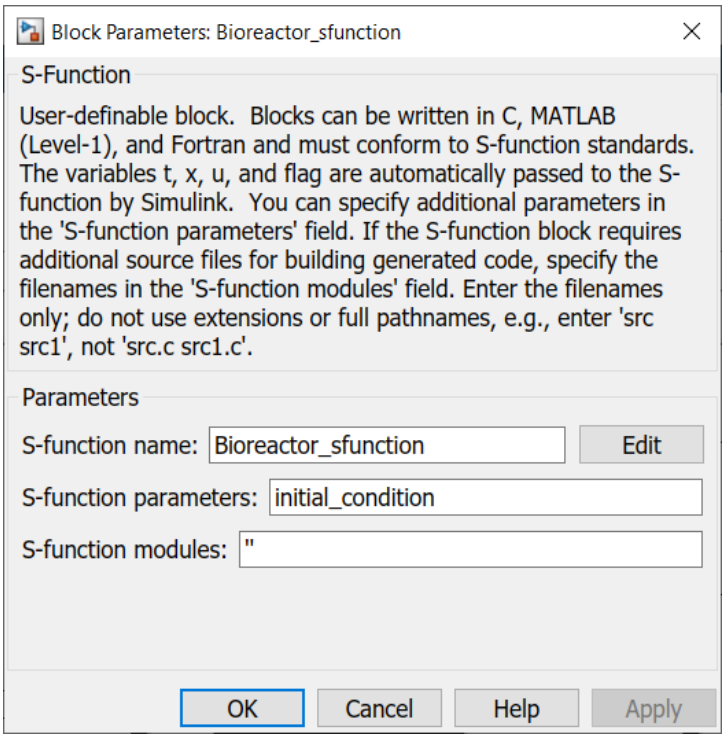

Figure 3-9 S-Function block parameters

To define the bioreactor system, the necessary elements for this block are the name of the S-function (Bioreactor_sfunction) and input parameters (initial_condition) that describe the system.

In this context, "S-function" refers to the system descriptor that must be defined as one to represent the bioreactor system. The required elements for defining an S-function are listed below:

- The number of system states, inputs and outputs, and their quantity should also be specified if the system has discrete states.
- Inputs and outputs of the system.
- Initial values of the system states.
- Differential equations describing the system.
- Equations describing the system's outputs.

By entering the above details into the S-function template available in MATLAB, the bioreactor system can be modelled in Simulink.

The diagram of the bioreactor's implementation in MATLAB is illustrated in Figure 3.12. The S-function has been utilized to implement all the differential equations discussed. The primary components of the blocks consist of differential equations representing temperature, dissolved oxygen (DO), and all the components, including glucose, glutamine, lactic acid, and viable cells. The S-function in Figure 3.11 receives several inputs, including the substrate flow rate entering the bioreactor, the flow rate of the cooling agent (F_{ag}), the pH level, the rotation speed of the stirrer (N), and the superficial gas velocity (v_s). The various inputs are collectively combined and transmitted to the model. Simulink performs calculations and produces output simultaneously. The demultiplexer block separates the output into individual outputs for desired inputs or their graphs.

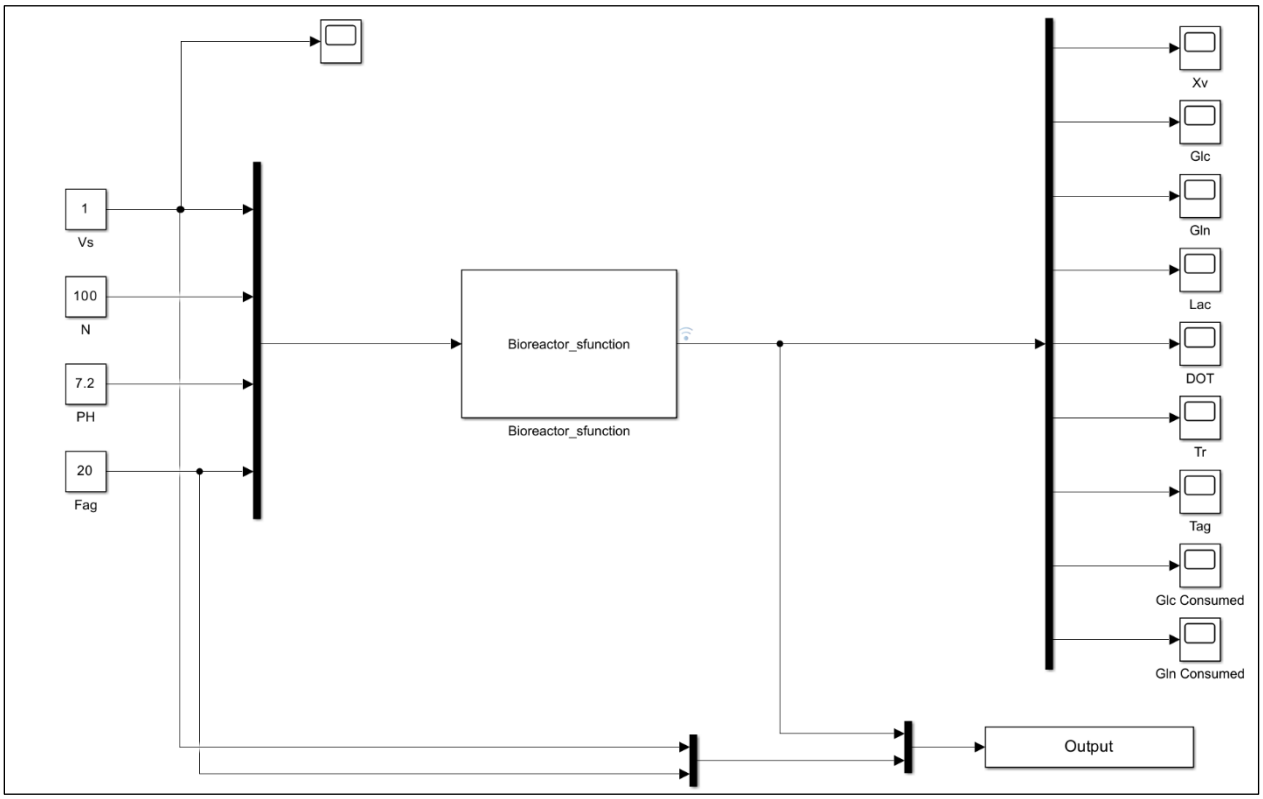

Figure 3-10 Implementation of bioreactor's Simulink in MATLAB

3.4.2 Bioreactor Closed Loop PID

The output, representing the controller action, can be obtained by employing the PID Controller block in Simulink and providing the error signal as input. The basis for calculating the controller action has been explained in Chapter 2. For each of the control loops, a PID controller is considered separately. As evident in the figure below, in this block, one can specify the type of controller. needed (P, I, PI, PD, PID), the continuity (discrete or continuous) of the control system, control coefficients, and other parameters.

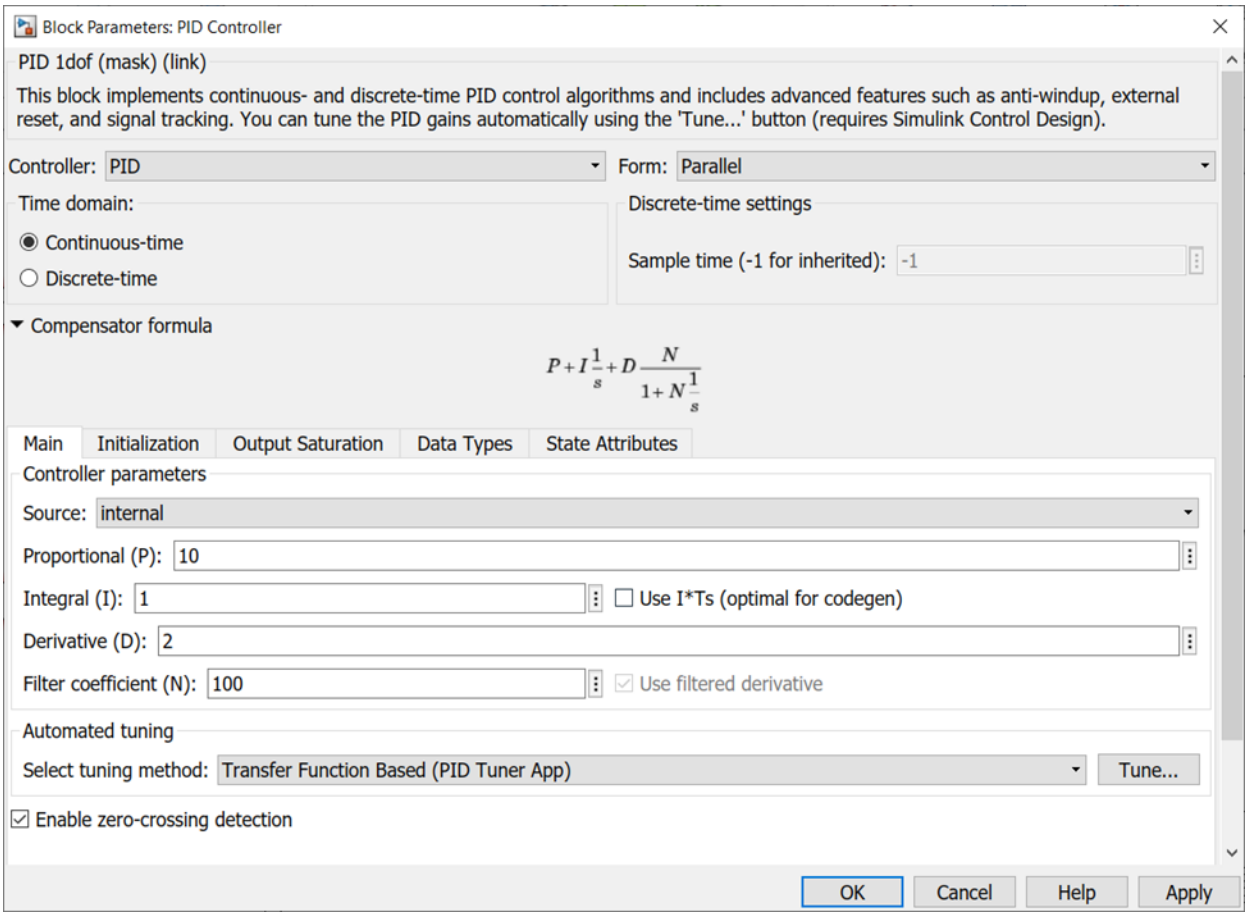

Figure 3-11 Block parameters of PID controller in Simulink

A saturation block has been used in the path of the PID controller action to prevent negative values for airflow and cooling agent flow. This limitation can be implemented in the output saturation section of the PID block. In Figure 3.12, the implementation of the temperature can be observed in the controller in Simulink. The temperature signal from the bioreactor, which is the output of the S-function block related to the bioreactor, is compared to the defined setpoint; subsequently, the error signal is input into the PID controller.

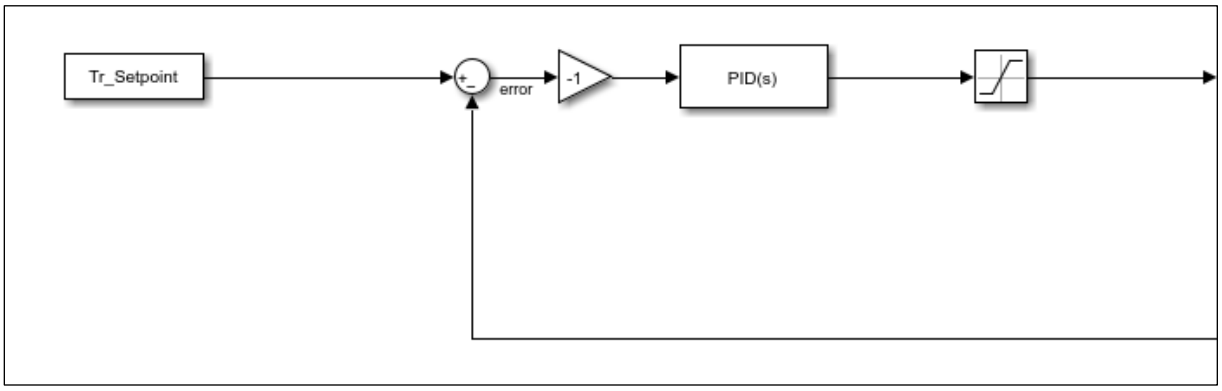

Figure 3-12 Implementation of saturation block

The closed loop PID control system simulation for a bioreactor was designed in Figure 3.13. At first, by loading the parameters from the `'parameter.mat'` file, it simulates the closed-loop control system using a Simulink model named `'Bioreactor_Closeloop_PID'`. It simulates a specified time duration. The solver method used to solve the system's differential equations numerically is `'ode23tb'`, which is a good choice for solving dynamic systems. The results are stored in variables such as `'Closeloop_PID'.` In order to analyze the system's behaviour, the data is processed and plotted to represent various variables visually. These variables include X_v (cell concentration), Glucose Consumption, Lactate production, dissolved oxygen tension (DOT), bioreactor temperature, and control actions for oxygen and cooling agent flow rates. The findings will be thoroughly discussed in Chapter 4. Then, the system also compares the system's performance with and without a PID controller and includes plots illustrating the effects of DOT (dissolved oxygen tension) on specific growth rates and the controller's actions.

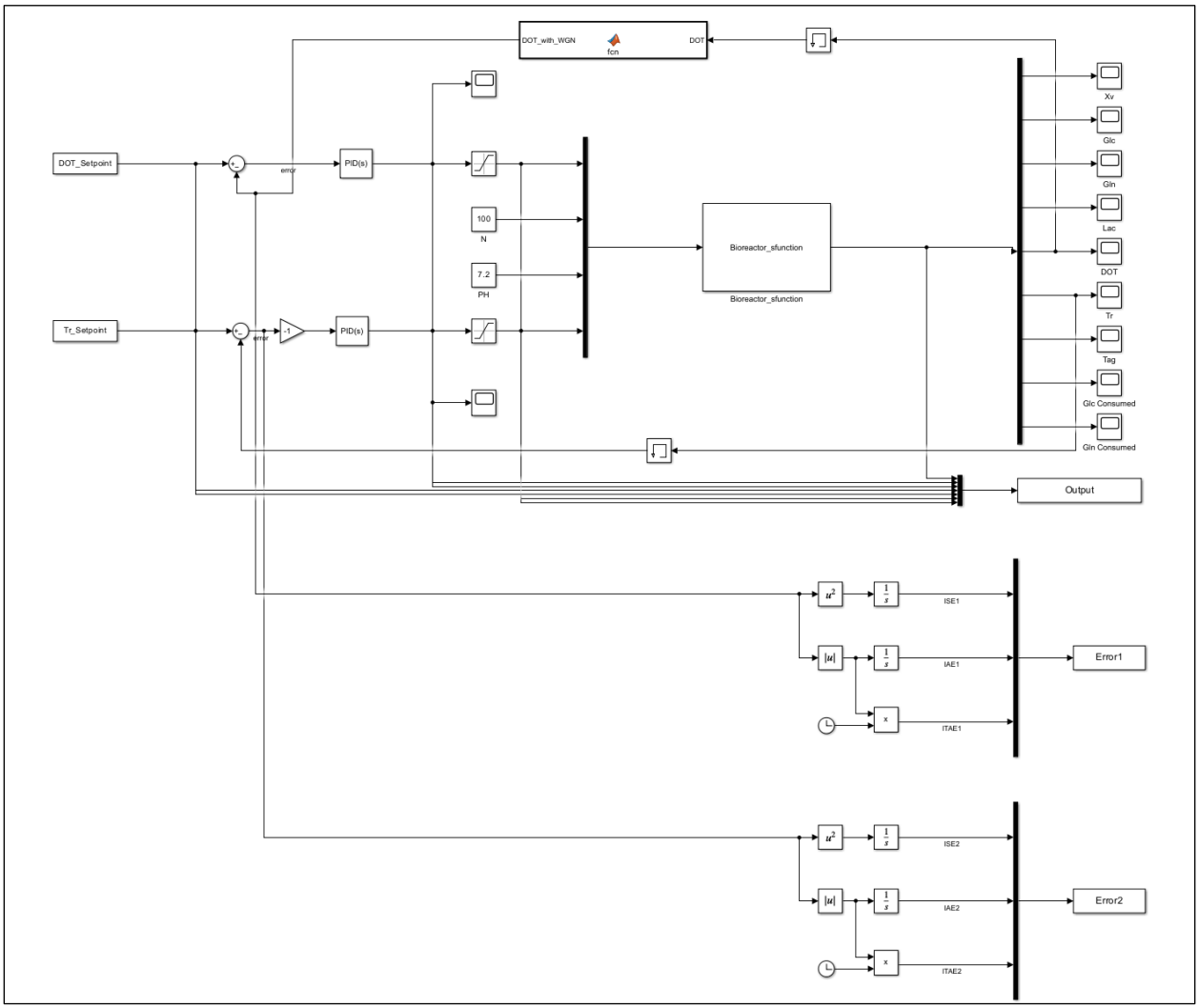

Figure 3-13 Simulink Block Diagram of PID Controller

3.4.3 Bioreactor Closed Loop MPC Controller

The MPC Controller block has been used within the Simulink environment to implement the MPC controller, as evident in Figure 3.14. The reference signal (corresponding to the setpoint values for bioreactor temperature and DOT) and the measured output (referring to the signals of bioreactor temperature and DOT as output from the bioreactor S-function) are included as inputs. In this section, consideration can also be given to measured disturbances, referring to observed and

quantifiable external influences or changes that affect the controlled system's behavior. These disturbances are incorporated into the control strategy to enhance performance and stability.

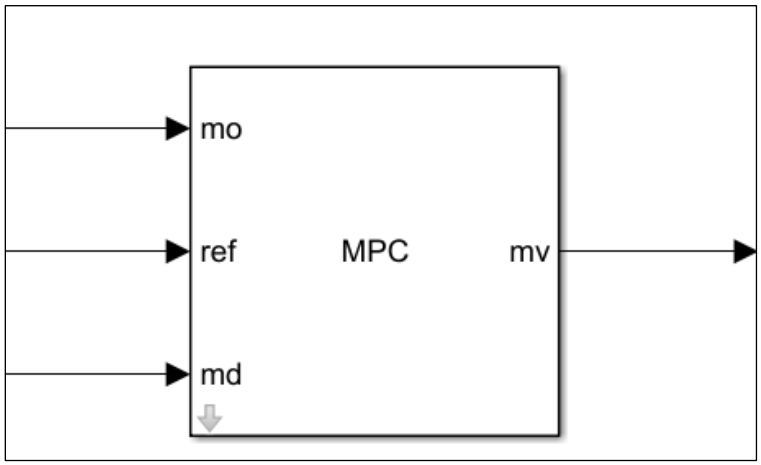

Figure 3-14 MPC block in Simulink (mo: measured output, md: measured disturbance, mv: manipulated variable)

The following section will outline the requirements for using this block. To use the MPC controller, it is necessary to provide the MPC object created in MATLAB. The creation process involves the following steps:

- Linearization of the nonlinear system:

  In this section, we linearize the open-loop bioreactor system by specifying input and output nodes. The linearized system, represented in the following format, is introduced to the MPC:

$$\dot{x}(t) = Ax(t) + Bu(t)$$

$$y(t) = Cx(t) + Du(t)$$

The bioreactor's model is linearized with linearization function in MATLAB due to implementing MPC controller. The linearization of a bioreactor model using MATLAB and Simulink starts by opening a Simulink model named `'Bioreactor_Openloop_Model'` and then simulating the model to ensure it is valid. The linearization process specifies input and output which are air flow rate, cooling agent flow, DOT, and temperature within the model. The '`linio`' function is used for this purpose. After defining these linearization points, the code linearizes the model using the `'linearize'` function, resulting in a transfer function representation '`sys`'. As the linearized model is non-minimal order, it then applies minimal-order reduction using `'minreal'` to limit uncontrollable or unobservable states (there are several different reaction taking place in the bioreactor some of the state variables that have similar changes), resulting in `'sysr'`.

A, **B**, **C**, and **D** for linearize function:

```
sys =

  A =
                Bioreactor_s  Bioreactor_s  Bioreactor_s  Bioreactor_s  Bioreactor_s
   Bioreactor_s       0.01577         101.8         16.17        -203.7             0
   Bioreactor_s    -2.366e-07     -0.001526    -0.0002425      0.003056             0
   Bioreactor_s    -0.0001943        -1.254         -1.78          2.51             0
   Bioreactor_s     1.593e-08     0.0001027     1.633e-05      -0.07995       0.07974
   Bioreactor_s             0             0             0         1.739        -1.939

  B =
                    Vs    Fag
   Bioreactor_s      0      0
   Bioreactor_s      0      0
   Bioreactor_s  4.767      0
   Bioreactor_s      0      0
   Bioreactor_s      0  -0.24

  C =
             Bioreactor_s  Bioreactor_s  Bioreactor_s  Bioreactor_s  Bioreactor_s
   Demux/5              0             0             1             0             0
   Demux/6              0             0             0             1             0

  D =
              Vs  Fag
   Demux/5     0    0
   Demux/6     0    0
```

A, **B**, **C**, and **D** for minreal:

```
sysr =

  A =
           x1       x2       x3       x4
   x1   -81.77   -11.05    4.217   -38.96
   x2     41.2    3.987   -1.973    20.09
   x3   -17.07   -2.246  -0.9816   -8.352
   x4    157.5    21.41   -8.376    74.98

  B =
       Air Flow Rat  Cooling Agen
   x1       -0.3376    -1.108e-14
   x2        -3.846        0.1289
   x3         -2.73       -0.1942
   x4        0.6066      -0.05713

  C =
                       x1        x2        x3        x4
   DOT           -0.07083   -0.8068   -0.5726    0.1273
   Bioreactor T    0.8924   0.05595   -0.0918    0.4383

  D =
                 Air Flow Rat  Cooling Agen
   DOT                      0             0
   Bioreactor T             0             0
```

- Specification of Parameters:

  We define parameters such as Prediction Horizon, Control Horizon, Weights, and Optimizer.

- Introduce constraints to the model:

  Constraints that can be applied to this controller are determined based on software help, including:

  1. Minimum output variable constraints
  2. Maximum output variable constraints
  3. Minimum manipulated variable constraints
  4. Maximum manipulated variable constraints

5. Manipulated variable constraint matrix
6. Controlled output constraint matrix

For this problem, we have imposed constraints of the "minimum manipulated variable" type to prevent negative values for airflow and cooling agent flow. Additionally, minimum/maximum output variable constraints can be applied to mitigate overshoot/undershoot in the system.

In Figure 3.15, a Simulink block diagram of the MPC controller is designed. The controller object `'mpcobj'` is created and configured with properties like prediction and control horizons, manipulated variables' constraints, and output variables' weights. The prediction horizon is 90 h, and the control horizon is 80 h. Constraints are set for the manipulated variables, and weights are assigned to output variables. After setting up the MPC controller, the Simulink model called `'Bioreactor_Closeloop_MPC'` where the MPC controller is implemented. It defines the simulation options and runs the closed-loop simulation using the specified solver `'ode15s'`, which indicates that the simulation should use the `'ode15s'` solver for solving the differential equations within the Simulink model. `'ode15s'` is a stiff ODE (Ordinary Differential Equation) solver commonly used for solving stiff and non-stiff systems of ODEs [87]. In this thesis the system is considered continuous as the time steps are very small.

In Figure 3.15, the MPC model for the bioreactor is illustrated. The model includes several blocks. The first block is the MPC controller which contains the controller that has manipulated output , references (DOT and temperature setpoint), and manipulated variables. The second block, labelled "fnc" applies White Gaussian noise (WGN) to the DOT signal [26]. The third block, named as Bioreactor_sfunction contains the bioreactor's ODE models which receives all the initials parameters necessary for simulating the upstream process. The output block displays setpoints for DOT and temperature and all other state variables (glucose, glotamine, lactic acid, X_v). At the right

side of Figure 3.15 the blocks are related to errors are shown for DOT (Error1) and temperature (Error2).

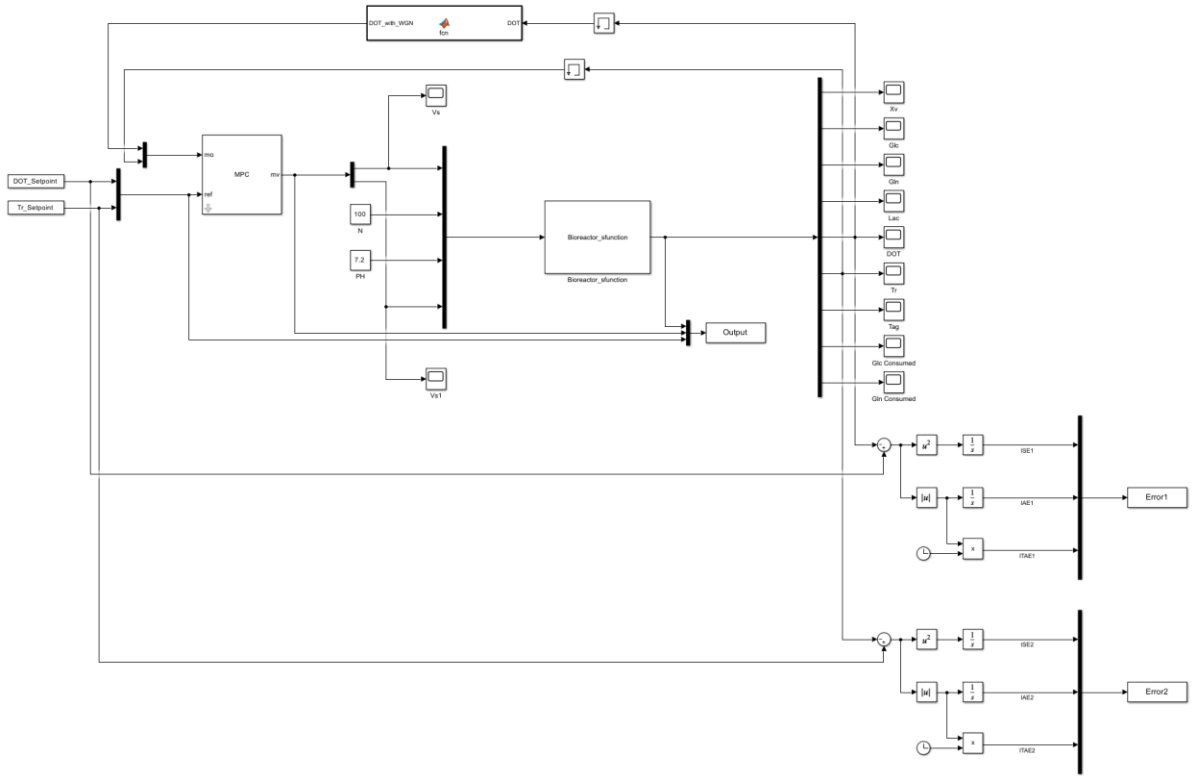

Figure 3-15 Simulink Block Diagram of MPC Controller

Chapter 4

Simulation Results and Discussions

The control algorithms for the AAV bioreactor that have previously been discussed are evaluated based on the outcomes of the simulation in MATLAB. This research aimed to control DOT and temperature in the bioprocess system; when each variable is regulated at its designated value, known as the setpoint, the growth rate of the cells will achieve their optimal level, leading to an increase in cell concentration and product yield. This chapter analyzes the results for PID and MPC controllers with and without measurement noise.

4.1 PID Controller

The PID controller has been assigned to each control loop previously discussed, and the figures below clearly represent the outcomes. The first section showcases the results when measurement noise is not considered, whereas the second section demonstrates the results after introducing noise.

4.1.1 Without Measurement Noise

Figure 4.1 shows the PID controller's performance on temperature and DOT control and tracking errors. Figure 4.1a analyzes dissolved oxygen during 90 hours of AAV production by applying the PID controller. The setpoint for DOT is 40%, shown in orange, and the PID controller performance in blue. It can be observed that the overshoot from the setpoint in the first hours of the process is above 40%, and then the controller tries to stay in on the setpoint. After t = 70 h, the controller could not control DOT above 40%, dropping to less than 40%. The controller has satisfactorily controlled temperature, as shown in Figure 4.1b; the output temperature follows the set point at

T=37˚C.

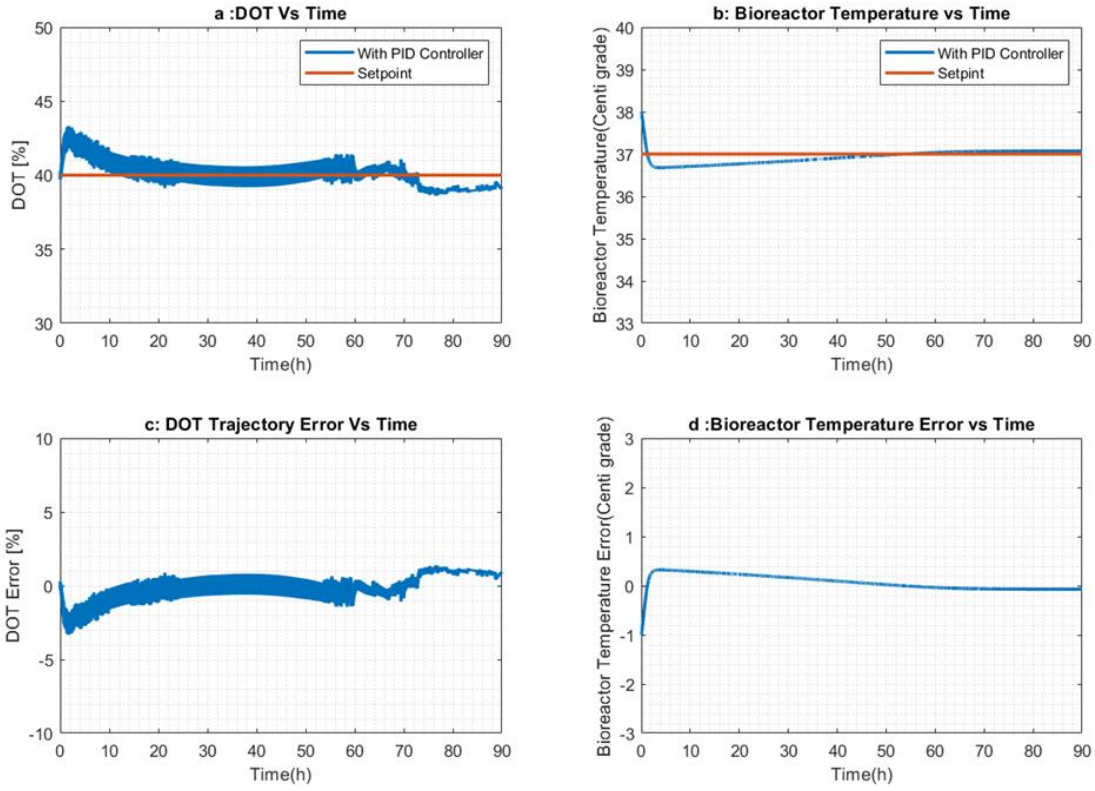

Figure 4-1 Performance of PID controller for DOT (a, c) and Temperature (b, d)

Figure 4.2 depicts the dynamic behaviour of the AAV bioprocess with and without the PID controller. Figure 4.2a shows the logarithmic-scale variation of viable cell concentration over time, which is the exponential phase of cell growth. As expected, the concentration reaches a constant value after a specific duration, and it will no longer have an increasing trend due to the equal mortality rate of cells and cell growth in the bioprocess. In the absence of the PID controller, DOT values drop to lower than 40%, which is the setpoint for the culture's demand for oxygen. Figure 4.2 (b-d) are plotted considering the change of components according to their consumption or production rate. Figures 4.2b and 4.2d show glucose and glutamine consumption as the substrates for cell growth. According to Table 3.2 (ODEs expression for Glc and Gln concentration), the

amount of substrate consumed increases with the production of cells in the system. Lactic acid is produced in this bioreactor alongside the consumption of glucose, which is the amount of substrate conversion to biomass (Figure 4.2c).

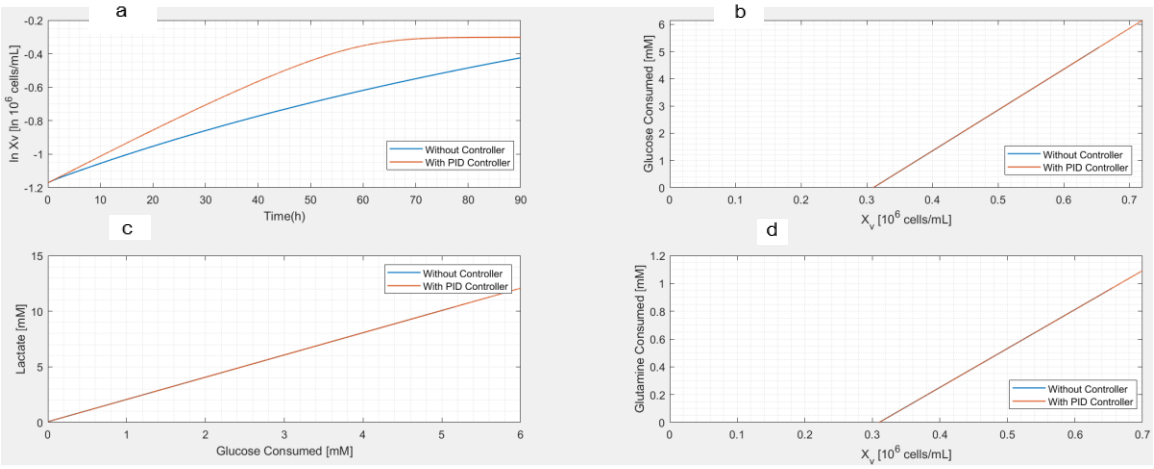

Figure 4-2 a) Cells growth pattern with PID controller, and consumption and production of b) Glucose, c) Lactic acid, d) Glutamine

Figure 4.3a shows the action associated with the oxygen flow rate (ml/min) in the PID controller. In the case of lacking DO or drop in oxygen, the PID controller, for instance, must activate the hardware for injecting oxygen into the bioreactor and then stop the injection. However, as shown in Figure 4.3a, the action produced from PID is wildly oscillating and shows negative values for the flow rate as it cannot get constraints as maximum or minimum for the control output. If we divide the graph into three sections, the first section (t=0 h to t=20 h) and the third (t=55 h to t=90 h) show more aggressive oscillation than the middle section. These actions occur due to the fluctuation in oxygen flow rate as the demand for oxygen, and the PID controller could not respond smoothly to the change in the system.

Meanwhile, Figure 4.3b displays the action of PID related to the temperature controller's cooling agent flow rate (l/h). In this graph, the cooling agent flow rate obtained negative values as the temperature was established at 37˚C, and it does not need any cooling action to reduce the bioreactor's temperature, which is a drawback for the PID controller in our system. As mentioned, MPC controllers have an advantage in including constraints in the control system. On the other hand, PID controllers do not possess this advantage.

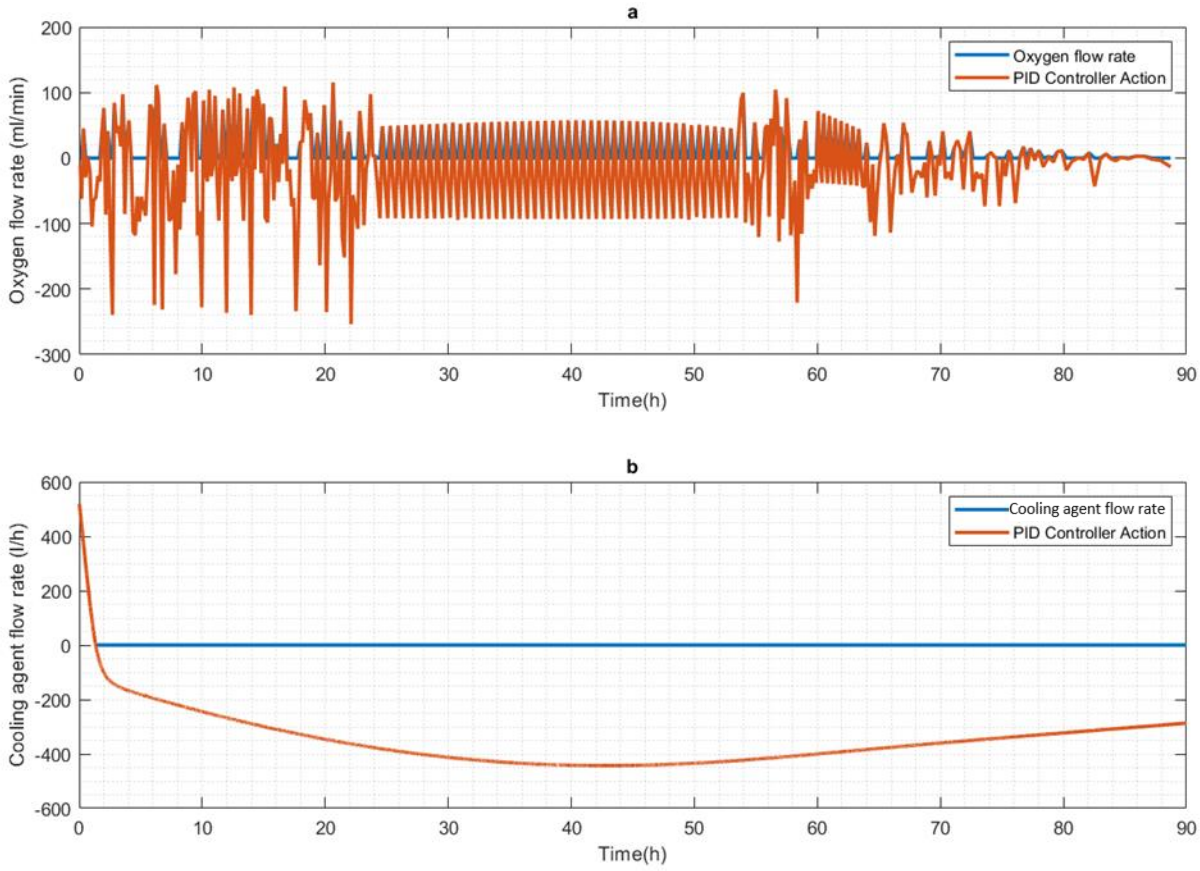

Figure 4-3 PID controller action for a) DOT and b) temperature

As a result, the action obtained from the PID controller in Figure 4.3 generates negative values for both the flow rate. This is problematic since the flow rate is a physical quantity that can only take positive or zero values. This being so, an actuator has been considered in the controller's output for

the closed-loop control PID system to function effectively, similar to how control valves behave in natural systems. The purpose of this component is to pass through the controller's output, which represents the input oxygen flow rate or temperature to the bioreactor. If the value is positive, it passes through the element without any changes, and if it is negative, it sends a control command of zero to the unit. The operation of the actuator is illustrated in Figure 4.4.

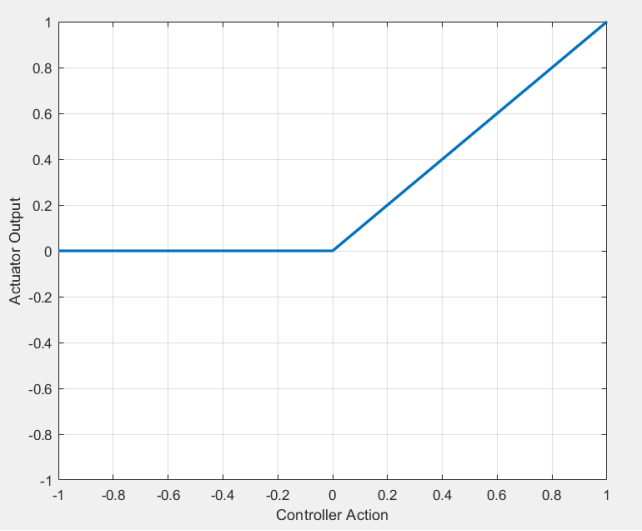

Figure 4-4 Actuator action on the output of PID control to eliminate negative values

4.1.2 With Measurement Noise

The earlier approach of this study provides an estimation of bioreactor state variables. Estimating these state variables primarily involves the integration of the ODEs using given initial conditions. A primary issue of these methodologies is the need for more consideration given to random errors and natural noise within the procedure and data [88]. In the context of a batch, fed-batch, and continuous system, it is necessary to make certain assumptions regarding mixing, which

may only sometimes be fulfilled. Additionally, variations in the working volume can occur, leading to wall growth.

Moreover, notable inaccuracies can arise when measuring gas flow rate and, to a lesser extent, the concentrations of O_2 and CO_2. Calculating the measurements' average helps reduce the noise's magnitude but still needs to eliminate the issue [88].

Closed-loop control systems, by default, require the addition of feedback, which can be obtained through many means, such as sensor-based measurements, observer-based estimations, or a mix of both. The representation of a measured signal can be expressed as follows:

$$signal = x + e_s + e_r \quad (4\text{-}1)$$

signal represents the noise adding to the DOT, x represents the variable's actual value under measurement, es denotes the systematic error, and er refers to the random error (measurement noise). The systematic error refers to a variable deviation from the x value caused by inherent errors associated with the sensor or observer. These errors may arise due to poor calibration of sensors or inaccuracies in the observer's model. Random error, or measurement noise can arise from various sources. In the case of sensors, electromagnetic interference is frequently identified as a prominent contributor to this type of error. The average or expected value of a random error tends to approach zero as the number of samples increases. This study aims to examine the impact of random error and error on measured output of the system on the efficacy of the model predictive control method [26, 89].

One common challenge encountered in industrial applications is the occurrence of measurement noise. In this context, we examine the effects of standard white Gaussian noise [24] on the DOT. For this analysis, it was associated with a signal-to-noise ratio (SNR) value of 20 dB to characterize the noise. After trying different SNR in SNR= 20 dB the observable change occurred.

In Figure 4.5, the graph depicts the PID controller's ability to regulate temperature and DOT and monitor errors with white noise only applied to the DOT. Noise can apply disturbance to the system,

and in the case of a suitable controller, it must regulate the variable (DO) to the setpoint. As observed, the PID controller produces oscillating signals for DOT compared to the setpoint. Regrettably, the controller struggles to effectively control DOT to the desired level, indicating that it may not be suitable for scenarios with noise or other disturbances. It shows an overshoot from the setpoint due to the limitation in applying constraints in this traditional type ofPID controller. Nonetheless, subsequent sections will reveal the MPC controller's proficiency in managing noise, one of its key benefits. Figure 4.5 b and d, the performance of the PID controller on temperature that does not have noise.

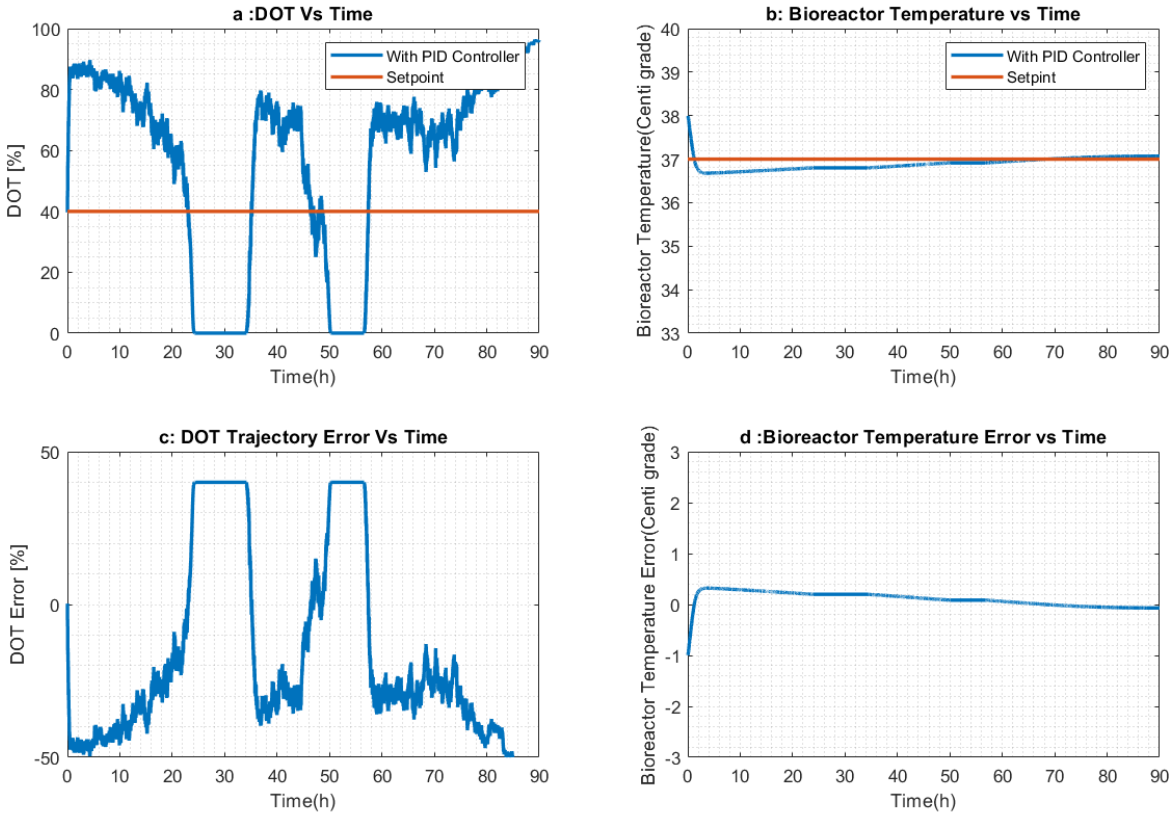

Figure 4-5 a) PID action on DOT with White Gaussian noise (SNR=20 dB), b) PID action on temperature. The errors of PID controller in c) DOT and d) temperature

The graph in Figure 4.6 shows the exponential phase of cell growth (X_v) associated with the PID controller in the presence of noise (Figure 4.6a) and without noise (Figure 4.6b). Nevertheless, it is imperative to acknowledge that measurement noise (Figure 4.6a) substantially affects the production rate, resulting in an extended period to achieve the specified amount of X_v compared to a condition without any measurement noise (Figure 4.6b). At t= 60hr, $ln\, X_v$ is higher in no-noise condition. This is due to inadequate control of the DOT, as seen in Figure 4.5a, which has caused a decrease in the growth rate compared to when proper DOT control is implemented. This decline in the cells' growth rate ultimately affects the final cell concentration and the concentration of other components, as they depend on each other's consumption rate. Another observation from Figure 4.6a is that two time steps occur due to the DOT's controller action, which shows in Figure 4.5a that the PID controller drops to zero and does not follow the setpoint.

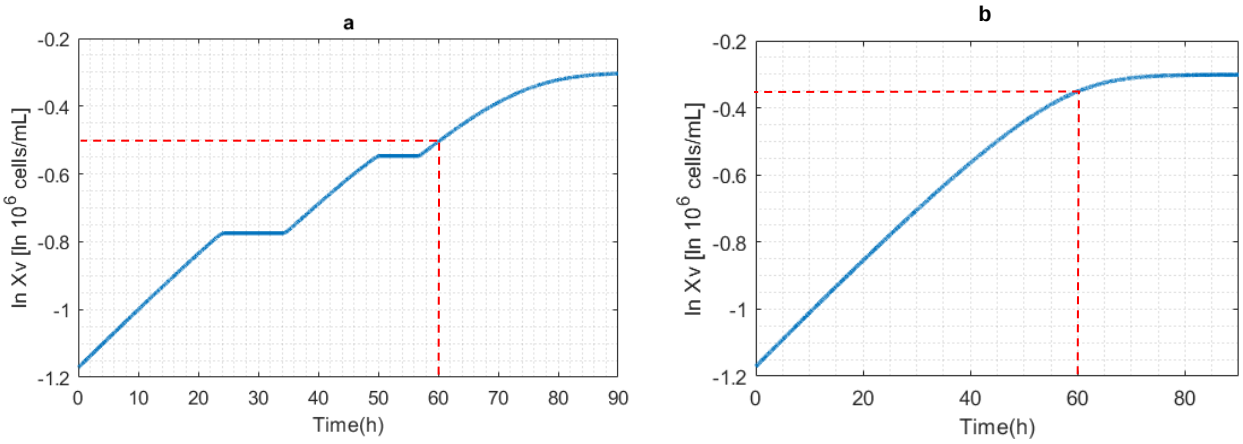

Figure 4-6 Impact of white noise on X_v with PID controller, a) with white noise (SNR=20dB), b) without noise. (At t = 60 h, the growth rate of X_v is higher in the absence of noise.)

Figure 4.7a depicts the action associated with the oxygen flow rate (ml/min) in the PID controller in the presence of SNR=20 dB. As mentioned earlier, these controllers must have an actuator at their output to prevent them from getting negative values. Regarding the control action that PID is showing for oxygen flow rate, it is observed that the control action is more oscillating than without noise, and the parts that got to zero are related to the parts that DOT drops to zero in Figure 4.5a. Figure 4.7b illustrates the action of the temperature controller with no noise, and it shows negative values for the cooling agent flow as the temperature was at 37 ˚C.

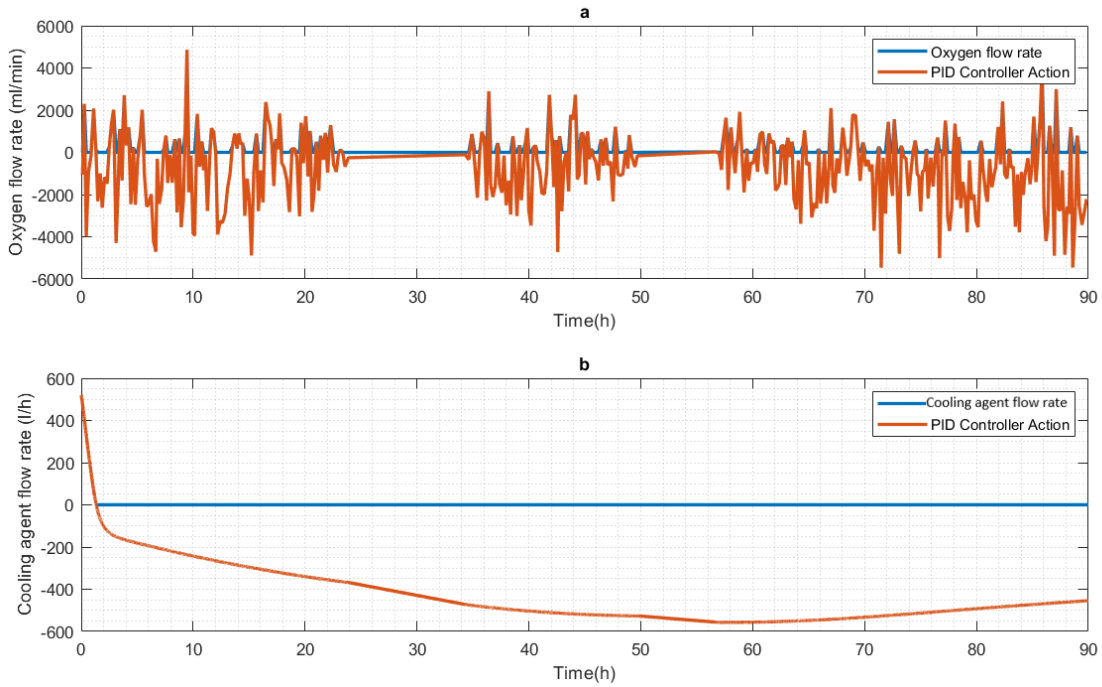

Figure 4-7 a) Action of DOT controller with noise, b) Action of temperature controller with noise

In Table 4.1 is shown the values of ISE (Integral of Squared Error), IAE (Integral of Absolute Error), and ITAE (Integral of Time-weighted Absolute Error) for DOT and temperature control loops in both conditions with/without measurement noise. An increase in these indices is also noticeable in the presence of measurement noise, which means the error in the presence of noise is

higher than in standard situations. Thus, the PID controller could not show the desired performance in controlling DOT in the bioreactor for predicting the system.

Table 4-1 Errors for PID controller with/without measurement noise

Closed Loop PID	*ISE*	*IAE*	*ITAE*
DOT	1.45×10^5	3.61×10^3	3.5×10^3
DOT (with SNR=20dB)	3.91×10^5	5.18×10^3	8.6×10^3
Temperature	1.90	1.01×10	4.82
Temperature(with SNR=20dB on DOT)	2.92	12.97	6.13

4.2 MPC Controller

This section will explore the outcomes generated by the MPC controller. The MPC controller is expected to perform better than the PID controller, particularly in control action. This projection comes from integrating control effort into the objective function, which should result in a smoother control action. In contrast, the PID controller produces excessive oscillations, rendering it unsuitable for practical use. Furthermore, considering the capabilities offered by the use of the MPC controller, by imposing constraints on the controller action, which in both control loops is of the flow type, the controller is ultimately designed to avoid negative values for flow.

Another vital aspect to consider is the impact of measurement noise. As previously mentioned, MPC controllers benefit from performing smoothly when noise or disturbances are present. It has been observed that the controller we designed is also highly effective in such scenarios.

4.2.1 Results without Measurement Noise

The performance of the MPC controller in temperature and DOT regulation and the tracking error are depicted in Figure 4.8. The controller has notably effectively regulated the output

variables to their designated setpoints. Figure 4.8a shows the performance of DOT with the MPC controller in the bioreactor. As can be seen, the controller output of DOT follows the setpoint (40%) very smoothly. Although the PID controller output follows the setpoint of DOT in Figure 4.1a, it has oscillation. Figure 4.8c is the DOT trajectory error that is near zero. Figure 4.8b is the MPC controller for temperature that the control output masks the setpoint of 37˚C, and the error from the setpoint is zero in the MPC controller for temperature.

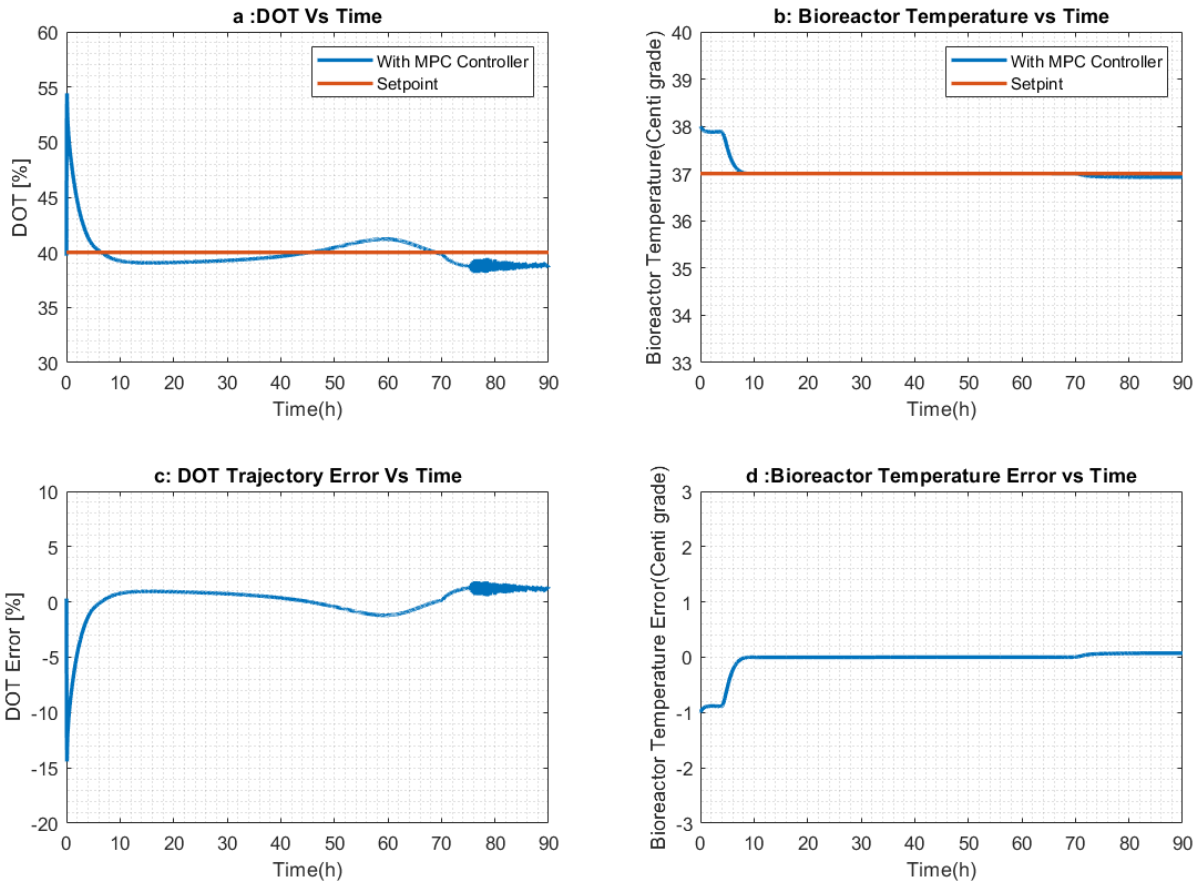

Figure 4-8 Performance of MPC controller on a) DOT and b) temperature and errors (c, d)

Figure 4.9a shows the exponential cell growth pattern for AAV production in the bioreactor with the MPC controller on DOT and temperature over time. As anticipated, the concentration of Xv gradually stabilizes after a specific duration, indicating no further upward trend. This pattern is comparable to the general exponential growth phase observed in the cell growth pattern and other bioprocesses, as discussed in earlier Chapters. Figures 4.9b and 4.9d simultaneously illustrate glucose and glutamine consumption alongside increased cell count, which is the substrate in our system. This bioprocess produces lactic acid while glucose and glutamine are consumed, as shown in Figure 4.9c.

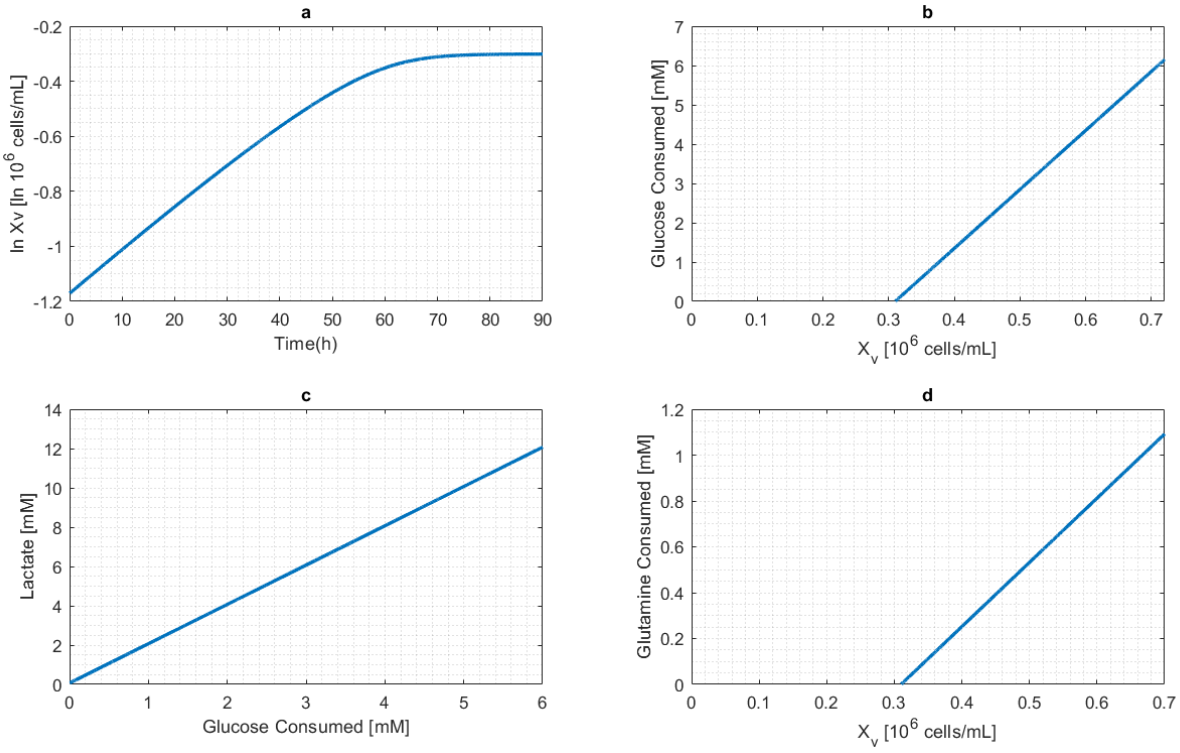

Figure 4-9 a) Cells growth pattern with MPC controller, and consumption and production of b) Glucose, c) Lactic acid, d) Glutamine

Figure 4.10a displays the action of the MPC controller for DOT, and Figure 4.10b shows the action of the MPC temperature controller. As mentioned earlier, one of the advantages of MPC controllers is the ability to add constraints to the control system. Therefore, by adding constraints to the control system, we can ensure that the control action generated by this controller provides non-negative values for flow rates. The constraints in our model are $35 \leq DOT \leq 45$. Another noteworthy aspect regarding the control action is that, unlike PID controllers, the control action is entirely smooth in MPC controllers. This characteristic is of significant importance when considering the application of these controllers in industry.

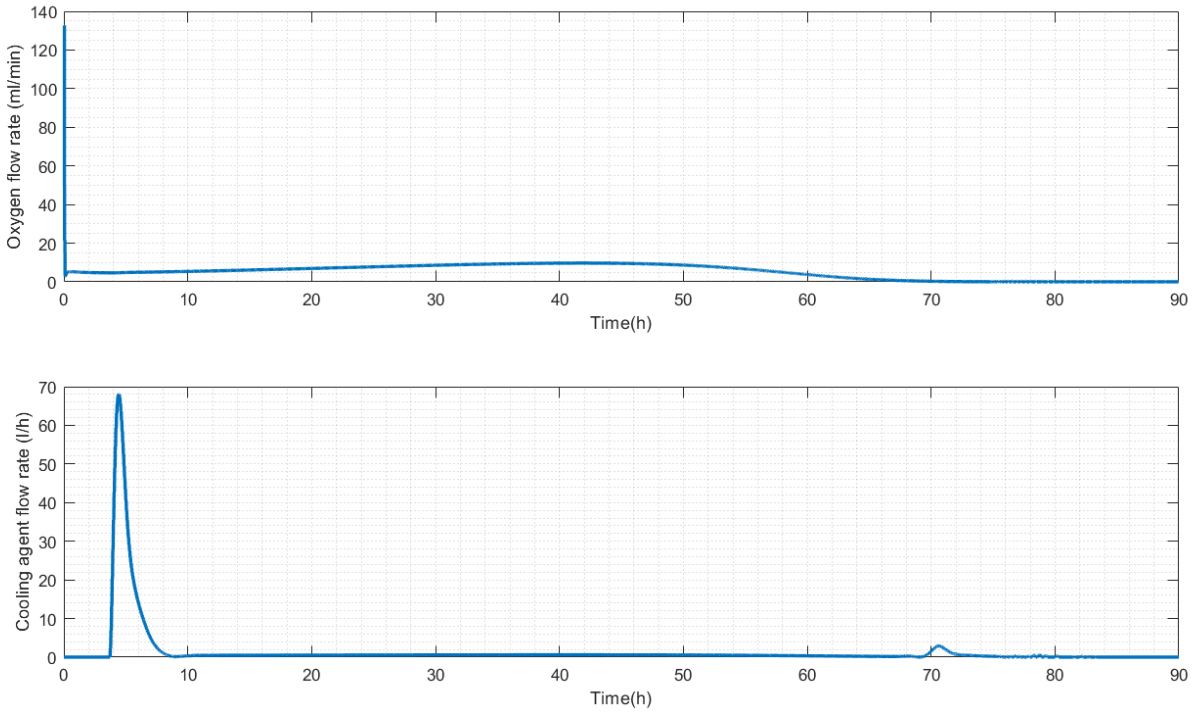

Figure 4-10 The action of the MPC controller on DOT

4.2.2 With Measurement Noise

This section analyzes the performance of MPC controllers in reducing disturbances and noise introduced into the system. This section examines the presence of standard white Gaussian noise on the DOT, comparable to the closed-loop system regulated by the PID controller. The signal-to-noise ratio (SNR) for the applied noise is assumed to be 20 dB.

The performance of the MPC controller in temperature and DOT regulation, together with the corresponding tracking errors, is depicted in Figure 4.11. As expected, in contrast to the PID controller, the MPC controller has exhibited notable efficacy in regulating the DOT variable to its setpoint, and the influence of measurement noise (SNR=20 dB) has not detrimentally impacted the controller's ability to handle this variable effectively as MPC can control the dynamic changes in the system and controller output follows the setpoint. The noise was not applied to the temperature; thus, it shows the same response as before.

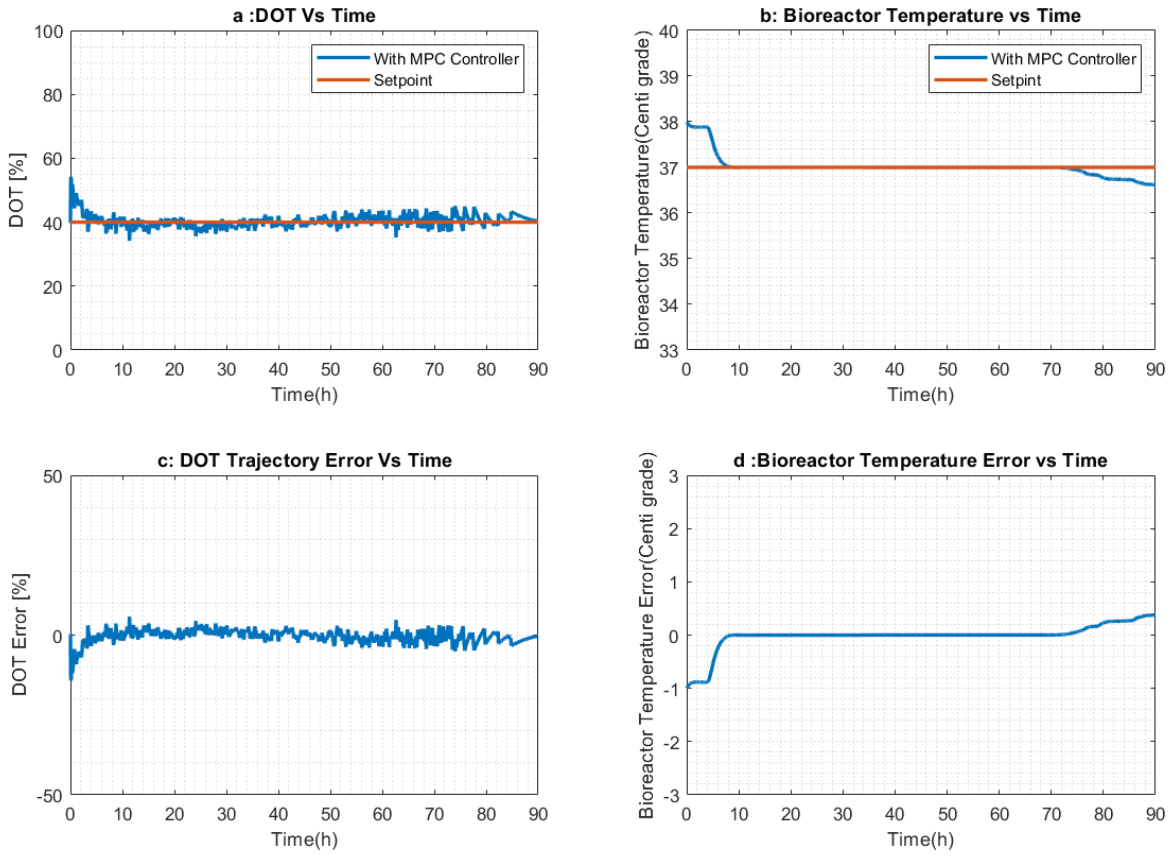

Figure 4-11 The performance of the MPC controller on a) DOT in the presence of white noise and b) temperature with no noise

Figure 4.12a displays the trend of viable cell concentration changes over time, plotted on a logarithmic scale. Despite measurement noise, the controller's performance has not been significantly impacted, and components' consumption and production rates remain unaffected (Figure 4.12b,c,d). Adequate control of DOT in the presence of noise has ensured a consistent growth rate, resulting in no significant deviations in the graphs. This is different from a system model where measurement noise is neglected. The effect of DOT on the specific growth rate has been factored in, and no significant changes have been observed.

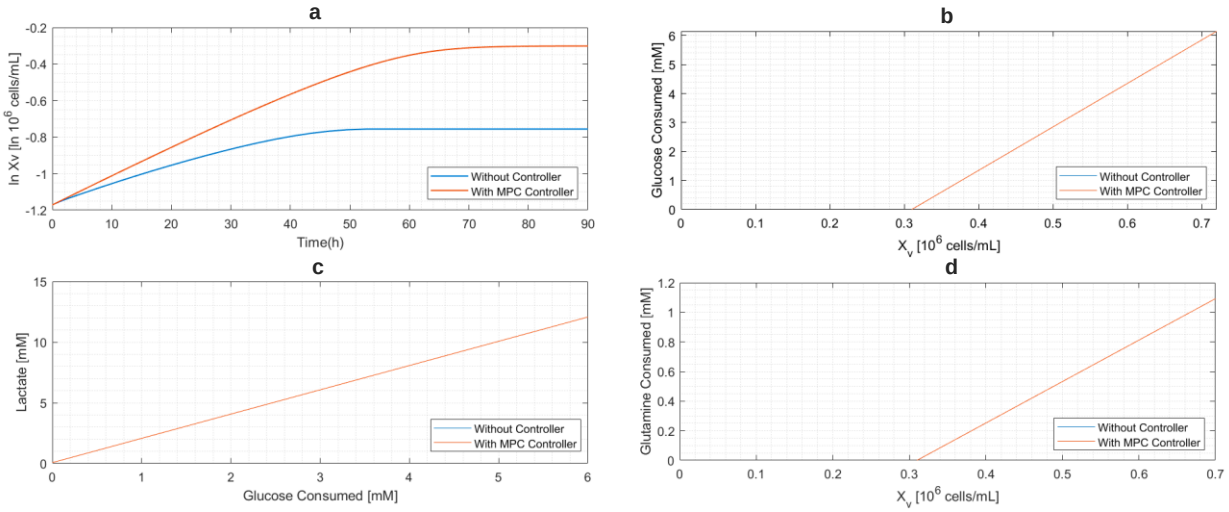

Figure 4-12 Performance of MPC controller in the presence of white noise (SNR=20 dB) on cell growth

Figure 4.13a shows the MPC controller action for DOT with the white noise of SNR=20 dB, and Figure 4.13b shows the temperature controller action without noise. The impact of measurement

noise on the controller action is not as fluctuating as the PID response. MPC controller tried to keep the flow rate as smooth as possible.

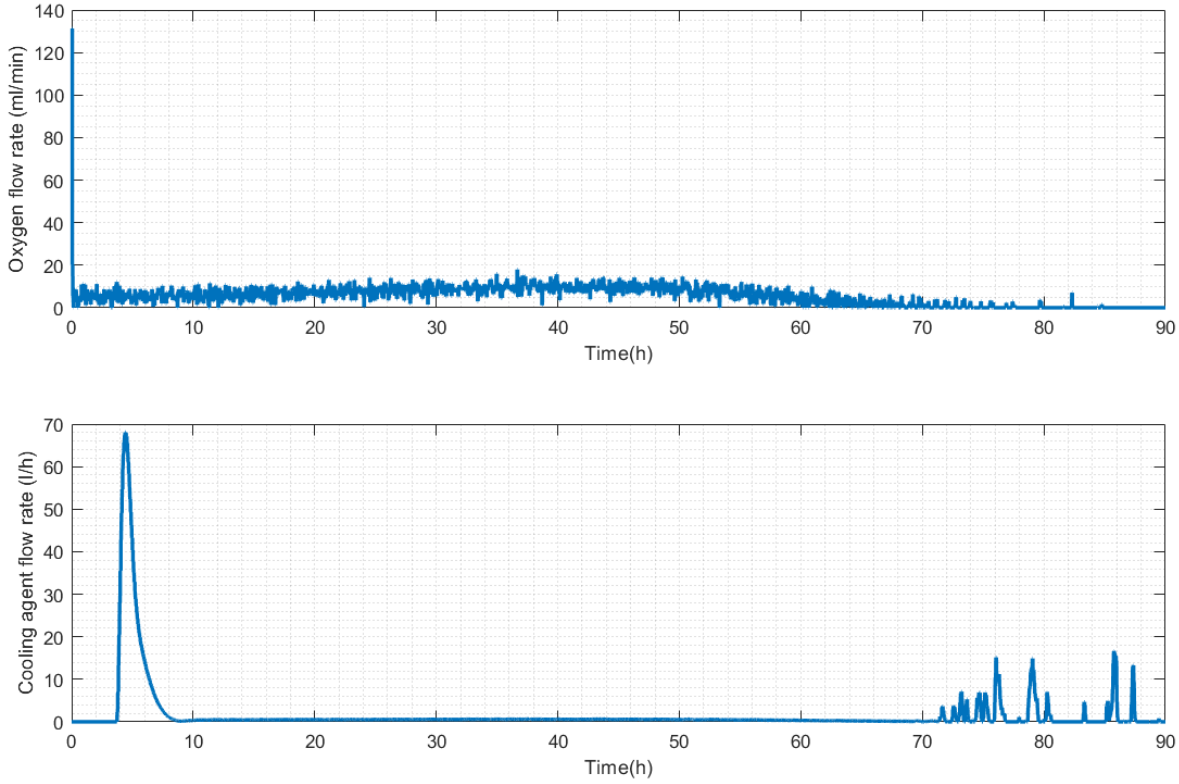

Figure 4-13The action of the MPC controller on a) DOT with white noise (SNR=20 dB) and b) temperature

Table 4.2 shows DOT and temperature MPC control loops' ISE, IAE, and ITAE values. By comparing these values to those of the PID controller, it is clear that the MPC controller maintains proper control action and has significantly lower values for ISA, IAE, and ITAE in DOT control. The PID controller manages temperature effectively, as shown by the reported ISA, IAE, and ITAE values, because it can control the linear system better than nonlinear ones. In the case of nonlinear PID, it must manipulate its parameters to respond reasonably. However, it is worth noting that the MPC controller's action is much smoother, even in temperature control. Table 4.2 also shows the

ISE, IAE, and ITAE values for both control loops, and while there is an increase in these indices in the presence of measurement noise, it is not significant. For DOT with noise, the drop in the ITAE value indicates the controller might respond quicker to noise; however, this adjustment does not reduce the occurrence of a more significant error.

Table 4-2 Performance of MPC controller with/without measurement noise

Closed Loop MPC	*ISE*	*IAE*	*ITAE*
DOT	2.23×10^2	8.81×10	1.09×10^2
DOT (with SNR=20dB)	3.65×10^2	1.28×10^2	2.68×10
Temperature	4.05	6.23	6.57
Temperature(with SNR=20dB)	4.99	8.75	3.37×10

4.3 Impact of Different Measurement Noise

This part aims to analyze the influence of the amplitude of applied noise on the performance of MPC and PID controllers. The findings will indicate that even when subjected to low signal-to-noise ratio (SNR) values, the MPC controller will perform satisfactorily. In contrast, when the noise values are elevated, the performance of the PID controller will be unsatisfactory.

Figure 4.14 presents the performance analysis of both controllers on X_v concentration under the influence of random white Gaussian noise, with varying signal-to-noise ratio (SNR) values of 80 dB, 40 dB, 20 dB, and 5 dB in Figure 4.14 (a), (b), (c), and (d), respectively. The observed trend in the above diagram reveals that the decrease in signal-to-noise ratio (SNR), denoting increased levels of introduced noise, does not significantly impact the performance of the MPC controller.

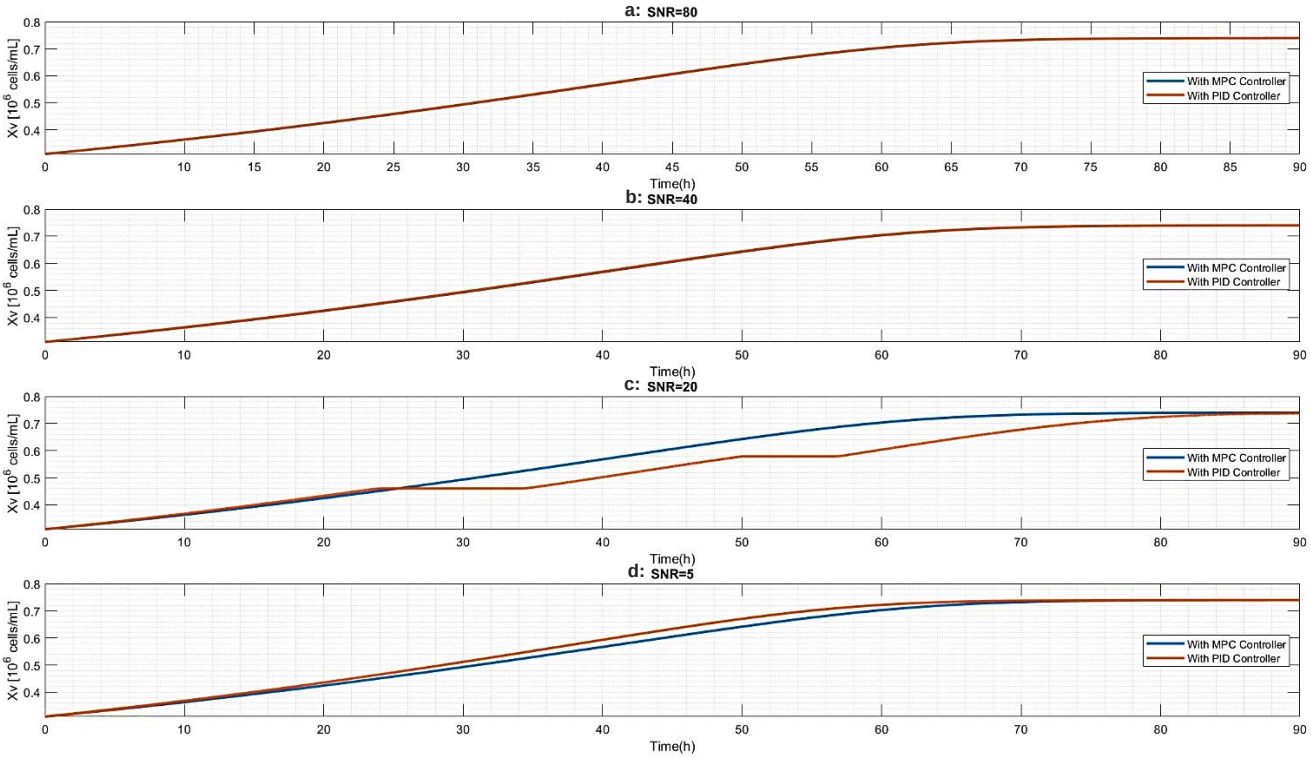

Figure 4-14 Impact of white noise on MPC and PID controller with a) SNR=80 dB, b) SNR=40 dB, c) SNR=20 dB, and d: SNR=5 dB on cell growth

On the other hand, the PID controller demonstrates reduced effectiveness, struggling to maintain the desired setpoint due to its inability to adhere to constraints for output control variables (Figure 4.14d).

In Figure 4.15, the behavior of both the PID and MPC controllers with respect to the control of the DOT value toward its desired setpoint is observed. The crucial factor here is the signal-to-noise ratio (SNR), which reflects the ratio of the signal's strength to the strength of the noise present in the system. As the SNR decreases, the PID controller gradually loses its ability to control the DOT value effectively. This means that when there is a low SNR (e.g., SNR=20 dB or SNR=5 dB), which will produce intense noise, the PID controller struggles to control the DOT value, and its

performance deteriorates significantly. This degradation occurs because the PID controller becomes more sensitive to the noise in the measurements, making it challenging to regulate the DOT value precisely. X_v is higher in PID than MPC in Figure 4.14d because PID could not maintain DOT near 40%, and it increased to above 90% and showed an increase in cell growth as it cannot have constraints. Moreover, it is in contrast with the real world.

On the other hand, the MPC controller exhibits different behaviour. Even as the SNR decreases, the MPC controller's control performance remains robust and unaffected. It continues to regulate the DOT value to its setpoint effectively alongside the setpoint, regardless of the noise level in the measurements. This resilience to noise is a notable advantage of the MPC controller, as they are designed to handle disturbances and measurement noise carefully, ensuring stable and accurate control even in challenging conditions. The MPC controller performed much better than the PID controller in facing random measurement noise.

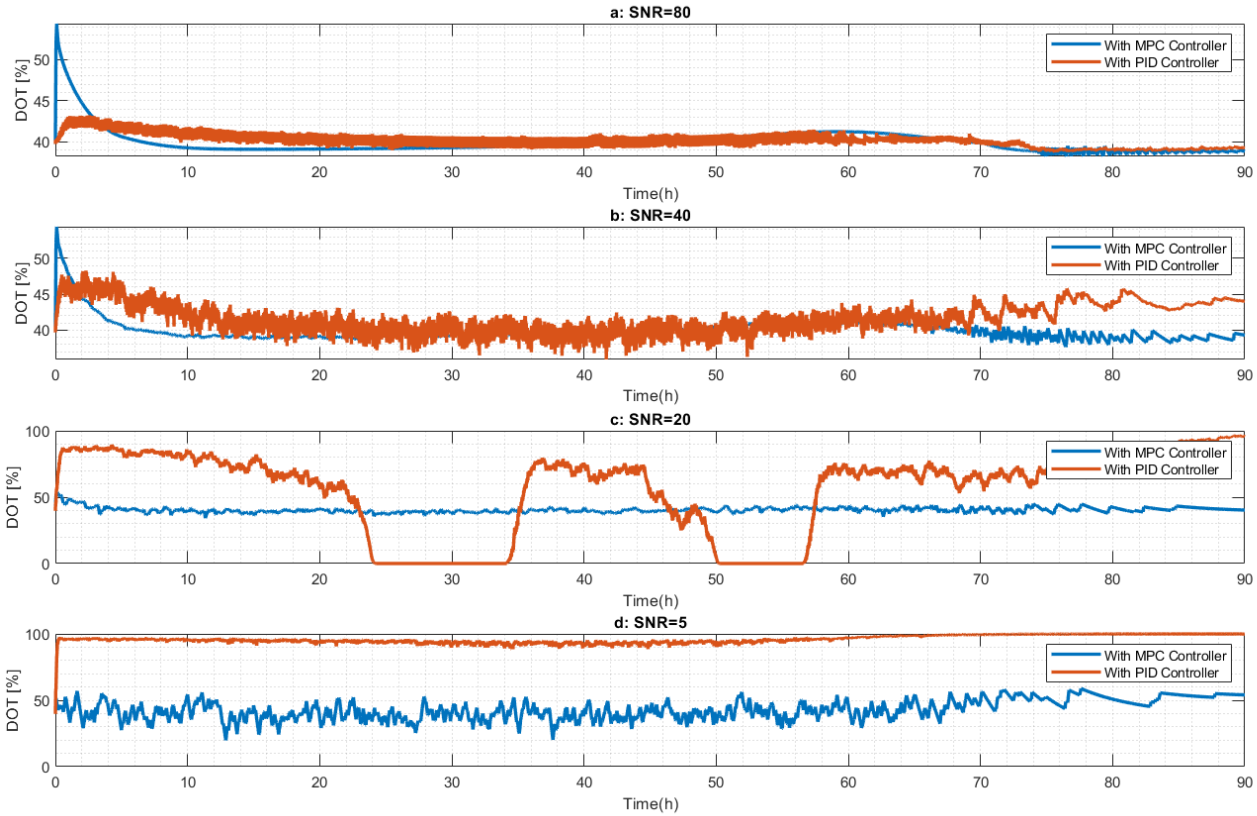

Figure 4-15 Impact of different white noise on DOT in MPC and PID controller for a) SNR=80 dB, b) SNR=40 dB, c) SNR=20 dB, and d) SNR=5 dB

Figure 4.16 illustrates the MPC and PID control action, specifically the controller responsible for managing the DOT. Regarding the behaviour of the control action, it is worth noting that the situation progressively worsens for the PID controller, as seen in Figure 4.16 (e-h). The observed actions become exceedingly sharp, making them practically inapplicable. Furthermore, even with these sharp control actions, the PID controller still cannot effectively control the DOT value to its setpoint (Figure 4.15). A controller's action represents the control effort it applies to the system in response to errors or deviations from the desired setpoint. In the PID controller shown in Figure 4.16, as SNR decreases, the actions it generates become increasingly aggressive and erratic. These sharp actions are impractical for real-world applications, especially in bioprocess systems, as they can lead to undesirable consequences, such as instability or damage to the controlled process.

Moreover, despite the aggressive actions in Figure 4-16, the PID controller struggles to achieve precise control of the DOT value. This difficulty arises because the PID controller's sensitivity to measurement noise becomes more pronounced as SNR decreases. Consequently, the controller's actions become more exaggerated to counteract the noise, but this approach proves ineffective in maintaining the DOT value at the desired setpoint. In contrast, as previously discussed, the MPC controller maintains smooth and effective control actions even in decreased SNR values. This characteristic highlights the MPC controller's superiority in handling noisy and challenging control environments, ensuring stable and accurate control over the DOT value and other variables.

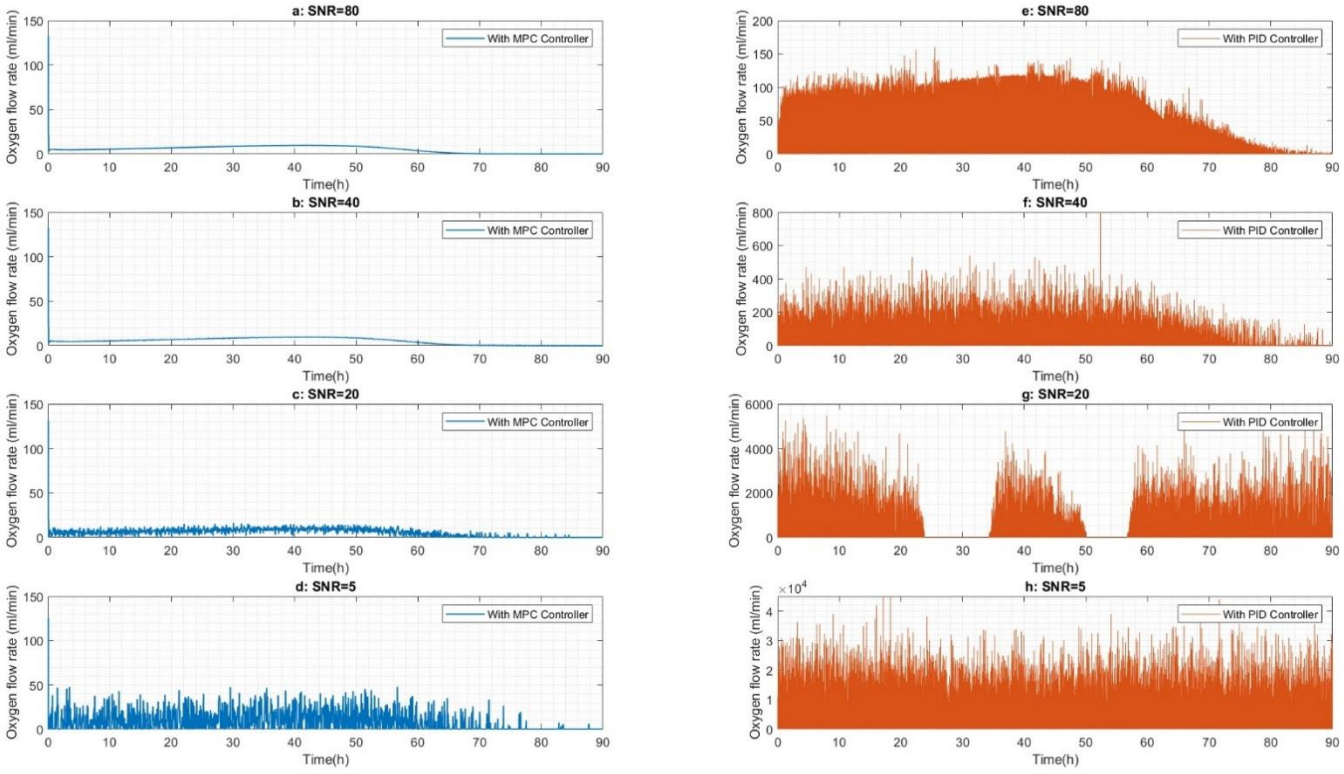

Figure 4-16 MPC and PID control action of DOT for SNR= 80, 40, 20, 5 dB

4.4 MPC Control of Different Data

We compare the good data generated with the model in steady-state conditions to observe the MPC controller performance better while neglecting all measurement noises, input variable fluctuation, or setpoint changes with anomaly data. For this purpose, in the following section, the performance of the MPC model is analyzed with two different measurement noises on DOT.

In Figure 4.17, we observe the behaviour of control outputs for DOT in the MPC control system. The steady-state control output (blue line) exhibits a smooth response to the control model, staying within the specified setpoint range between the maximum (45%) and minimum (35%) constraints.

In this ideal condition, the control system performs as expected. However, when noise is introduced into the model, the control outputs display oscillatory behaviour compared to the steady-state condition. These oscillations become more pronounced as the level of noise increases, going from an SNR of 40 dB (red line) to SNR=20 dB (yellow line). Despite these oscillations, it is notable that the MPC system continues to follow the setpoint and remains within the acceptable operating range.

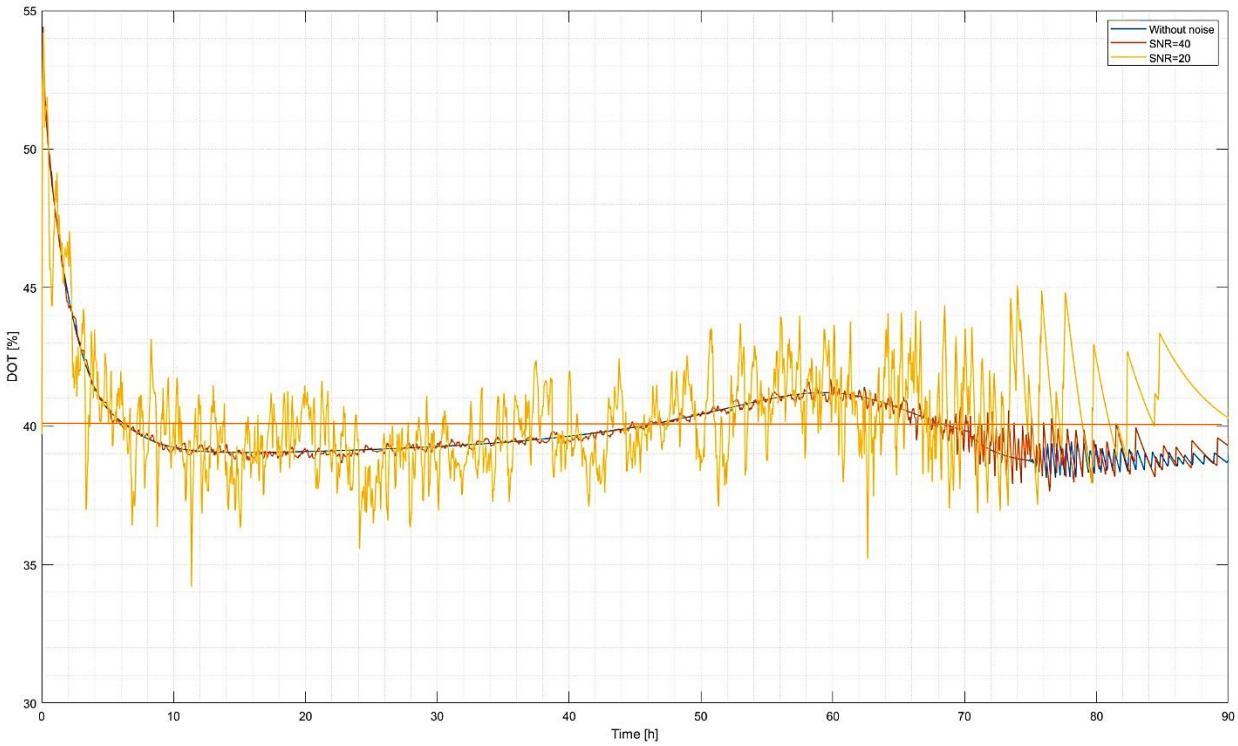

Figure 4-17 Applying measurement noise to the steady-state bioprocess; steady-state (blue line), SNR=40 dB (red line), SNR=20 dB (yellow line), DOT setpoint (green line)

Figure 4.18 further proves the control system's performance under noisy conditions. In this graph, we can see the response of the MPC controller on X_v, which represents a process variable. As measurement noise is introduced into the DOT control loop, the viable cell density remains largely

unaffected by the DOT fluctuations. This consistent behaviour is observed across different profile of measurement noise. It is worth noting that due to fluctuations in DOT and the oxygen flow rate, there is a possibility of a slight increase in the oxygen flow rate within the bioreactor. As shown in Figure 4.18c, the yellow line representing SNR=20 dB exhibits a higher value than the steady state. This increase can be the reason for the increase in the oxygen flow rate, which can lead to a corresponding increase in viable cell density. This increase is due to the MPC's difficulty controlling the DOT in its setpoint. Overall, Figure 4.18 demonstrates that the MPC controller effectively predicts and manages the state of the process even in the presence of environmental changes and noise. Despite the amplitude in DOT and oxygen flow rate, the control system maintains reasonable performance, ensuring that the process operates within acceptable bounds and achieves the desired control objectives.

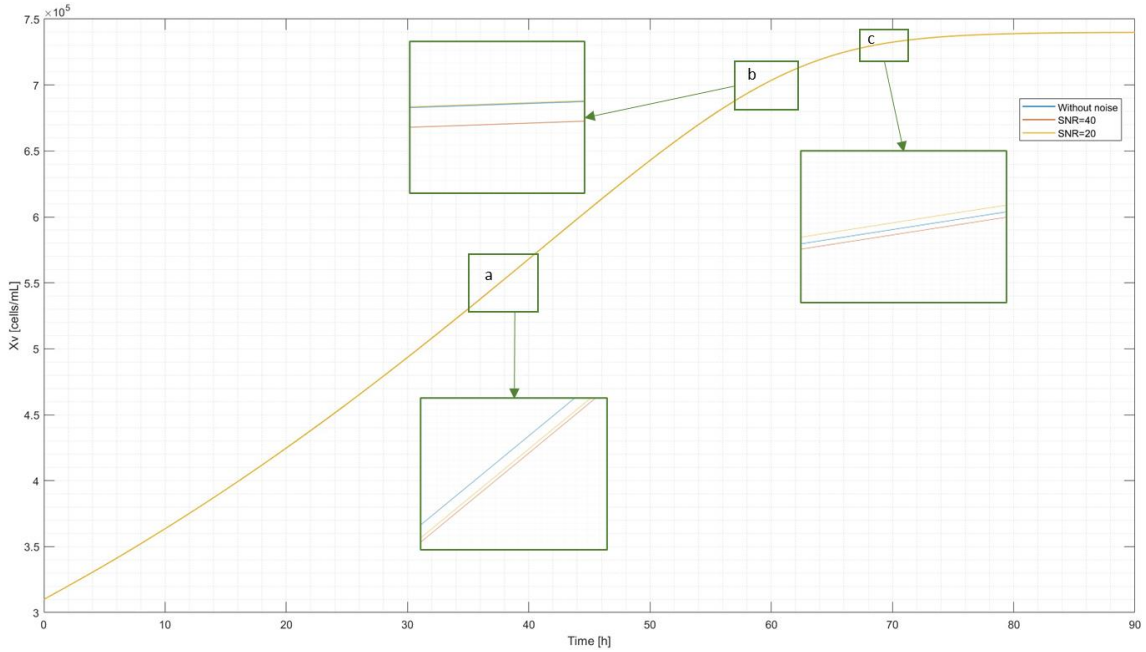

Figure 4-18 Response of MPC controller to steady-state and noisy data data, t=39h (a), t=60h (b), t=70h (c)

Chapter 5

Conclusion and Future Works

This chapter provides thesis overview, highlighting significant contributions and results. Additionally, it highlights potential domains for further investigation and discoveries.

5.1 Summary and Contribution

As mentioned before, manufacturing stable Adeno-associated virus (AAV) viral vectors for gene therapy is challenging due to low titers and inconsistent quality during the triple transfection process. Managing dissolved oxygen and temperature as environmental parameters during large-scale fermentation is crucial for optimal growth and product output. Hybrid models and creative strategies combining mechanical and data-driven approaches are necessary to improve the monitoring and automation of the process for rAAV. This thesis presents a mechanistic kinetic model for simulating the upstream process of AAV and developing the MPC controller to address these critical challenges.

Ordinary Differential Equations (ODEs) define each component in a bioreactor simulation, encompassing growth rate, cell concentration, and nutrient levels. This optimization process results in precise predictions and enhances the production of coveted products. These ODEs were implemented in the Simulink environment in MATLAB to simulate the steady state condition of AAV production. The initial conditions were obtained from experimental data, and other parameters were collected from various literature. The proposed model successfully simulated the upstream process, similar to other bioprocesses. The next step was to implement the Model Predictive Control (MPC) controller to regulate Dissolved Oxygen Tension (DOT) and temperature to achieve a higher concentration of cell growth. The MPC model was developed using MATLAB and demonstrated satisfactory control performance on DOT and temperature, even with varying

measurement noise. It has been determined that the MPC controller outperforms the designed PID controller's capacity to adapt to changing conditions and effectively reduce discrepancies between controlled variables and their target set point. The MPC's superior ability can be attributed to its innate inner tuning capabilities, allowing for swift and seamless adjustments to sudden changes. Based on the results, it can be concluded that implementing an MPC controller led to an increase in viable cell X_v for the system. While the parameters used in this study were not directly derived from experimental data, the visual outcome matched previous research in this area.

5.2 Future work

In Chapter 3, we presented the model for the MPC controller that merits additional investigation in future studies. As mentioned in Chapter 3, the parameters needed for developing ODE models and controllers include initial concentrations, environmental conditions and boundaries, constants of the ODE models, and all of the characteristics related to heat transfer in the bioreactor. Some parameters are collected from experimental data from McGill University (X_{v0}, pH, agitated rotational velocity, preferred temperature, DO concentration, initial substrate and biomass concentrations). Initial specific growth rates are obtained from estimation by NODE and Bayesian Inference [4] based on the same experimental data of AAV's production in the bioreactor. The parameters related to the temperature model are collected from [15] for yeast fermentation, which can slightly be similar to rAAV production. This being so, enhancing primary parameter values from a single AAV production trial could facilitate a more precise simulation and control of the upstream process for AAV.

The model must also encompass all state variables involved in the upstream process. In that case, adding the kinetic model of ammonia formation to the other substrates and product models can complete the simulation of AAV's production process to see the effect of all components on the

cell growth concentration, such as limitations or inhibitions, and it can provide the better representation of the internal condition of the bioprocess.

In order to ensure optimal performance, it is crucial to conduct lab-scale experiments to test the effectiveness of this model under real-world conditions. For this approach, the proposed model-based system can be combined with a data-driven system with software sensors and create a hybrid method for monitoring and controlling the bioprocess of AAV as one of the important materials in gene therapy. Experimental data can help adjust the bioprocess model parameters of crucial state variables to lead to more realistic control prediction.

In the industry, there is a continuous desire towards transitioning from traditional manufacturing to digital technologies [90]. However, there are limitations in using on-line sensors in bioprocesses due to the reactions and environmental conditions during the processes. To address this, developing soft sensors based on the MPC controller can give us real-time knowledge regarding the complex bioprocess and improve product quality. By coupling the smart soft sensors to bioprocess mechanisms, the goal of the industry can be achieved specifically for the production of AAV [90].

References

[1] Lukashev AN, Zamyatnin AA. Viral Vectors For Gene Therapy: Current State And Clinical Perspectives. Biochemistry (Moscow) 2016; 81: 700–708.

[2] Weber T. Anti-AAV Antibodies In AAV Gene Therapy: Current Challenges And Possible Solutions. Front Immunol 2021; 12: 658399–658399.

[3] Manfredsson FP, Benskey MJ. Viral Vectors For Gene Therapy : Methods And Protocols. Book, New York: Humana Press, 2019.

[4] Iglesias CF, Xu X, Mehta V, et al. Monitoring The Recombinant Adeno-Associated Virus Production Using Extended Kalman Filter. Processes 2022; 10: 2180.

[5] Gimpel AL, Katsikis G, Sha S, et al. Analytical Methods For Process And Product Characterization Of Recombinant Adeno-Associated Virus-Based Gene Therapies. Mol Ther Methods Clin Dev 2021; 20: 740–754.

[6] Penaud-Budloo M, François A, Clément N, et al. Pharmacology Of Recombinant Adeno-Associated Virus Production. Mol Ther Methods Clin Dev 2018; 8: 166–180.

[7] Joshi PRH, Venereo-Sanchez A, Chahal PS, et al. Advancements In Molecular Design And Bioprocessing Of Recombinant Adeno-Associated Virus Gene Delivery Vectors Using The Insect-Cell Baculovirus Expression Platform. Biotechnol J 2021; 16: 2000021.

[8] Brignoli Y, Freeland B, Cunningham D, et al. Control Of Specific Growth Rate In Fed-Batch Bioprocesses: Novel Controller Design For Improved Noise Management. Processes 2020; 8: 679.

[9] Galvanauskas V, Simutis R, Levišauskas D, Urniežius R. Practical solutions for specific growth rate control systems in industrial bioreactors. Processes. 2019 Oct 2;7(10):693.

[10] Hitzmann B. Bioprocess Monitoring And Control. Basel, Switzerland: MDPI - Multidisciplinary Digital Publishing Institute, 2020.

[11] Simutis R, Lübbert A. Bioreactor Control Improves Bioprocess Performance. Biotechnol J 2015; 10: 1115–1130.

[12] Dochain D, Tali-Maamar N, Babary JP. On Modelling, Monitoring And Control Of Fixed Bed Bioreactors. 1997.

[13] Ramaswamy S, Cutright TJ, Qammar HK. Control Of A Continuous Bioreactor Using Model Predictive Control. Process Biochemistry 2005; 40: 2763–2770.

[14] Dewasme L, Fernandes S, Amribt Z, c. State Estimation And Predictive Control Of Fed-Batch Cultures Of Hybridoma Cells. J Process Control 2015; 30: 50–57.

[15] Nagy ZK. Model Based Control Of A Yeast Fermentation Bioreactor Using Optimally Designed Artificial Neural Networks. Chem Eng J 2007; 127: 95–109.

[16] De Tremblay M, Perrier M, Chavarie C, et al. Optimization Of Fed-Batch Culture Of Hybridoma Cells Using Dynamic Programming: Single And Multi Feed Cases. 1992.

[17] Joiner J, Huang Z, Mchugh K, et al. Process Modeling Of Recombinant Adeno-Associated Virus Production In HEK293 Cells. Curr Opin Chem Eng 2022; 36: 100823.

[18] Srivastava A, Mallela KMG, Deorkar N, et al. Manufacturing Challenges And Rational Formulation Development For AAV Viral Vectors. J Pharm Sci 2021; 110: 2609–2624.

[19] Liu S. Bioprocess engineering: kinetics, sustainability, and reactor design. Elsevier; 2020 Apr 7.

[20] Liu S. How Cells Grow. In: Bioprocess Engineering. Elsevier, 2017, Pp. 629–697.

[21] Jagschies G, Lindskog E, Lacki K, Galliher PM, editors. Biopharmaceutical processing: development, design, and implementation of manufacturing processes. Elsevier; 2018 Jan 18.

[22] Siegwart P, Côté J, Male K, Et Al. Adaptive Control At Low Glucose Concentration Of HEK-293 Cell Serum-Free Cultures. Biotechnol Prog 1999; 15: 608–616.

[23] Assadzadeh A, Jamuar SS. Development And Simulation Of Biochemical Reactor By Using MATLAB. In: 2010 12th International Conference On Computer Modelling And Simulation. Proceeding, IEEE, 2010, Pp. 456–461.

[24] Craven S, Whelan J, Glennon B. Glucose Concentration Control Of A Fed-Batch Mammalian Cell Bioprocess Using A Nonlinear Model Predictive Controller. J Process Control 2014; 24: 344–357.

[25] Chitra M, Pappa N, Abraham A. Dissolved Oxygen Control Of Batch Bioreactor Using Model Reference Adaptive Control Scheme. IFAC Papersonline 2018; 51: 13–18.

[26] Jabarivelisdeh B, Carius L, Findeisen R, et al. Adaptive Predictive Control Of Bioprocesses With Constraint-Based Modeling And Estimation. Comput Chem Eng 2020; 135: 106744.

[27] Lopéz-Peréz PA, Rodriguez-Mata AE, Hernández-González O, et al. Design Of A Robust Sliding Mode Controller For Bioreactor Cultures In Overflow Metabolism Via An Interdisciplinary Approach. Open Chem 2022; 20: 120–129.

[28] Zhao B, Li X, Sun W, et al. Biodt: An Integrated Digital-Twin-Based Framework For Intelligent Biomanufacturing. Processes 2023; 11: 1213.

[29] Atchison RW, Casto BC, Hammon WMD. Adenovirus-associated defective virus particles. Science 1965; 149: 754–756.

[30] Hoggan MD, Blacklow NR, Rowe WP. Studies Of Small DNA Viruses Found In Various Adenovirus Preparations: Physical, Biological, And Immunological Characteristics. Proc Natl Acad Sci U S A 1966; 55: 1467–1474.

[31] Blacklow NR, Hoggan MD, Rowe WP. Isolation Of Adenovirus-Associated Viruses From Man. Proc Natl Acad Sci U S A 1967; 58: 1410.

[32] Wang D, Tai PWL, Gao G. Adeno-Associated Virus Vector As A Platform For Gene Therapy Delivery. Nature Reviews Drug Discovery 2019 18:5 2019; 18: 358–378.

[33] Hastie E, Samulski RJ. Adeno-Associated Virus At 50: A Golden Anniversary Of Discovery, Research, And Gene Therapy Success—A Personal Perspective. Hum Gene Ther 2015; 26: 257–265.

[34] Rose JA, Berns KI, David Hoggan M, et al. Evidence for a single-stranded adenovirus-associated virus genome: formation of a DNA density hybrid on release of viral DNA. Proceedings Of The National Academy Of Sciences 1969; 64: 863–869.

[35] Carter BJ, Khoury G, Denhardt DT. Physical Map And Strand Polarity Of Specific Fragments Of Adenovirus-Associated Virus DNA Produced By Endonuclease R-Ecori. J Virol 1975; 16: 559–568.

[36] Carter BJ, Khoury G, Rose JA. Adenovirus-Associated Virus Multiplication IX. Extent Of Transcription Of The Viral Genome In Vivo. J Virol 1972; 10: 1118–1125.

[37] William W. Hauswirth And Kenneth I. Berns. Origin And Termination Of Adeno-Associated Virus DNA Replication. Virology 1977; 78: 488–499.

[38] Cheung AK, Hoggan MD, Hauswirth WW, Berns KI. Integration of the adeno-associated virus genome into cellular DNA in latently infected human Detroit 6 cells. Journal of virology. 1980 Feb;33(2):739-48.

[39] Kotin RM, Berns KI. Organization of adeno-associated virus DNA in latently infected Detroit 6 cells. Virology. 1989 Jun 1;170(2):460-7.

[40] Roizman B, Palese P, Linden RM, et al. Site-Specific Integration By Adeno-Associated Virus. Proceedings Of The National Academy Of Sciences 1996; 93: 11288–11294.

[41] Myers MW, Carter' BJ. Assembly Of Adeno-Associated Virus. Virology 1980; 102: 71–82.

[42] Naso MF, Tomkowicz B, Perry III WL, Strohl WR. Adeno-associated virus (AAV) as a vector for gene therapy. BioDrugs. 2017 Aug;31(4):317-34.

[43] Snyder RO, Moullier P, editors. Adeno-associated virus: methods and protocols. Humana Press; 2011.

[44] Burg M, Rosebrough C, Drouin LM, et al. Atomic Structure Of A Rationally Engineered Gene Delivery Vector, AAV2.5. J Struct Biol 2018; 203: 236–241.

[45] Heiser WC. Gene Delivery To Mammalian Cells, Volume 2. Book, Totowa: Humana Press, 2003. Epub Ahead Of Print 2003. DOI: 10.1385/1592596509.

[46] Siegwart P. Modélisation Et Contrôle Adaptatif De La Croissance De Cellules HEK-293 En Milieu Sans Sérum. École Polytechnique De Montréal, Https://Publications.Polymtl.Ca/6925/ (1998).

[47] Nguyen TNT, Sha S, Hong MS, Et Al. Mechanistic Model For Production Of Recombinant Adeno-Associated Virus Via Triple Transfection Of HEK293 Cells. Mol Ther Methods Clin Dev 2021; 21: 642–655.

[48] Moser A. Bioprocess Technology. DOI: Https://Doi.Org/10.1007/978-1-4613-8748-0.

[49] Spier M, Vandenberghe L, Medeiros A, et al. Application Of Different Types Of Bioreactors In Bioprocesses. Bioreactors: Design, Properties And Applications 2011; 53–87.

[50] Heinzle E, Dunn IJ, Ingham J, Přenosil JE. Biological Reaction Engineering: Dynamic Modeling Fundamentals with 80 Interactive Simulation Examples. John Wiley & Sons; 2021 Apr 14.

[51] Nag A. Biofuels refining and performance. NICE (News & Information for Chemical Engineers). 2008;26(2):165-.

[52] Springham DG, Moses V, Cape RE. The Science And The Business: An Introduction. In: Biotechnology - The Science And The Business. United States: Taylor & Francis Group, 1999.

[53] Liljequist V. Development Of A Bioreactor Simulator For Supporting Automation Software Test And Verification (Master's Thesis). Uppsala University , 2017.

[54] Tyson JJ, Novak B. Control of cell growth, division and death: information processing in living cells. Interface focus. 2014 Jun 6;4(3):20130070.

[55] Shishodia V, Jindal D, Sinha S, Singh M. Analysis of Cell Growth Kinetics in Suspension and Adherent Types of Cell Lines. In Animal Cell Culture: Principles and Practice 2023 Feb 1 (pp. 251-265). Springer International Publishing.

[56] Kovárová-Kovar K, Egli T. Growth kinetics of suspended microbial cells: from single-substrate-controlled growth to mixed-substrate kinetics. Microbiology and molecular biology reviews. 1998 Sep 1;62(3):646-66.

[57] González-Figueredo C, Flores-Estrella RA, Rojas-Rejón OA. Fermentation: Metabolism, Kinetic Models, And Bioprocessing. In: Shiomi N (Ed) Current Topics In Biochemical Engineering. Rijeka: Intechopen 2018. DOI: 10.5772/Intechopen.82195.

[58] Kitano H. Computational Systems Biology. Nature 2002; 420: 206–210.

[59] Yang R, Rodriguez-Fernandez M, St. John PC, et al. 8 - Systems Biology. In: Carson E, Cobelli C (Eds) Modelling Methodology For Physiology And Medicine (Second Edition). Oxford: Elsevier, Pp. 159–187.

[60] Fernandes-Platzgummer A, Badenes SM, Silva CL, et al. Bioreactors For Stem Cell And Mammalian Cell Cultivation. In: Bioprocessing Technology For Production Of Biopharmaceuticals And Bioproducts. Bookitem, Hoboken, NJ, USA: John Wiley & Sons, Inc, 2018, Pp. 131–173.

[61] Boudreau MA, McMillan GK. New directions in bioprocess modeling and control: maximizing process analytical technology benefits. ISA; 2007.

[62] Lyubenova V, Ignatova M, Roeva O, Junne S, Neubauer P. Adaptive Monitoring of Biotechnological Processes Kinetics. Processes. 2020 Oct 17;8(10):1307.

[63] Nikita S, Mishra S, Gupta K, et al. Advances In Bioreactor Control For Production Of Biotherapeutic Products. Biotechnol Bioeng 2023; 120: 1189–1214.

[64] Visioli Antonio. Practical PID Control. 1st Ed. 2006. Book, London: Springer London, 2006. DOI: 10.1007/1-84628-586-0.

[65] Johnson MA, Moradi MH. PID Control New Identification And Design Methods. 1st Ed. 2005. Book, London: Springer London, 2005. 2005. DOI: 10.1007/1-84628-148-2.

[66] Rawlings JB, Mayne DQ, Diehl MM, et al. Model Predictive Control: Theory, Computation, And Design 2nd Edition, Http://www.Nobhillpublishing.Com.

[67] Holkar KS, Waghmare LM. An overview of model predictive control. International Journal of control and automation. 2010 Dec;3(4):47-63.

[68] Qin JS, Badgwell TA, Qin SJ. An Overview Of Industrial Model Predictive Control Technology, Https://Www.Researchgate.Net/Publication/2773527 (1997).

[69] H. Chen, F. Allgöwer. Nonlinear Model Predictive Control Schemes With Guaranteed Stability. In: NATO ASI Series. Springer, Dordrecht, 1998, Pp. 465–494.

[70] Morari M, Lee JH. Model predictive control: past, present and future. Computers & chemical engineering. 1999 May 1;23(4-5):667-82. [71] Rawlings JB. Tutorial Overview Of Model Predictive Control. IEEE Control Syst 2000; 20: 38–52.

[72] Camacho EF, Bordons C. Model Predictive Control. In: Advanced Textbook In Control And Signal Processing. Springer Science And Business Media, 1999. DOI: 10.1007/978-0-85729-398-5.

[73] Rossiter JA. Model-based predictive control: a practical approach. CRC press; 2017 Jul 12.

[74] Wang L. Model Predictive Control System Design And Implementation Using MATLAB. Springer London, 2009. Epub Ahead Of Print 2009. DOI: 10.1007/978-1-84882-331-0.

[75] Forbes MG, Patwardhan RS, Hamadah H, Et Al. Model Predictive Controlin Industry: Challenges And Opportunities. In: IFAC-Papersonline. 2015, Pp. 531–538.

[76] Hastie T, Tibshirani R, Friedman JH. The Elements Of Statistical Learning: Data Mining, Inference, And Prediction. 2009; 2: 1–758.

[77] Thoma M, Allgöwer F, Morari M. Lecture Notes In Control And Information Sciences 384.

[78] Pachauri N, Rani A, Singh V. Bioreactor Temperature Control Using Modified Fractional Order IMC-PID For Ethanol Production. Chemical Engineering Research & Design 2017; 122: 97–112.

[79] Clarke KG. Microbial kinetics during batch, continuous and fed-batch processes. Bioprocess Engineering. 2013:97-146.

[80] Peleg M, Corradini MG. Microbial Growth Curves: What The Models Tell Us And What They Cannot. Crit Rev Food Sci Nutr 2011; 51: 917–945.

[81] Ross T, Dalgaard P. Secondary Models. Modeling Microbial Response In Food 2004; 63–150.

[82] Shuler ML. Bioprocess Engineering : Basic Concepts. Third Edition. Book, Boston: Prentice Hall, 2017.

[83] Vieth WR. Bioprocess Engineering : Kinetics, Mass Transport, Reactors, And Gene Expression. Book, New York: Wiley, 1994.

[84] Popović M, Niebelschütz H, Reuss M. Oxygen solubilities in fermentation fluids. European journal of applied microbiology and biotechnology. 1979 Mar;8:1-5.

[85] Pirt SJ. Principles Of Microbe And Cell Cultivation. Book, New York: Wiley, 1975.

[86] Joshi PR, Bernier A, Moço PD, Schrag J, Chahal PS, Kamen A. Development of a scalable and robust AEX method for enriched rAAV preparations in genome-containing VCs of serotypes 5, 6, 8, and 9. Molecular Therapy-Methods & Clinical Development. 2021 Jun 11;21:341-56.

[87] Shampine LF, Reichelt MW. The MATLAB ODE Suite. SIAM Journal On Scientific Computing 1997; 18: 1–22.

[88] Stephanopoulos G, San K-Y. Studies On On-Line Bioreactor Identification. I. Theory. Biotechnol Bioeng 1984; 26: 1176–1188.

[89] Steenson L V., Phillips AB, Turnock SR, et al. Effect Of Measurement Noise On The Performance Of A Depth And Pitch Controller Using The Model Predictive Control Method. In: 2012 IEEE/OES Autonomous Underwater Vehicles (AUV). Proceeding, IEEE, 2012, Pp. 1–8.

[90] Rathore AS, Mishra S, Nikita S, Et Al. Bioprocess Control: Current Progress And Future Perspectives. Life (Basel) 2021; 11: 557.